EXPLORING THE ROLE OF THE SYNTHETIC FOOD COLOURANT ALLURA RED AC IN THE DEVELOPMENT OF COLITIS

EXPLORING THE ROLE OF THE SYNTHETIC FOOD COLOURANT ALLURA RED AC IN THE DEVELOPMENT OF COLITIS

By

YUN HAN KWON, M. Sc

A thesis submitted to the School of Graduate Studies in Partial Fulfillment of the Requirements for the Degree Doctor of Philosophy

McMaster University DOCTOR OF PHILOSOPHY (2022) Hamilton, Ontario

(Medical Science – Infection & Immunity)

TITLE	Exploring the role of the synthetic food colourant Allura Red AC in the development of colitis
AUTHOR	Yun Han Kwon, M. Sc
SUPERVISOR	Dr. Waliul I. Khan, MBBS, Ph. D., FRCPath
SUPERVISORY COMMITTEES	Dr. Alison C. Holloway, Ph. D. Dr. Michael G. Surette, Ph. D.
NUMBER OF PAGES:	xvii, 157

LAY ABSTRACT

Epidemiological and experimental studies suggest a potential link between inflammatory bowel disease (IBD) and diet. The Western diet, often characterized by a high intake of processed foods, is associated with the growing incidence of IBD. Allura Red AC (AR) is a popular artificial food dye found in highly common processed foods, yet little is known about its impact on human health and disease. Serotonin, a key molecule in the gut, has been implicated in large bowel inflammation. Herein, the potential role of AR in the development of colitis was examined. Across multiple models, AR exposure heightened vulnerability to colitis in mice, an effect attenuated by reduced serotonin production in the gut. The effect of AR in enhancing colitis vulnerability occurred via gut microbiota-dependent and -independent pathways. These studies have identified how AR promotes colitis, findings that may advance public health awareness and impact the health of patients with IBD.

ABSTRACT

Environmental factors such as diet contribute to the pathogenesis of inflammatory bowel disease (IBD). Epidemiological evidence suggests a robust linkage between IBD and the Western diet, which is often characterized by a high intake of food additives. These additives, including synthetic colourants, are widely used, leading to significant human exposure. Allura Red AC (AR) is one of the most popular synthetic colourants, yet little is known about its impact on human health and the role of AR in the pathogenesis of colitis remains elusive. Serotonin (5-hydroxytryptamine; 5-HT), which regulates various gut physiological processes, has been shown to modulate the gut microbiota and enhance susceptibility to colitis. In this thesis, it was discovered that chronic exposure to AR, at a dose found in commonly consumed dietary products, exacerbated dextran sulfate sodium (DSS)-induced colitis and triggered early onset of disease in the $CD4^{+}CD45RB^{high}$ T cell-induced colitis model. AR also induced low-grade colonic inflammation in naïve C57BL/6 mice. Exposure to AR was associated with increased colonic 5-HT levels and impaired intestinal barrier function via activation of the myosin light chain kinase (MLCK) pathway. However, AR did not promote colitis in mice lacking tryptophan hydroxylase 1 (Tph1), the rate-limiting enzyme responsible for colonic 5-HT synthesis. Further, AR increased colonic 5-HT levels in germ-free (GF) mice and perturbed the gut microbiota composition in specific pathogen-free (SPF) mice. Transfer of this altered microbiota from the dye-exposed SPF mice to GF mice conferred enhanced susceptibility to DSS-induced colitis.

Mechanistically, AR induced reactive oxygen species (ROS) generation and promoted 5-HT secretion via the NF-κB pathway in BON cells. Data in this thesis indicate that the widely used synthetic colourant, AR, promotes colitis via colonic 5-HT in microbiota-dependent and -independent pathways. Collectively, these findings provide important information on enhancing public awareness of its detrimental effects on human health.

PUBLICATIONS DURING GRADUATE STUDIES

1. **Kwon, Y. H.***, Wang, H.*, Denou, E.*, Ghia, J-E., Rossi, L., Fontes, M. E., Bernier, S. P., Shajib, M. S., Banskota, S., Collins, S. M., Surette, M. G., Khan, W. I. (2019). Modulation of Gut Microbiota Composition by Serotonin Signaling Influences Intestinal Immune Response and Susceptibility to Colitis. *Cellular and Molecular Gastroenterology and Hepatology*, 7(4), 709-728. ***co-authorship**.
2. Wang, H. *, **Kwon, Y. H.** *, Dewan, V. *, Vahedi, F., Syed, S., Fontes, M. E., Ashkar, A. A., Surette, M. G., Khan, W. I. (2019). TLR2 Plays a Pivotal Role in Mediating Mucosal Serotonin Production in the Gut. *The Journal of Immunology*, 202(10), 3041-3052. ***co-authorship**.
3. Grondin, J. A., **Kwon, Y. H.**, Far, P. M., Haq, S., Khan, W. I. (2020). Mucins in intestinal mucosal defense and inflammation: learning from clinical and experimental studies. *Frontiers in Immunology*, 11, 2054.
4. Banskota, S., Wang, H., **Kwon, Y. H.**, Gautam, J., Gurung, P., Haq, S., Hassan, F. M., Bowdish, D., Kim, J-A., Carling, D., Fullerton, M. D., Steinberg, G. R., Khan, W. I. (2020). Salicylates Ameliorate Intestinal Inflammation by Activating Macrophage AMPK. *Inflammatory Bowel Disease*, izza305.
5. Banskota, S., Brim, H., **Kwon, Y. H.**, Singh, G., Sinha, S. R., Wang, H., Khan, W. I., Ashktorab, H. (2021). Saffron Pre-Treatment Promotes Reduction in

Tissue Inflammatory Profiles and Alters Microbiome Composition in Experimental Colitis Mice. *Molecules*, 26(11), 3351.

6. Yousefi, Y., Haq, S., Banskota, S., **Kwon, Y. H.**, Khan, W. I. (2021). Trichuris muris Model: Role in Understanding Intestinal Immune Response, Inflammation and Host Defense. *Pathogens*, 10(8), 925.
7. Haq. S., Wang. H., Grondin, J., Banskota, S., Marshall, J. K., Khan, I. I., Chauhan, U., Cote, F., **Kwon, Y. H.**, Philpott, D., Brumell, J. H., Surette, M. G., Steinberg, G. R., Khan, W. I. (2021). Disruption of autophagy by increased 5-HT alters gut microbiota and enhances susceptibility to experimental colitis and Crohn's disease. *Science Advances*, 7(45), eabi6442.
8. Barra, N. G., **Kwon, Y. H.**, Morrison, K. M., Steinberg, G. R., Wade, M. G., Khan, W. I., Vijayan, M. M., Schertzer, J. D., Holloway, A. C. (2022). Increased gut serotonin production in response to bisphenol A structural analogues may contribute to their obesogenic effects. *American Journal of Physiology Endocrinology and Metabolism*. **In Press**.
9. **Kwon, Y. H.**, Khan, W. I. (2022). Peripheral Serotonin: Cultivating Companionship with Gut Microbiota in Intestinal Homeostasis. *American Journal of Physiology Cell Physiology*. **In Press**.
10. **Kwon, Y. H.**, Banskota, S, Wang, H., Rossi, L., Grondin, J. A., Syed, S. A., Schertzer, J. D., Morrison, K. M., Wade. M. G., Holloway, A. C., Surette, M. G., Steinberg, G. R., Khan, W. I. (2022). Synthetic food colorant Allura Red AC promotes colitis via colonic serotonin. *Nature Communications*. **In Revision**.

COURSE COMPLETED DURING PH. D. STUDIES

1. MEDSCI 740 – *Drug Receptor Interactions*. Instructor: Dr. Ram Mishra.

AWARDS DURING PH. D. STUDIES

1. **Young Investigator Award** (2019).

   Issued by *Digestive Disease Week – American Gastroenterological Association*.

2. **Department Graduate Student Research Excellence Scholarship** (2019).

   Issued by *Department of Pathology and Molecular Medicine, McMaster University*.

3. **In This Issue** (2019).

   Issued by *The Journal of Immunology*.

4. **CMGH Trainee Article of the Year** (2020).

   Issued by *Cellular and Molecular Gastroenterology and Hepatology*.

ACKNOWLEDGEMENTS

I would like to start by thanking my supervisor, Dr. Waliul Khan, for providing me with an opportunity to continue basic science research and to realize my potential as a scientist during 7 years of unforgettable memory in his laboratory. I have greatly appreciated your advice regarding both professional and personal matters. I am grateful to have received your guidance during my doctoral studies.

Thank you to my supervisory committee, Dr. Alison Holloway, and Dr. Michael Surette, for your academic guidance and insightful feedback. Your expertise provided the direction of my thesis which I could not have thought about and developed my critical thinking skills in anticipation of your criticisms. Thank you for the faith that you have shown in me and your encouragement. May the years bless you and your family with continued good health, wealth, and happiness.

I would like to thank collaborators and colleagues in the Farncombe Institute at McMaster University for their support. I would also like to thank my past and present lab members for their guidance and support during my doctoral studies. To my brother, Dr. Suhrid Banskota, I am very fortunate to have you to sit beside me and support throughout my doctoral studies. You have taught me how to think about life in a new way, especially the way to appreciate every moment and strive to make the best use of it even though there are ups and downs.

To my soccer buddies, Dr. Alberto Caminero, and Dr. Justin McCarville, I will miss our times running on the artificial turf field at the back of the rec centre at McMaster University, especially during sizzling summer days. The best part I will not forget is grabbing beers after the matches though there were more times that we lost the games. Because of the pandemic, we couldn't get together on the field, but I was fortunate to be on the team and grateful to have you as teammates.

To my best friends, Jacob Baek, Jimmy Choi, Daniel Ohn, and Ryan Yoo, I consider myself as the luckiest person to have you as my friends. I am thankful to you for understanding and accepting me just the way I am.

Finally, and most importantly, I am wholeheartedly thankful to my beloved family who started a new beginning in Canada. My hard-working parents have sacrified their lives for my sister and myself and provided unconditional love and care. Without your continuous support and indescribable faith in me, I could not have achieved anything on this journey.

TABLE OF CONTENTS

LIST OF ABBREVIATIONS

ADI	Acceptable daily intake
AhR	Aryl hydrocarbon receptor
APC	Antigen presenting cell
AR	Allura Red AC
ATG16L1	Autophagy related 16 like 1
BB	Brilliant Blue FCF
BSA	Bovine serum albumin
CARD15	Caspase recruitment domain-containing protein 15
CD	Crohn's disease
CgA	Chromogranin A
CMC	Carboxymethylcellulose
COX-2	Cyclooxygenase-2
CS	*p*-Cresidinesulfonic acid
CYBB	Cytochrome b-245 beta chain
DAI	Disease activity index
DC	Dendritic cell
DMEM	Dulbecco modified Eagle medium
DNBS	Dinitrobenznesulfonic acid
dNTP	Deoxynucleoside triphosphate
DSS	Dextran sulfate sodium
EC	Enterochromaffin

EEC	Enteroendocrine cell
EHEC	Enterohemorrhagic *E. coli*
ELISA	Enzyme-linked immunosorbent assay
ENS	Enteric nervous system
EPEC	Enteropathogenic *E. coli*
ER	Endoplasmic reticulum
FACS	Fluorescent activated cell sorting
FBS	Fetal bovine serum
FDA	Food and Drug Administration
FITC	Fluorescein isothiocyanate
GF	Germ-free
GI	Gastrointestinal
GLP	Glucagon-like peptide
GPBAR	G protein-coupled bile acid receptor
GPCR	G protein-coupled receptor
GTPase	Guanosine triphosphatase
GWAS	Genome-wide association studies
H&E	Hematoxylin and eosin
HEPES	4-(2-hydroxyethyl)-1-piperazineethanesulfonic acid
HTAB	Hexadecyltrimethylammonium bromide
I3A	Indole-3-carboxaldehyde
IAA	Indole-3-acetic acid
IBD	Inflammatory bowel disease

IDO	Indoleamine 2,3-dioxygenase
IEC	Intestinal epithelial cell
IFN	Interferon
IL	Interleukin
IPA	Indole-3-propionic acid
Kyn	Kynurenine
L-AADC	L-Amino acid decarboxylase
LD_{50}	Lethal dose
Lgr5	leucine-rich repeat-containing G-protein-coupled receptor 5
Lipocalin-2	Lcn-2
LPS	Lipopolysaccharide
LTB_4	leukotriene B_4
MAO	Monoamine oxidase
mEGF	Mouse epidermal growth factor
MEM	Minimum Essential Medium
MLC	Myosin II regulatory light chain
MLCK	Myosin light chain kinase
MPO	Myeloperoxidase
NaB	Sodium butyrate
NOD2	Nucleotide-binding oligomerization domain-containing protein 2
NOX2	NADPH oxidase 2
P-80	Polysorbate-80
PAS	Periodic acid-Schiff

PBS	Phosphate buffer saline
*p*CPA	*para*-chlorophenylalanine
PCR	Polymerase chain reaction
PIC	Protease inhibitor cocktail
PIEZO	Piezo type mechanosensitive ion channel
Pparg	Peroxisome proliferator activated receptor gamma (*Pparg*)
PTM	Post-translational modification
PVDF	Polyvinylidene difluoride
QS	Quorum sensing
RAG1	Recombination activating gene 1
Reg	Regenerating islet-derived protein
RIPA	Radioimmunoprecipitation assay
ROS	Reactive oxygen species
SA	Sulfanilic acid
SCFA	Short-chain fatty acid
SCID	Severe combined immunodeficient
SDS	Sodium dodecyl sulfate
Ser	Serine
SERT	Serotonin reuptake transporter
SSRI	Selective serotonin reuptake inhibitor
SY	Sunset Yellow
Syn	Synaptophysin
TBST	Tris-buffered saline tween 20

TER	Transepithelial resistance
TGM	Transglutaminase
Th	T helper
TLR	Toll-like receptor
TNBS	2,4,6-trinitrobenzenesulfonic acid
TNF	Tumour necrosis factor
TNFR	TNF-α receptor
Tph	Tryptophan hydroxylase
T_{reg}	Regulatory T
Trp	Tryptophan
TRPA	Transient receptor potential cation channel subfamily A
TY	Tartrazine Yellow
UC	Ulcerative colitis
VMAT	Vesicular monoamine transporter
WT	Wild -type
ZO	Zonula occludens
5-HIAA	5-hydroxyindoleacetic acid
5-HT	5-hydroxytryptamine
5-HTP	5-hydroxytryptophan
5-HTR	5-HT receptor

—CHAPTER 1—

INTRODUCTION

1.1 Inflammatory Bowel Disease

Inflammatory bowel disease (IBD) is a group of chronic inflammatory diseases that include Crohn's disease (CD) and ulcerative colitis (UC). Chronic disruption of mucosal homeostasis accompanied by exaggerated immune responses underlies the pathophysiology of IBD (Korzenik et al., 2006). Although UC and CD have overlapping clinical and pathological features, these clinically defined forms of IBD have several distinct hallmarks. The most common hallmark that distinguishes CD from UC is discontinuous or skip lesions which can occur in any region throughout the gastrointestinal (GI) tract; lesions are typically localized to the ileum and the colon. While UC is largely characterized by superficial inflammation limited to the gut mucosa and confined to the colon and the rectum, CD is a transmural disease which can involve all intestinal layers of the gut. In these conditions, activated immune cells from both innate and adaptive immune systems infiltrate the mucosa and contribute to extensive ulcerative lesions, which can ultimately lead to abscesses, fistulas and/or subsequent fibrosis (Yoo et al., 2020). Disease diagnosis often occurs within the first three decades of life; however, recent evidence indicates that IBD can manifest at any age (Kaplan et al., 2019). Pediatric IBD accounts for approximately 15% of all cases (Benchimol et al., 2011; Carroll et al., 2019; Duricova et al., 2014; Vernier–Massouille et al., 2008), suggesting that exposure to environmental factors in early childhood may be closely linked with the later onset of IBD.

1.2 Factors affecting the development of IBD

IBD is a multifactorial disorder which is thought to result from exaggerated mucosal immune responses toward enteric microbes in combination with the influence of different environmental factors in a genetically susceptible host (De Souza et al., 2016). Currently, more than 3 million people around the world live with these conditions that accompany, at times, debilitating physical and psychological symptoms, often leading to a poor quality of life (Jairath et al., 2020) and decreased life expectancy (Peery et al., 2015). With recent advances in modern technology, including next-generation sequencing and high-throughput -omics data generation, investigations into the human genome and the gut microbiome have brought forth unprecedented insights regarding the pathogenesis of IBD. Animal models of colitis and human clinical samples have also provided substantial understanding in this regard, leading to improved therapeutic strategies to control mucosal inflammation.

1.2.1 Genetic factors

Large-scale genome-wide association studies (GWAS) and subsequent meta-analyses have helped to unveil the genetic architecture of IBD. To date, more than 200 confirmed risk loci have been reported (Jostins et al., 2012). However, these risk loci are not exclusively associated with IBD; some genes have opposite outcomes in different diseases, such as type 1 diabetes and rheumatoid arthritis (Liu et al., 2015). For instance, *IL23R*, the gene encoding the subunit of the receptor for the pro-inflammatory cytokine interleukin-23 (IL-23), was also identified using IBD-based

GWAS, and this gene was found to be strongly associated with CD (Duerr et al., 2006). Previous work has, however, demonstrated a requirement for IL-23 in animal models of IBD, rheumatoid arthritis, and autoimmune encephalitis (Cua et al., 2003; Murphy et al., 2003; Yen et al., 2006). In contrast, several alleles specifically associated with CD have been identified. Single-nucleotide polymorphisms in Autophagy related 16 like 1 (*ATG16L1*) have been strongly associated with an increased risk of developing CD (Hampe et al., 2007). Deficiency of this gene results in a decreased release of antimicrobial proteins due to disruption of the secretory functions in Paneth cells, and unresolved endoplasmic reticulum (ER) stress that leads to spontaneous apoptosis (Adolph et al., 2013; Cadwell et al., 2008). The most well-known gene associated with CD, however, is nucleotide-binding oligomerization domain-containing protein 2 (*NOD2*) (previously known as caspase recruitment domain-containing protein 15, CARD15) (Hugot et al., 2001). *NOD2*, also known as IBD protein 1 (*IBD1*), is an intracellular pattern recognition receptor which plays an important role in detecting the bacterial peptidoglycan product called muramyl dipeptide (MDP) (Kobayashi et al., 2005). Importantly, the frequency of NOD2/CARD15 mutations in non-Caucasian populations including Africans and Pacific Asians is diminished in comparison to populations of either European or Jewish ancestry (Bernstein et al., 2006; Dassopoulos et al., 2010; Inoue et al., 2002; Leong et al., 2003; Yamazaki et al., 2013). The remarkable heterogeneity in the disease susceptibility across diverse ethnicities and populations with geographical variation suggests that genetic influences are not the sole contributing factor associated with IBD pathogenesis.

1.2.2 Gut Microbiota

Trillions of microorganisms inhabit the GI tract, with the distal ileum and colon being the largest reservoir. Of these microorganisms, including bacteria, fungi, and viruses, bacteria are, by far, the most characterized and colonize the majority of the colon with approximately 10^{12} bacteria consisting of predominantly obligate anaerobes (Rigottier-Gois, 2013; Sekirov et al., 2010). Critical in maintaining intestinal homeostasis, the interactions between microbes and their host consist of finely tuned mechanisms through interlinked metabolic networks and processes closely monitored by the mucosal immune system (Cerf-Bensussan et al., 2010). Recent advances catalyzed by a rapid development of modern technology have facilitated the concept that the gut microbiome is not just a bystander, but actively carries out essential functions, aiding in nutrient metabolism and providing a healthy barrier against pathogenic infections (Hooper et al., 2010). It is also becoming increasingly apparent that the gut microbiota efficiently tailors the host immune system and limits resources available to pathobionts (Kamada et al., 2013).

Microbial-derived metabolites including short-chain fatty acids (SCFAs) are important for mucosal barrier function, which are an important fuel for intestinal epithelial cells (IECs) and immune cells, such as naïve CD4+ T cells. For instance, butyrate, which is produced through anaerobic bacterial fermentation of dietary fibres, exerts anti-inflammatory and barrier protective effects in the colon (Hamer et al., 2008; Plöger et al., 2012). It has previously been shown that butyrate enhances the intestinal epithelial barrier function by maintaining the integrity of the epithelial tight junction

(Kelly et al., 2015). Similarly, butyrate treatment also facilitated the assembly of tight junctional proteins and increased MUC2 synthesis, the main component of the intestinal mucus layer (Burger-van Paassen et al., 2009; Chen et al., 2018; Fachi et al., 2019; Grondin et al., 2020; Peng et al., 2009). Moreover, butyrate induces the differentiation of functional colonic $CD4^+$ regulatory T (T_{reg}) cells via T-cell intrinsic epigenetic upregulation of the *Foxp3* gene, mediating host-microbial crosstalk for maintaining immune homeostasis in the colon (Furusawa et al., 2013). However, the beneficial host-butyrate relationship can be hindered during periods of intestinal inflammation as evidenced by several clinical studies. In patients with IBD, which is strongly associated with gut microbial dysbiosis, there is a lower abundance of butyrate-producing bacteria such as *Roseburia hominis* and *Faecalibacterium prausnitzii* (Machiels et al., 2014; Wang et al., 2014). Additionally, impairments of butyrate utilization which result from the reduction of its uptake through downregulation of the monocarboxylate transporter have been observed in the inflamed colonic mucosa of patients with IBD (Chapman et al., 1994; De Preter et al., 2012; Thibault et al., 2007). Given that restoration of butyrate, alone or as a cocktail of SCFAs, by enema has been shown to ameliorate colonic inflammation in patients with IBD (Harig et al., 1989; Scheppach et al., 1992), insufficient butyrate levels may be involved in the pathogenesis of IBD. Although alterations in the gut microbiota composition, as well as its metabolome, have been closely associated with chronic inflammation through studies using animal models of colitis, the definitive cause-effect relationship between dysbiosis and IBD has been difficult to unravel.

1.2.3 Immune activation and intestinal barrier function

The GI mucus layer, largely composed of the glycoprotein, MUC2, not only provides lubrication but also supplies a critical physical barrier, protecting the host from the invasion of commensals and pathogens alike (Grondin et al., 2020). This bilayer is continuously refreshed with goblet cells providing, among other mucins, the structural support of MUC2 (Johansson et al., 2008; Paone et al., 2020). It is important to note that disruption of the gut microbiome by a wide range of environmental stimuli is often accompanied by a loss of intestinal epithelial integrity, mediated by immune activation (Nagalingam et al., 2012). In IBD, histopathological processes are often linked with unchecked immune activation. Determined by the specialized tight and adherens junctional proteins connecting each polarized epithelial cell, compromised intestinal epithelial barrier function and subsequent permeation of luminal microorganisms and noxious molecules can lead to these pathological processes.

Given the importance of the intestinal epithelium as a primary interface between the body and the external environment, tumour necrosis factor-alpha (TNF-α) is one of the major pro-inflammatory effectors that facilitates diverse cellular processes, such as inflammatory mediator production, cell death/survival, and proliferation (Braegger et al., 1992; Leppkes et al., 2014). Substantial evidence indicates that Th1-type cytokines, such as TNF-α and interferon-gamma (IFN-γ), are associated with disruption of the intestinal epithelial barrier function (Fish et al., 1999; Gibson, 2004; Günther et al., 2013; Neurath, 2014). For instance, IFN-γ treatment on cultured epithelial monolayers led to a reduction in the parameters of IEC barrier function, such as transepithelial

resistance (TER), and increased fluorescein isothiocyanate (FITC)-dextran flux, which were accompanied by an increased expression of TNF-α receptor (TNFR) (Fish et al., 1999). In this setting, treatment with TNF-α further induced a reduction in TER, and increased FITC-dextran flux, suggesting synergistic effects of these cytokines on the epithelial permeability (Fish et al., 1999). Consistent with this work, TNF-α treatment, only upon priming of the cultured epithelial monolayers with IFN-γ, induced intestinal epithelial barrier dysfunction through a mechanism that requires activation of myosin light chain kinase (MLCK) (Wang et al., 2005). MLCK plays a central role in the pathophysiological regulation of the intestinal epithelial barrier, which is necessary for TNF-α induced barrier loss through phosphorylation of myosin II regulatory light chain (MLC) (Cunningham et al., 2012; Zolotarevsky et al., 2002). Importantly, intestinal epithelial barrier regulation via MLCK activation has been observed in murine models of colitis and in inflamed colonic tissues of IBD patients with phosphorylation of MLC at Serine (Ser) 19 (Ferrier et al., 2003; Moriez et al., 2005; Scott et al., 2002; Blair et al., 2006).

Patients with IBD often display elevated levels of mucosal and serum IFN-γ following microbial infection (Camoglio et al., 1998; Holland et al., 2008; Rafa et al., 2010; Sasaki et al., 1992). IFN-γ-induced impairment of the epithelial barrier function allows increased permeation of gut luminal antigens, including commensal bacteria and unprocessed dietary antigens, into the mucosa which subsequently induces pathological inflammation (Smyth et al., 2011; Turner, 2009). Furthermore, increased IFN-γ levels can affect intestinal epithelial barrier function, greatly diminishing the epithelial

resistance by perturbing apical actin organization and reducing expression of the tight junction proteins, such as zonula occludens (ZO)-1, and occludin (Madara et al., 1989; Youakim et al., 1999).

Besides professional antigen-presenting cells (APCs), including dendritic cells (DCs), monocytes/macrophages, and B lymphocytes, IECs have the capacity to function as non-professional APCs. It has previously been shown that IECs communicate with CD4+ T cells in maintaining intestinal homeostasis. For instance, IECs isolated from IBD patients preferentially stimulated CD4+ T cell proliferation, a process associated with significant IFN-γ secretion (Dotan et al., 2007). This effect is also present when IECs from healthy controls are co-cultured with normal CD4+ T cells, though to a much lesser extent (Dotan et al., 2007). Thus, it can be surmised that factors driving activation and differentiation of CD4+ T cells can alter the intricate network between immune cells and IECs, which may drive the pathogenesis of intestinal inflammation. Furthermore, excessive activation of effector CD4+ T cells or the loss of tolerance to gut luminal and microbial antigens can contribute to the development of colitis (Zenewicz et al., 2009). CD4+ T cells have been shown to promote cytotoxicity by recruiting and activating other immune cells, including macrophages and neutrophils, as well as produce cell subset-specific cytokines (e.g., IL-17, IL-23, and IFN-γ). Thus, it is not surprising that considerable evidence indicates $CD4^+$ T cells, especially T helper (Th) 1 and Th17 subsets, are important in the pathogenesis of colitis in both humans and mice (He et al., 2021; Ito et al., 2006; Khor et al., 2011; Neurath et al., 2002; Powrie et al., 1993; Takeuchi et al., 2016; Yen et al., 2006).

Both Th1- and Th17-type immune responses have been characterized in murine models of colitis using dextran sulfate sodium (DSS) and $CD4^{+}CD45RB^{high}$ T cells (P. P. Ahern et al., 2010; Alex et al., 2009; Ito et al., 2006; Lee et al., 2009; Ostanin et al., 2006). DSS is one of the most widely used experimental models of colitis, in which intestinal inflammation is induced by the administration of DSS via drinking water (Kiesler et al., 2015; Morgan et al., 2013). DSS, a sulfated polysaccharide, damages the colonic epithelium by directly inducing cell injury and altering mucosal barrier function, thereby enabling the entry of commensal bacteria and bacterial components into the lamina propria (Kiesler et al., 2015; Wirtz et al., 2007). In this model, inflammation is limited to the colon and characterized by erosion/ulcer-type lesions, loss of crypts, and infiltration of granulocytes (Cooper et al., 1993; Okayasu et al., 1990). Importantly, innate immune cells are sufficient to induce mucosal inflammation in the DSS model; inflammation can notably develop in the absence of T cell-mediating adaptive immunity, as in severe combined immunodeficient (SCID) and recombination activating gene 1-deficient (*Rag1*$^{-/-}$) mice (Krieglstein et al., 2002).

In contrast, $CD4^{+}CD45RB^{high}$ T cell transfer model of colitis is currently the best characterized chronic model that closely resembles the development of human IBD, especially CD (Ostanin et al., 2006; Powrie et al., 1993; Sandborn et al., 2002). In this model, adoptive transfer of naïve CD4+ T cells ($CD4^{+}CD45RB^{high}$ T cells) from donor mice into lymphopenic SCID or *Rag1*$^{-/-}$ recipient mice leads to primarily colonic inflammation in 5-10 weeks (Kiesler et al., 2015). Here, colonic inflammation is driven by enteric antigens as well as polarization, expansion, and trafficking of naïve CD4+ T

cells to the intestine, disrupting the architecture of the epithelium, depleting goblet cell numbers and driving increased infiltration of immune cells to the mucosa (Ostanin et al., 2006; Powrie, 1995). Notably, expression of IFN-γ by $CD4^+$ T cells is shown to be critical for $CD4^+CD45RB^{high}$ T cell-induced colitis (Ito et al., 2006; Neurath, 2014), and, as previously mentioned, IFN-γ is highly upregulated in both CD and UC (Nava et al., 2010; Singh et al., 2016; Verma et al., 2013). Moreover, genetic mutations associated with IFN-γ have been identified as one of the risk loci for IBD (Jostins et al., 2012), and antibody-based therapies targeting CD4+ T cell-derived cytokines, including IFN-γ, are found to be effective in IBD trials (Hommes et al., 2004; Reinisch et al., 2006).

It should also be noted that experimental evaluation of intestinal epithelial barrier function and immune activation have been further substantiated by the recent development of organoids (Altay et al., 2019; Nakamura, 2019; Xu et al., 2018). Organoid cultures harbour the unique ability of a self-organizing nature and intestinal renewal arising from leucine-rich repeat-containing G-protein-coupled receptor 5 (Lgr5)-positive stem cells, which mediates crypt-villus structures with all differentiated intestinal cell types *in vitro* (Sato et al., 2009). It has recently been shown that IFN-γ increased the epithelial barrier permeability, and reduced ZO-1 and E-cadherin expression in intestinal organoids derived from wild-type (WT) mouse and CD patients (Bardenbacher et al., 2019; Xu et al., 2021). Likewise, treatment of CD patient-derived intestinal organoids with a cytokine cocktail containing TNF-α and IFN-γ increased the epithelial paracellular permeability, which was accompanied by increased MLCK signaling and decreased E-cadherin (Xu et al., 2021). Thus, when the mucosal barrier

is breached, translocation of the gut microbiota and exaggerated immune response can drive intestinal inflammation.

1.2.4 Environment

Ever since the first case of UC was reported in 1859 (Wilks, 1859), the prevalence and incidence of IBD have steadily increased around the world (Kaplan et al., 2021), with the global prevalence increasing by 31% from 1990 to 2017 (Piovani et al., 2020). Currently, approximately 1% of the Canadian population is suffering from IBD, with the disease prevalence estimated to reach 403,000 people by 2030 (Coward et al., 2019). Although significant progress has been made to identify IBD susceptibility genes through GWAS as well as to understand the immunological mechanisms underlying these conditions, approximately one-third of patients with IBD still do not respond appropriately to existing therapies, including immunosuppressive agents (e.g., azathioprine, corticosteroids, cyclosporine, methotrexate, and 6-mercaptopurine), and biologics targeting specific cytokines (e.g., TNF-α and IL-23) or α4β7 integrin due to low efficacy, an increased risk of infection, and high medication costs (Baumgart et al., 2012; Cui et al., 2021; Sandborn et al., 2020; Torres et al., 2017; Villablanca et al., 2022). The increasing emergence of IBD in Western countries and, particularly, countries undergoing rapid Westernization, has renewed the interest in understanding the effects of environmental factors. Urbanization of societies, which is associated with dietary changes, antibiotic use, hygiene status, microbial exposures, pollutants, and toxicants, has been implicated in this epidemiological evolution (Ananthakrishnan et

al., 2018; Ho et al., 2019). These environmental factors can evoke intestinal inflammation, which not only drives dysbiosis in the gut, but also trigger disruption of the intestinal epithelial barrier integrity (Arthur et al., 2012; Ayres et al., 2012; Lewis et al., 2015; Lupp et al., 2007; Zeng et al., 2016). Several epidemiological studies have also shown that children born to individuals who relocate from regions of low IBD prevalence to areas of high disease prevalence acquire greater risk (Benchimol et al., 2015; Kaplan et al., 2017; Ng et al., 2017), implicating the critical role played by environmental factors in IBD pathogenesis. Collectively, these previous findings suggest that exposures to environmental factors are strongly linked to the development of IBD.

2.1 Peripheral serotonin and the gut

2.1.1 Brief background of Serotonin

In the 1930s, with an interest in the smooth muscle constricting and contracting properties of various amine substances, Dr. Vittorio Erspamer isolated a substance from GI mucosal extracts of vertebrates (Whitaker-Azmitia, 1999). This substance was identified as an indolalkylamine secreted by EC cells (Erspamer et al., 1937; Whitaker-Azmitia, 1999). Building on the discovery of this “enteramine” (Erspamer, 1948; Erspamer et al., 1951; Erspamer et al., 1937), Drs. Irvine Page and Maurice Rapport discovered an endogenous vasoconstricting factor with an indole nucleus from a purified concentration of bovine serum and chemically identified it as "5-hydroxytryptamine" (5-HT) (Page, 1968; Rapport et al., 1948a, 1948b). 5-HT was later

dubbed as "serotonin", a term obtained from its derivative "*ser*um" and its ability to modulate tone ("*-tonin*") within blood vessels (Rapport et al., 1948a). Later, work involving the total gastroenterectomy of rats, which resulted in a substantial reduction in 5-HT levels and the predominant metabolite, 5-hydroxyindoleacetic acid (5-HIAA) in urine, revealed that the gut is the main hub of 5-HT biosynthesis (Bertaccini, 1960). This evidence, along with intact 5-HT levels in the brain after total gastroenterectomy (Bertaccini, 1960), suggested that neuronal 5-HT biosynthesis is independent of its gut-derived counterpart.

5-HT is an evolutionarily ancient and phylogenetically conserved biogenic amine (Whitaker-Azmitia, 2001). It appears as though 5-HT emerged very early in the evolutionary process; intriguingly, plants exploit the light-absorbing properties of the indole ring structure of tryptophan to generate 5-HT, known as phytoserotonin, via photosynthesis (Azmitia, 2020). Further, driven by evolutionary selective pressure, the serotonergic system is conserved across different species; 5-HT is found in protozoa (e.g., *Tetrahymena*), metazoa (e.g., *Planarian*, and *Polycelis*), arthropods (e.g., *Homarus*, *Cherax*, and *Drosophila*), bacteria, and mammals (Johnson et al., 2015; Lent, 1985; Sun et al., 2020; Turlejski, 1996). Though the neuropsychological and cognitive functions of 5-HT (e.g., appetite, social behaviour, mood, pain, and sleep) have garnered the most attention in the past, an astonishing number of biological processes mediated by 5-HT, including immune modulation, have recently gained interest.

2.1.1 Enterochromaffin cells

The intestinal epithelium serves as an important interface in translating external environmental cues to host signaling for the regulation of intestinal physiology. Within this epithelium, enteroendocrine cells (EECs), which collectively constitute the largest endocrine tissue in the body, represent approximately 1% of the total epithelial cell population (Rehfeld, 2004). These cells, interspersed throughout the epithelium, are isolated from one another by non-endocrine epithelial cells. EECs are sensory sentinels, responding to a plethora of luminal antigens, including dietary nutrients, non-nutrient chemicals, irritants, food-borne toxins, and microorganisms (Furness et al., 2013; Gunawardene et al., 2011; Zeve et al., 2022). Strategically situated between the luminal environment and the enteric neurons in the mucosa, EECs release a wide array of biologically active molecules, integrating important messages from the gut lumen and, thus, coordinating physiological processes at both local and distant sites (Bellono et al., 2017; Worthington et al., 2018).

Amongst EEC subtypes, enterochromaffin (EC) cells are the most common within the GI epithelium, constituting more than 70% of the EEC population in the proximal colon (Cristina et al., 1978). EC cells are widely distributed throughout the intestine and comprise approximately 0.5% of the total mucosal cells (Lund et al., 2018). EC cells are classical open-type flask-shaped EECs, which display a pyramidal-shaped morphology sporting an apical cytoplasmic protrusion with microvilli that extend towards the gut lumen. The wider base of these cells hosts basal processes that extend towards adjacent epithelial cells (Capella et al., 1995; Lund et al., 2018; Sjölund et al.,

1983).

EC cells are responsible for synthesizing and secreting about 95% of the body's total 5-HT content; a small fraction of 5-HT is also secreted by I cells in the ileum and L cells in the colon (Gershon, 2013; Kendig et al., 2015). Apart from being the major producer of the body's 5-HT, EC cells are chief sentinels that respond to various luminal stimuli (e.g., chemical, mechanical, and microbial-derived metabolites) and express a repertoire of ion channels and surface receptors, including piezo type mechanosensitive ion channel component 2 (PIEZO2) (Alcaino et al., 2018), transient receptor potential cation channel subfamily A member 1 (TRPA1) channels (Bellono et al., 2017; Nozawa et al., 2009), 5-HT receptors (5-HTRs) (Linan-Rico et al., 2016), toll-like receptors (TLRs) (Bogunovic et al., 2007), G protein-coupled bile acid receptor 1 (GPBAR1) (Ward et al., 2013), and receptors for recognizing short-chain fatty acids (SCFAs) and other gut hormones (Lund et al., 2018). Notably, EC cells in the small intestine are devoid of nutrient metabolite sensing receptors (Lund et al., 2018). However, these cells are enriched with high levels of glucagon-like peptide 1 (GLP-1) receptor and, thus, are capable of sensing nutrient metabolites indirectly through a paracrine mechanism involving GLP-1 secreting L cells (Lund et al., 2018). Unlike in the small intestine, EC cells in the colon express various G-protein coupled receptors (GPCRs), which act as sensors for microbial metabolites allowing direct detection of luminal chemical contents (Lund et al., 2018).

2.2 Serotonin synthesis, release, and metabolism

2.2.1 Synthesis

Dietary L-tryptophan (Trp) is an essential amino acid, which serves as an important biosynthetic precursor of numerous compounds, including 5-HT and melatonin (Alkhalaf et al., 2015). Readily available in protein-rich foods including meat, bananas, cheese, chocolate, oats, fish, eggs, and beans, exogenous sources of Trp, often acquired via diet, are crucial to the human body. Approximately 99% of ingested Trp is used for the manufacturing of proteins within the body (Peter et al., 1991). The majority of free Trp then enters the kynurenine (Kyn) pathway, which accounts for approximately 90% of Trp catabolism (Dougherty et al., 2008). Less than 5% of free Trp is directly transformed by intestinal microorganisms into various indoles (e.g., indole-3-acetic acid [IAA], indole-3-carboxaldehyde [I3A], and indole-3-propionic acid [IPA]) which serve as ligands of the aryl hydrocarbon receptor (AhR) (Agus et al., 2018; Dodd et al., 2017; Gao et al., 2018). Only a minor fraction (~3%) of the Trp pool is utilized for peripheral 5-HT synthesis (Hubbard et al., 2015; Richard et al., 2009), while the remaining is involved in the synthesis of 5-HT in the brain (Sandyk, 1992).

EC cells synthesize the majority of the body's 5-HT from Trp by the rate-limiting enzyme, tryptophan hydroxylase (TPH) 1, in response to various stimuli in the gut lumen; a small fraction of 5-HT is also synthesized by T lymphocytes and mast cells (Chen et al., 2015; Kushnir-Sukhov et al., 2007). TPH1 catalyzes the conversion of Trp to the immediate precursor of 5-HT, 5-hydroxytryptophan (5-HTP), which is further decarboxylated to 5-HT by L-amino acid decarboxylase (L-AADC). Once synthesized,

5-HT is packaged into granules and transported by vesicular monoamine transporter 1 (VMAT1), which is stored near both the apical and basal membrane of the EC cell. Secreted 5-HT regulates a wide range of physiological functions, namely motility, secretion, and immune modulation (Mawe et al., 2013). An isoform of TPH, TPH2, regulates 5-HT production in neuronal sources, including enteric neurons (Walther et al., 2003). In contrast with Trp and 5-HTP, 5-HT generated from the peripheral serotonergic system does not reach the brain due to its inability to cross the blood-brain barrier.

2.2.2 Signaling

Upon release, 5-HT acts locally by activating as many as 22 different receptors and subtypes located on enterocytes, enteric neurons, and immune cells and, therefore, mediates several autocrine-paracrine-endocrine functions (Ahern, 2011; Sharkey et al., 2002). 5-HT receptors in mammals are grouped into seven families based on their functional, structural, and signal transduction properties (Hoyer et al., 1994). Apart from the 5-HT type 3 receptor (5-HT3R) family, which consists of ligand-gated ion channels, all other 5-HTR families consist of GPCRs (Hannon et al., 2008). Upon binding to its receptors, 5-HT can initiate either plasma membrane depolarization or G-protein-mediated modifications to the levels of intracellular messengers. In the intestine, 5-HT1R, 5-HT2R, 5-HT3R, 5-HT4R, and 5-HT7R are expressed; each family contains different subtypes that are simultaneously influenced by 5-HT binding (Layunta et al., 2021). Apart from the classical receptor-mediated signaling pathway, it has been shown

that 5-HT is also capable of covalently incorporating itself into different effector proteins, such small guanosine triphosphatases (GTPases) and histones, via transamidation by transglutaminases (TGMs), a post-translational modification (PTM) known as “serotonylation” (Walther et al., 2003).

2.2.3 Metabolism and termination

To prevent any toxic effects from persistent extracellular 5-HT that may otherwise lead to desensitization of receptors on surrounding cells (Chen et al., 1998; Gershon et al., 1962), the bioactivity of 5-HT must be tightly regulated. In this process, two important proteins, namely serotonin reuptake transporter (SERT) and monoamine oxidase (MAO), are necessary to terminate serotonergic signaling. Clearance of extracellular 5-HT begins with active sequestration into adjacent enterocytes from both sides of the membrane by SERT. Subsequently, 5-HT is metabolized into 5-HIAA by MAO_A. The remaining 5-HT can also be sequestered by SERT and stored in platelets, allowing it to be efficiently transported throughout circulation (Mercado et al., 2010). Serving as a pathway by which endocrine functions can be carried out, 5-HT shuttled in this manner can directly act as a hormone on various cell types, including adipocytes, cardiomyocytes, hepatocytes and osteocytes (El-Merahbi et al., 2015). Moreover, platelets lack the ability to synthesize 5-HT due to the absence of TPH1. Though comparatively minor to monoamine oxidation in the intestinal epithelial cells, sequestration in platelets thus contributes to the termination of interstitial 5-HT bioactivity via MAO_B (Sandler et al., 1981). A schematic illustration summarizing 5-

HT synthesis, signaling, and metabolism in the gut is displayed in **Figure 1**.

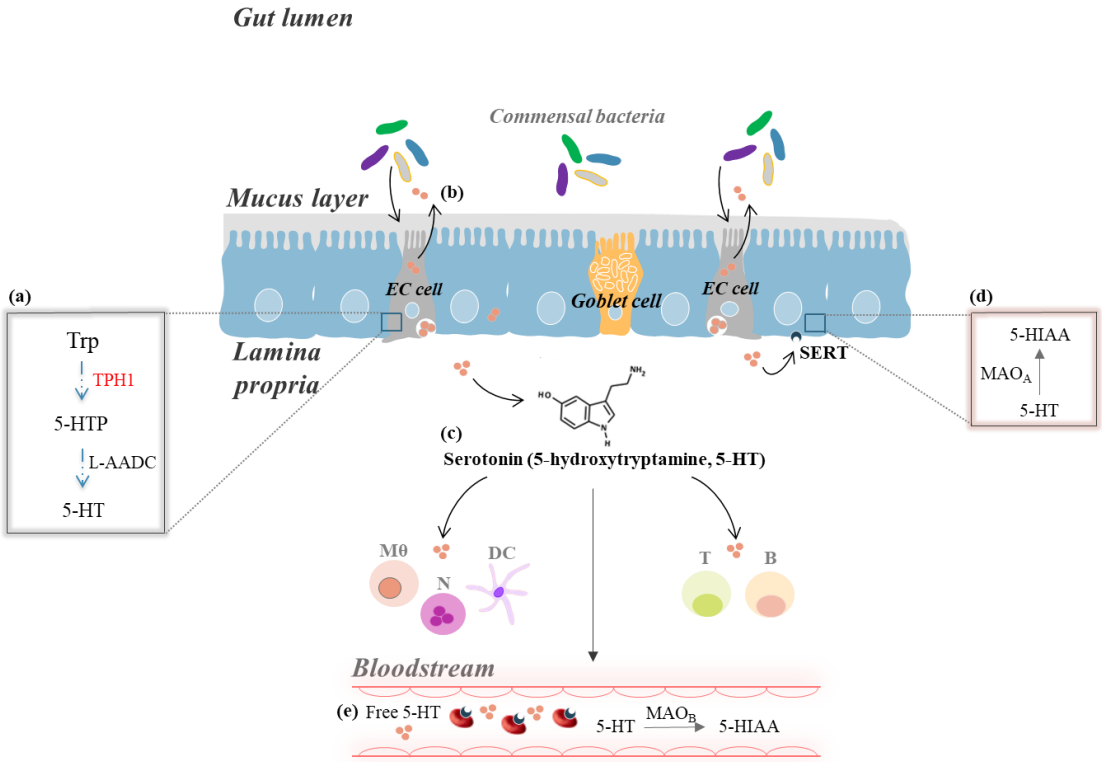
Gut lumen
Commensal bacteria
Mucus layer
(b)
EC cell
Goblet cell
EC cell
(a)
Trp
TPH1
5-HTP
L-AADC
5-HT
Lamina propria
SERT
(d)
5-HIAA
MAO$_A$
5-HT
(c)
Serotonin (5-hydroxytryptamine, 5-HT)
MΘ
DC
N
T
B
Bloodstream
(e) Free 5-HT
5-HT
MAO$_B$
5-HIAA

Figure 1: General overview of 5-HT synthesis, signaling, and metabolism in the gut. (**a**) Enterochromaffin (EC) cells convert dietary tryptophan (Trp) into 5-hydroxytryptophan (5-HTP) via the rate-limiting enzyme, tryptophan hydroxylase 1 (TPH1). 5-HTP is then further converted into 5-hydroxytryptamine (5-HT) or serotonin by L-amino acid decarboxylase (L-AADC). Synthesized 5-HT is rapidly packaged and carried in vesicular monoamine transporter 1 (VMAT1) to both apical and basolateral side of the cell membrane. (**b**) EC cells express various sensory receptors, acting as mechano- and chemo-sensors to continuously release 5-HT in response to stimuli in the gut lumen. Though comparatively minor to the release of 5-HT into the lamina propria, 5-HT is also released into the gut lumen. (**c**) Released 5-HT into the lamina propria activates 5-HT receptors (5-HTRs) on various immune cells and modulates immune responses. Serotonin reuptake transporter (SERT) and monoamine oxidase (MAO) play essential roles in maintaining physiological levels of 5-HT. (**d**) Extracellular 5-HT is actively sequestered by SERT in the surrounding intestinal epithelial cells (IECs), which is then metabolized to 5-hydroxyindoleacetic acid (5-HIAA) via MAO_A in the mitochondria. (**e**) The remaining 5-HT is also actively sequestered by platelets, which is either metabolized by MAO_B, or transported to distant target tissues. Mθ: macrophages; N: neutrophils; DCs: dendritic cells; T: T lymphocytes; B: B lymphocytes.

2.3 Physiological functions of 5-HT

Within EC cells, physicochemical signals are converted into biochemical endocrine signals, which promote the synthesis and release of 5-HT, both apically (to the lumen) and basolaterally (to the bloodstream). Being strategically situated between the gut lumen and nearby enteric neurons, 5-HT released from EC cells regulates various GI processes by stimulating the mucosal surfaces and afferent neurons of the enteric nervous system (ENS). For instance, mechanosensitive ion channels (PIEZO2) convert luminal forces, including postprandial disruptions, into 5-HT release (Alcaino et al., 2018; Bertrand, 2004). Similarly, EC cells can act as nutrient sensors; D-glucose, one of the many chemical signals present during food intake, was able to induce a concentration-dependent increase in 5-HT release from BON cells (a model for human EC cells) (Kim et al., 2001). This finding was further substantiated in colonic EC cells purified from guinea pigs, in which acute exposure to high levels of glucose spurred increased Ca^{2+} influx (Zelkas et al., 2015), a classic trigger of 5-HT secretion in endocrine cells (Chen et al., 2021). In addition, 5-HT plays an essential role as a GI physiological signaling molecule, conveying signals from the gut to the brain via intrinsic or extrinsic neurons. 5-HT regulates motor complexes by influencing the peristaltic reflex and intestinal propulsion (Bülbring et al., 1958; Heredia et al., 2009).

Apart from the well-documented physiological role in GI processes, substantial evidence indicates that 5-HT potently modulates an array of immune responses and inflammatory cascades by binding to specific receptors on the surface of various immune cells in the lamina propria. These immune cells not only express an array of

different 5-HT receptors but also are capable of synthesizing and sequestering 5-HT via TPH1 or SERT, respectively. For instance, mast cells, T cells, and monocytes/macrophages have been shown to express TPH1 (Kushnir-Sukhov et al., 2007; Mössner et al., 1998), while DCs, mast cells, T cells, and macrophages express SERT, allowing the uptake of extracellular 5-HT from the microenvironment (O'Connell et al., 2006). Moreover, it has also been shown that naïve CD4+ T cells predominantly express the 5-HT7R, and activation of CD4+ T cells was enhanced upon 5-HT stimulation *in vitro* (León-Ponte et al., 2007).

Platelet-stored 5-HT is released upon injury and/or inflammatory signals, such as platelet activating factor and complement components, thereby amplifying platelet aggregation and, thus, blood coagulation (Watts et al., 2012). It has also previously been shown that intracellular 5-HT, after being sequestered into platelets by SERT, serves, with the assistance of the endogenous transglutaminase, TG2, as a substrate for the small GTPases, Rab4 and RhoA (Walther et al., 2003). TG2 renders the aforementioned GTPases constitutively active and eventually boosts platelet aggregation (Walther et al., 2003). In addition, post-translational modification of α-actin via serotonylation is necessary for vascular smooth muscle contraction and, ultimately, regulation of vascular tone (Watts et al., 2009). Collectively, these findings suggest that coordination between the immune system and the serotonergic system in the gut mucosa is crucial for sensing environmental cues and prompting host defense, disruption of which may result in various GI disorders, including IBD.

2.4 Serotonin in intestinal inflammation

A growing body of data underpins the crucial impact of the host serotonergic system in the pathophysiology of IBD, in which peripheral 5-HT acts as a prominent regulatory molecule. Many studies emphasize increased peripheral 5-HT signaling in states of intestinal inflammation. Increases in EC cell number and 5-HT content have been observed in patients with IBD (Kidd et al., 2009; Manzella et al., 2020; Shajib et al., 2019) as well as in animal models of colitis induced by DSS, dinitrobenzene sulfonic acid (DNBS), and 2,4,6-trinitrobenzenesulfonic acid (TNBS) (Ghia et al., 2009; Khan et al., 2006; Kwon et al., 2019; MacEachern et al., 2018). Reduction in SERT expression was also observed in both humans and mice suffering from intestinal inflammation (Jørandli et al., 2020; Stavely et al., 2018). In a seminal study, the critical role of gut-derived 5-HT in the pathogenesis of colitis in experimental models of IBD has been unraveled by utilizing *Tph1*$^{-/-}$ mice, which have significantly lower amounts of 5-HT in the gut with intact 5-HT levels in the brain (Ghia et al., 2009). Upon induction of acute DSS colitis, these mice exhibited reduced severity of intestinal inflammation compared to *Tph1*$^{+/+}$ mice. Furthermore, replenishment of 5-HT with 5-HTP, its immediate precursor, intensified colitis severity (Ghia et al., 2009). To further substantiate the role of colonic 5-HT during inflammation, 5-HT synthesis in WT mice was halted by *Tph* inhibitors, *para*-chlorophenylalanine (*p*CPA), or telotristat etiprate (LX1032/LX1606), which delayed the disease onset and reduced the severity of DSS-induced colitis (Ghia et al., 2009; Kim et al., 2015). Similarly, SERT-deficient mice (*SERT*$^{-/-}$), which have augmented bioactivity of 5-HT in the gut lumen and lamina propria, showed enhanced

colitis severity (Bischoff et al., 2009), further supporting the notion that colonic 5-HT signaling contributes to the pathophysiology of colitis.

5-HTRs, as noted previously, are expressed on various immune cells, such as macrophages, neutrophils, DCs, and B and T lymphocytes; the presence or absence of 5-HT can alter their inflammatory potential (Banskota et al., 2019). Intriguingly, it has been previously shown that DCs isolated from *Tph1*$^{-/-}$ mice produced less IL-12p40 than their WT counterparts post-DSS (Li et al., 2011). Co-culture of CD4+ T cells with DCs isolated from DSS-induced *Tph1*$^{-/-}$ mice also led to lower levels of IL-17 and IFN-γ in the culture supernatant (Li et al., 2011), suggesting the essential role of 5-HT in potentiating the pro-inflammatory signals from immune cells during colitis. Supporting these findings, the severity of TNBS-induced colitis, or spontaneous colitis associated with IL-10 deficiency, was found to be increased when combined with the 5-HT-enhancing effects of SERT deficiency (Haub et al., 2010). T lymphocytes are also functionally responsive to 5-HT (Aune et al., 1993). It has been shown that naïve CD4+ T cells expressing 5-HT7 receptors can induce rapid T cell responses upon 5-HT exposure *ex vivo*, a response which was abrogated by the 5-HT7R antagonist, SB-269970 (León-Ponte et al., 2007). The pro-inflammatory effect of 5-HT7R activation is further supported by a previous study showing that pharmacological blockade of this receptor can ameliorate DSS-induced colitis in C57BL/6 mice (Kim et al., 2013). Together, these previous studies highlight 5-HT's role as a pro-inflammatory mediator in the process of inflammation.

2.5 Serotonin and the gut microbiota

2.5.1 Microbial regulation of the host serotonergic system

Predominantly via microbial metabolites, which signal EC cells and prompt host machinery to generate 5-HT via Tph1, gut microbes are essential mediators of host 5-HT biosynthesis (Yano et al., 2015). The key role of the gut microbiota in manufacturing host 5-HT within EC cells is neatly illustrated by a recent study using germ-free (GF) and antibiotic-treated mice, which displayed a substantial reduction in peripheral 5-HT level, a phenomenon which was reversed upon colonization with normal gut microbes (Yano et al., 2015). Microbially-derived metabolites, such as SCFAs (e.g., acetate, butyrate, and propionate) that are generated through the anaerobic bacterial fermentation of various fibres and secondary bile acids (e.g., deoxycholate, cholate, and tyramine) act on EC cells and stimulate 5-HT synthesis via Tph1 in the colon, but not in the small intestine (Reigstad et al., 2015; Yano et al., 2015). Notably, spore-forming microbes from healthy human colonic microbiota increased colonic and blood 5-HT in GF mice, indicating that the serotonergic function of this community is conserved across mice and humans (Wikoff et al., 2009; Yano et al., 2015). While bacterial toxins, including cholera toxin and *Escherichia coli* lipopolysaccharide (LPS), have been shown to stimulate 5-HT release from EC cells (Bellono et al., 2017; Turvill et al., 2000), enteropathogenic *E. coli* (EPEC) can inhibit SERT expression and activity on IECs (Esmaili et al., 2009), illustrating the myriad effects of gut microbes on the serotonergic system.

As mentioned previously, EC cells express a wide array of surface receptors, including TLRs (e.g., TLR1, TLR2, and TLR4) (Bogunovic et al., 2007). Recently, several studies have shown that 5-HT biosynthesis from EC cells is dependent on the activation of TLR2. TLR2 activation decreases SERT expression and activity, while high levels of 5-HT yield a negative feedback effect on TLR2 expression (Latorre et al., 2016). In parallel, mice deficient in TLR2 show a reduction in colonic 5-HT levels and *Tph1* mRNA expression, and activation of TLR2 in nonhematopoietic cells (likely IECs), which were responsible for 5-HT production in the gut (Wang et al., 2019). These findings are supported by a previous observation that the outer membrane protein (Amuc_1100) of *Akkermansia muciniphila* promoted 5-HT biosynthesis via TLR2 signaling (Wang et al., 2021). Collectively, these data provide strong evidence that the gut microbiota can interact with the host to alter Tph1 expression and regulate 5-HT production.

With the discovery of analogous kynurenine pathways in microbes (Colabroy et al., 2005; Vujkovic-Cvijin et al., 2013) as well as the ability of *E. coli* and *Corynebacterium glutamicum* to produce Trp (Niu et al., 2019), microbes can also contribute to regulation of the host serotonergic system. Several bacteria, including *Bacteroides thetaiotaomicron* and *Bifidobacterium dentium*, have been shown to promote 5-HT synthesis by restoring EC cell networks through the effects of SCFAs (e.g., acetate and propionate) (Engevik et al., 2019; Modasia et al., 2020). *Clostridium ramosum* promotes 5-HT synthesis in the colon by programming the differentiation of intestinal stem cell progenitors towards a secretory 5-HT-producing lineage (Mandić et

al., 2019). Additionally, intragastric administration of *B. pseudolongum* has been shown to reduce colonic 5-HT levels by diminishing EC cell numbers, whereas *Lactobacillus rhamnosus* GG supernatants upregulate SERT expression in the colon (Cao et al., 2018; Tatsuoka et al., 2022). Furthermore, there is evidence that some bacteria (e.g., *E. coli*, *Klebsiella pneumoniae*, and *L. plantarum*) can directly metabolize Trp for *de novo* 5-HT biosynthesis (Chudzik et al., 2021) and, akin to this, some *Staphylococci* express the staphylococcal AADC (SadA) gene that is responsible for converting 5-HTP to 5-HT (Luqman et al., 2018).

2.5.2 Host serotonergic regulation of microbes

Apart from the direct influence of gut microbiota in promoting 5-HT synthesis within EC cells, there are relatively few studies on the inverse effects of the host serotonergic system on bacteria. It has been shown that mice lacking Tph1 harbour altered levels of fecal SCFAs and show distinct gut microbial composition compared to WT mice (Kwon et al., 2019). It has also been demonstrated that exposure to high levels of 5-HT can significantly inhibit the growth of many gut-residing bacteria, namely *B. thetaiotaomicron*, *Enterococcus faecalis*, *E. coli*, and *Ruminococcus gnavus.* Notably, *in vitro* exposure to 5-HT inhibited the growth of *A. muciniphila* in a concentration-dependent manner (Kwon et al., 2019). In parallel, *SERT*$^{-/-}$ mice showed a substantial reduction in the abundance of *A. muciniphila* compared to WT mice (Singhal et al., 2019). These findings are of particular interest as *A. muciniphila* is known to mediate protective effects in the development of DSS-induced colitis via its extracellular

vesicles (Chelakkot et al., 2018; Kang et al., 2013) and promote the intestinal barrier integrity (Alam et al., 2016; Everard et al., 2013), suggesting that certain bacteria in the gut communicate with the host serotonergic system for optimal colonization.

Recent evidence has also helped further clarify the direct influence of elevating intestinal 5-HT levels on gut microbes. For instance, *Turicibacter sanguinis* expresses a neurotransmitter sodium symporter-related protein with sequence and structural homology to mammalian SERT (Fung et al., 2019). In this way, *T. sanguinis* imports 5-HT through a mechanism which is inhibited by the selective serotonin reuptake inhibitor (SSRI), fluoxetine (Fung et al., 2019). Likewise, SERT deficiency increases fecal 5-HT levels and enriches *Turicibacter* in $SERT^{+/-}$ mice compared with WT mice (Fung et al., 2019).

Bacterial virulence and invasive properties are influenced not only by local environmental factors, such as pH changes and nutrient availability, but also by host signals (Freestone, 2013). 5-HT has previously been shown to induce the invasion of commensal *E. coli* (BW25113) without altering the virulence of the bacteria due to loss of host tolerance to the bacteria through impairment of the intestinal epithelial barrier (Banskota et al., 2017). Additionally, amines secreted from the noradrenergic and dopaminergic nerve terminals within the gut mucosa have also been shown to induce adhesion of enterohemorrhagic *E. coli* (EHEC) on the colonic surface by altering the virulence (Bansal et al., 2007; Chen et al., 2003). In contrast, a recent study showed that 5-HT can decrease virulence gene expression by EHEC and *Citrobacter rodentium* (a

murine model of EHEC) via the histidine sensor kinase CpxA that serves as a bacterial 5-HT receptor (Kumar et al., 2020).

5-HT can also indirectly influence the abundance of microbial species via quorum sensing (QS). QS is a cell-to-cell communication mechanism in which individual bacteria carry out colony-wide functions, including biofilm formation and virulence factor expression (Pena et al., 2019). QS bacteria respond to changes in cell density in the external environment and produce hormone-like molecules (called autoinducers), which allow bacteria to either compete or cooperate with other species (Surette et al., 1999). Previously, it has been demonstrated that high levels of 5-HT activate the *las* QS system and enhance the virulence of the opportunistic bacteria, *Pseudomonas aeruginosa* (Knecht et al., 2016), indicating that at least some bacteria utilize host molecules (i.e., social cheating) to enhance their QS networks. Utilization of another organism's molecules by bacteria to socialize with other species within their communities may be attributed to the conserved prosocial functions of serotonergic signaling across evolution (Edsinger et al., 2018; Kiser et al., 2012). Collectively, these findings, and those noted in the above section, support the emerging concept that bidirectional signaling pathways exists between the host serotonergic system and the gut microbiota, the disturbance of which can lead to disease states.

2.6 Microbes, intestinal inflammation, and serotonin

Considering the impact of the gut microbiota in the production of 5-HT within host EC cells, the 5-HT-microbiota axis has a potential role in the pathogenesis of

colitis. Recently, it was shown that higher mucosal 5-HT levels select for more colitogenic gut microbiota composition and increase susceptibility to DSS-induced colitis. Specifically, the severity of DSS-induced colitis in GF mice after colonization with the microbiota from *Tph1*$^{-/-}$ mice was reduced compared to GF mice colonized with WT microbiota (Kwon et al., 2019). These findings were paired with lower abundances of *Akkermansia*, disruption of intestinal epithelial barrier permeability as well as inhibition of the production of the antimicrobial peptides, β-defensins (Kwon et al., 2019).

Additionally, increased Tph1 and reduced SERT expression were also reported in inflamed colonic tissues from patients with IBD compared to both non-inflamed colonic tissues from patients with IBD and healthy controls (Shajib et al., 2019). A significant increase in both plasma and serum 5-HT levels were also reported in patients with IBD (Manzella et al., 2020; Shajib et al., 2019). Further, a recent study showed that the autophagic process is disrupted in inflamed colonic tissues of CD patients, which was associated with elevated plasma 5-HT levels compared to healthy controls (Haq et al., 2021). These previous findings showing high 5-HT content in patients with IBD could be explained by recent clinical findings that patients with IBD exhibited lower serum and fecal Trp levels than healthy controls, which were significantly correlated with increased C-reactive protein (Lamas et al., 2016; Nikolaus et al., 2017). The lower levels of Trp in the gut lumen were further associated with microbial dysbiosis, which is strongly linked with IBD (Lamas et al., 2016; Nikolaus et al., 2017). Trp, which can be shunted to the Kyn pathway or, to a lesser extent, the serotonergic

pathway, has a complex relationship with inflammation in its role as a precursor. In contrast to the pro-inflammatory role of the 5-HT pathway during intestinal inflammation, the role of kynurenine is still relatively controversial. The current consensus is that activation of the Kyn pathway, mediated by indoleamine 2,3-dioxygenase (IDO) 1, appears to exert immunoregulatory effects by providing homeostatic balance between immunity and tolerance (Acovic et al., 2018; Ciorba, 2013). Identifying factors influencing the gut microbiota and the metabolism of Trp (particularly when angled towards the serotonergic pathway) and, thus, its influence on 5-HT synthesis within EC cells is of great interest. Taken together, these findings provide strong evidence that alterations in Trp metabolism and the serotonergic system may have an active role, not only in influencing the microbial composition of the gut, but also in the pathogenesis of colitis.

3.1 Food additives and intestinal inflammation

Over the past few decades, human exposure to foods supplemented with various additives, due to shifts in food quality, has increased. These additives are routinely introduced during the manufacturing processes of countless dietary products. Generally, there are two types of food additives: those that are essential for food preservation and others with a more cosmetic role. Concerns about the impact of food additives on human health are becoming increasingly global. While initial research focused largely on adverse reproductive effects following exposure to endocrine-disrupting chemicals (Kumar et al., 2020), there is growing interest in examining the

impact of myriad food additives on intestinal inflammation. Further, these highly prevalent food additives are often underappreciated as potentially harmful dietary components in the Western diet, despite having been shown to evoke gut microbiome reconfiguration, promote overgrowth of microorganisms and adversely impact host immunity (Christ et al., 2019; Devkota et al., 2012; Martinez-Medina et al., 2014).

Recent studies substantiate that the exacerbated inflammatory response, which can be initiated by chemicals in the diet, is maintained by loss of gut epithelial integrity, increased permeability, and impaired mucin production. For instance, dietary emulsifiers (carboxymethylcellulose [CMC] or polysorbate-80 [P-80]), promote colitis by altering the gut microbiota and increasing the pro-inflammatory potential in both mice and humans (Chassaing et al., 2015; Chassaing et al., 2017; Naimi et al., 2021). The effect of these emulsifiers was found to be mediated by the gut microbiota, as GF mice did not develop colitis (Chassaing et al., 2015). Food thickeners, such as carrageenan and maltodextrin, have also been shown to adversely affect the intestinal epithelial barrier and inflammation. Carrageenan, an extract of red seaweed, is commonly found in infant formula, soymilk, dairy products, and processed meats. In human colonic epithelial cells, carrageenan has been shown to induce the activation of NF-κB and IL-8 secretion, thus inducing inflammation (Borthakur et al., 2007). In addition, maltodextrin, a polysaccharide polymer, has been shown to promote mucus depletion and suppress antimicrobial defense mechanisms by inducing ER stress in the intestine (Laudisi et al., 2019). The above evidence thus reinforces the growing interest that food additives can have impacts on human health.

3.2 Synthetic colourants

It has become increasingly apparent that the Western diet, characterized by an energy-dense meal that includes ultra-processed foods (e.g., ready meals, breakfast cereals, confectionery, snacks, and condiments), and low intakes of fibres, has permeated the modern lifestyle of a substantial proportion of the population. The Western lifestyle are causally linked to the leading health problems (e.g., obesity, type II diabetes, cardiovascular disease, and IBD) in Westernized nations (Christ et al., 2019; Rizzello et al., 2019).

Notably, the Western diet increases 5-HT synthesis in rats (Bertrand et al., 2011). Colourants, especially rich in the Western diet, are often added to foods and beverages during processing to improve the sensory attributes of the final products and do not have nutritional value. The use of synthetic colourants (or azo dyes) in dietary products has dramatically increased during the past few decades (Vojdani et al., 2015), leading to significant human exposure. There are currently nine certified colourants approved for usage by the US Food and Drug Administration (FDA) and Health Canada. Approximately 0.7 million tons of azo dyes are produced each year, and there are now more than 3000 recognized azo dyes that are used across the food, cosmetic, and pharmaceutical industries (Feng et al., 2012). A previous report showed beverages contained a wide range of concentrations from 5 to 200 ppm (1.2 mg/240 mL to 48 mg/240 mL) (Committee, 1968), which was consistent with a recent report where the range was found to be 0.2 to 52.3 mg/240 mL in commonly consumed beverages (Stevens et al., 2014). In a similar vein, when the amounts of synthetic colourants in

commonly consumed foods and sweets were measured, it was found that children, on average, consumed 100 mg to 200 mg per day of synthetic dyes (Stevens et al., 2015). Despite their important role in the food industry, an increasing body of literature has revealed that exposure to synthetic colourants could pose a serious threat to human health (Claus et al., 2016; Feng et al., 2012; Platzek et al., 1999).

Although microsomal and cytosolic reductases of the liver and extra-hepatic tissues can reduce a variety of chemicals including synthetic colourants, the gut microbiota plays a major role in metabolizing these dyes (Feng et al., 2012). Azo dyes contain one or more azo bonds and are typically not absorbed in small intestine but are metabolized by resident colonic bacteria, producing colourless aromatic amines which are potentially harmful to the host. For instance, Tartrazine Yellow (TY), one of the most popular and commercially available synthetic colourants, is metabolized into sulfanilic acid (SA) by intestinal bacteria. SA has a similar moiety to hapten and is presumed to bind proteins in the colonic mucosa, which elicits immune responses in the TNBS-induced colitis model (Shoda et al., 2000). Oral administration of TY at 25 mg/ml per day for 12 days prior to the induction of colitis increased acute ulcer development and delayed mucosal healing in rats (Shoda et al., 2000), illustrating that TY promotes hapten-induced intestinal immune responses.

Allura Red AC (AR), also known as FD&C Red No. 40 or E129, is one of the most widely used synthetic colourant, with more than 2 million kg of annual production worldwide (Sharma et al., 2011). It is a synthetic coal tar and water-soluble mono-azo red dye derived from petroleum aromatic hydrocarbons, which is readily metabolized

by gut microbial azoreductases (Amchova et al., 2015; Rafii et al., 1997). Currently, the acceptable daily intake (ADI) of AR in humans is a maximum of 7 mg/kg of body weight per day, while the median lethal dose (LD_{50}) for AR is defined as >2,000 mg/kg of body weight in mice (Sasaki et al., 2002). The maximum allowance of AR in food products is currently 300 ppm, as defined by Health Canada (Ivusic Polic, 2018). In an assessment survey conducted in Italy, the amount of AR in various red-coloured beverages ranged from 10.9 mg/L in a red soft drink up to 55.9 mg/L in a red juice-based product. Extrapolating from this, the exposure assessment estimated a weighted average daily intake of AR from 6.5 to 25.0 mg/day, and from 13.9 to 33.0 mg/day, from juice-based and soft drinks, respectively (Fallico et al., 2011). In a later study assessing the daily consumption of artificial dye-containing foods, adults were found to be exposed to colour dyes 0.76 ± 0.15 times per day while children had 2.43 ± 0.35 exposures per day (one exposure was defined as any food item, beverage, medicine, gum, or candy containing one or more artificial colours) (Bell, 2013). In this study, AR was found to be the most frequently consumed dyes in both adults and children (Bell, 2013). High levels of Allura Red AC can also be found in baked food products, up to 1,240 mg/kg; a single serving of a 100 g cupcake may contain as much as 124 mg of the dye, suggesting that the potential concentration of the dye could reach as high as 10 mM in the adult intestine (Zou et al., 2020). This projection suggests that, although the amount of AR may be below physiologically relevant concentrations, dye consumption through select food products may reach high intestinal concentrations and accumulation over time may be a point of concern.

AR is considered toxic if consumed in excessive amounts (Brown et al., 1993) and has the potential to cause behavioural effects, including increased hyperactivity in children (McCann et al., 2007). Particularly, AR exerts pro-inflammatory effects, which promotes oxidative stress by increasing the production of reactive oxygen species (ROS) and enhances cyclooxygenase-2 (COX-2) expression in the rat liver and kidney (Khayyat et al., 2018). Moreover, AR induces leukocyte-endothelial cell adhesion by producing leukotriene B_4 (LTB_4) from blood neutrophils (Leo et al., 2018). Despite these pro-inflammatory effects and its high prevalence in the Western diet, very limited work has been performed exploring the impact that AR exposure has on the GI system and, further, the impact these dyes may have on immune dysfunction in the gut.

Thesis hypothesis and objectives

Synthetic colourants are small molecules, which can circumvent the host immune system and activate inflammatory cascades (Vojdani et al., 2015). Substantial increases in the use of synthetic colourants over the past 50 years (Vojdani et al., 2015), exaggerated cellular pro-inflammatory responses (Leo et al., 2018) and the induction of histopathological aberrations by these dyes (Khayyat et al., 2018) suggest synthetic colourants may have a potential role in the pathogenesis of colitis. Given that microbes, with the presence of azoreductases, are capable of metabolizing azo dyes in the gut lumen (Feng et al., 2012) and some of these dyes modulate 5-HT content (Bawazir, 2016), the exploration of whether there is any interplay among AR, 5-HT, and the gut microbiota in influencing susceptibility to colitis is sorely needed. It is thus *hypothesized* that the synthetic colourant, Allura Red AC, enhances susceptibility to colitis.

Research objectives

1. To explore the effect of Allura Red AC exposure on the development of colitis
2. To elucidate whether colonic 5-HT is essential for enhancing susceptibility to colitis by Allura Red AC exposure
3. To investigate whether Allura Red AC exposure alters the susceptibility to colitis by modulating the gut microbiota composition

—CHAPTER 2—

MATERIALS AND METHODS

Mice: C57BL/6N (Taconic Biosciences, Hudson, NY), C57BL/6J (Jackson laboratory, Bar Harbor, ME), *Rag1*$^{-/-}$ (Jackson laboratory, Bar Harbor, ME). Germ-free (GF) mice on the C57BL/6 background were derived and maintained under gnotobiotic conditions in the Axenic/Gnotobiotic Unit at McMaster University. Breeding pairs of *Tph1*$^{-/-}$ and *Tph1*$^{+/+}$ mice were obtained from CNRS, Paris, France, and were kept and bred under SPF conditions. Male and female mice aged 8-12 weeks were used in most of the experiments. All mice were kept in sterilized, ventilated cages under specific pathogen-free (SPF) conditions. All mice were housed in sterilized, ventilated cages, fed irradiated normal chow food (18% protein rodent diet; Teklad Global Diets, Madison, WI, USA), and sterile water at a temperature of 21–22°C, and with 12:12 hour light/dark cycle in SPF rooms of McMaster University Central Animal Facility. All mice were acclimatized for at least 7 days prior to the start of any experiments. All experiments were approved by the McMaster University animal ethics committee and conducted under the Canadian guidelines for animal research.

Allura Red AC: For diet experiments using Allura Red AC, custom diet TD.190960, irradiated normal chow diet coated with Allura Red AC (0.1 g/kg), was purchased from Teklad. For water experiments using Allura Red AC (0.01% w/v or 0.1 mg/ml), Allura red AC was purchased from Toronto Research Chemical. Intake of food or water containing Allura Red AC was simply measured as the difference in weight or volume between the food or water into the cage and that remaining at the end of every week.

DSS-induced colitis: Dextran sulfate sodium (DSS) (molecular weight 40 kDa; ICN, Biomedicals Incorporate, Solon, OH) was added to drinking water for a final concentration of 2.0% and 3.5% w/v for a total of 7 days. All experiments were carried out in accordance with the McMaster University animal utilization protocols and with approval from the McMaster University Animal Care Committee and McMaster Animal Research Ethics Board. All experiments were also conducted under the Canadian guidelines for animal research. Samples from all mice were kept at −80 °C before analysis.

$CD4^+CD45RB^{high}$ T cell-induced colitis: Colitis was induced in *Rag1*$^{-/-}$ mice (Jackson) by adoptive transfer of fluorescent activated cell sorting (FACS)-sorted $CD4^+CD45RB^{hi}$ T cells. Briefly, $CD4^+$ T cells were isolated from splenocytes of naïve C57BL/6J mice (Jackson) by EasySep^{TM} Mouse Naïve CD4+ T cell Isolation Kit (STEMCELL Technologies, Vancouver, Canada). Naïve CD4+ T cells were labelled with PE-cy7-conjugated anti-mouse CD3 (1:100) (BioLegend, San Diego, CA), APC-conjugated anti-mouse CD4 (1:100) (BD Biosciences, San Jose, CA), and FITC-conjugated anti-mouse CD45 (1:100) (BD Biosciences). $CD4^+CD45RB^{high}$ T cells were sorted using FACS Aria II flow cytometer (BD Biosciences). Cell viability was assessed using Trypan blue assay prior to injection. Recipients were intraperitoneally (i.p.) injected with approximately 5 x 10^5 cells of sorted T cells per mouse, while control *Rag1*$^{-/-}$ mice received vehicle (phosphate buffer saline, [PBS]). Samples from all mice were kept at −80 °C before analysis.

Assessment of colitis severity: Disease activity index (DAI) is a combined score of weight loss, stool consistency, and fecal bleeding, and was blindly assessed using a previously published scoring system (Kim et al., 2012). This scoring system was defined as follows: weight loss: 0 = no loss, 1 = 1–5%, 2 = 5–10%, 3 = 10–20%, 4 = 20%+; stool: 0 = normal, 2 = loose stool, 4 = diarrhea; and bleeding: 0 = no blood, 2 = Hemoccult positive (Hemoccult II; Beckman Coulter, Fullerton, CA), and 4 = gross blood (blood around anus). DAI was measured starting from day 0 of DSS treatment in C57BL/6N and *Tph1*$^{-/-}$ mice or starting from day 0 post-reconstitution with CD4^{+}CD45RB^{high} T cells in *Rag1*$^{-/-}$ mice. Macroscopic damage scores were blindly scored using a previously published scoring system for DSS-induced colitis (Kim et al., 2012). Briefly, the severity of colitis is macroscopically scored based on shortening of colonic length, colonic bleeding, fecal bleeding, loosening of stool consistency, and signs of rectal bleeding.

Histology and immunohistochemistry: Approximately 1 cm of colonic tissues (mid colon) were washed with PBS, fixed in 10% buffered formalin for 24 hours, washed with 70% ethanol twice, and embedded in paraffin. Hematoxylin and eosin (H&E)-stained colonic tissue sections are scored using a previously published system for the following measures: crypt architecture (normal, 0 - severe crypt distortion with loss of entire crypts, 3), degree of inflammatory cell infiltration (normal, 0 - dense inflammatory infiltrate, 3), muscle thickening (base of crypt sits on the muscularis mucosae, 0 - marked muscle thickening present, 3), goblet cell depletion (absent, 0-

present, 1) and crypt abscess (absent, 0- present, 1) (Kim et al., 2012). The histological damage score is the sum of each individual score. Formalin-fixed, paraffin-embedded sections of the mid colon were stained with periodic acid-Schiff (PAS) to detect colonic goblet cells. The number of PAS-positive cells per 10 crypts was counted in 4 different areas for each section. If the section was in poor condition (<25% damaged), one of the four sections was counted on the opposite side. If >25% of section is damaged, the section was not counted. Investigators were blinded to the study groups. All images of H&E and PAS staining were captured using a Nikon Eclipse 80i microscope and NIS-Elements Basic Research imaging software.

Cecal microbiota transfer: Cecal contents from each group of SPF C57BL/6 mice were pooled (equally weighed) and GF C57BL/6 mice were orally inoculated with 200 µl (diluted in warm PBS) for 3 days with a single dose each day.

Measurement of myeloperoxidase level: Colonic myeloperoxidase (MPO) levels were measured following a published protocol (Kim et al., 2012). Briefly, approximately 1 cm of colonic tissues (mid-distal colon) were weighed after removing any visible feces or fat. Hexadecyltrimethylammonium bromide (HTAB) buffer was added according to tissue weight. If tissue weight is less than 25 mg, add the buffer at a ratio of 12.5 mg/ml; if tissue weight is between 25 mg and 50 mg, add at a ratio of 25 mg/ml. Tissues in ice-cold 50 mmol/l potassium phosphate buffer containing 0.5% hexadecyl trimethyl ammonium bromide (Sigma-Aldrich, St. Louis, MO) were then

homogenized a Mixer Mill (MM 400, Retsch, Inc., Newtown, PA) at 30 frequency (1/s) for 4 minutes. Homogenates were centrifuged at 13,400 × g for 6 minutes and the supernatant was removed. Each sample (7 µl) was then added to a 96-well plate, and 200 µl of solution containing potassium phosphate buffer, *O*-dianisidine (Sigma), and hydrogen peroxide was added in each well. The absorbance was measured at 450 nm by a spectrophotometer (model EL808, Winooski, VT). MPO levels were expressed in units per milligram of wet tissue, where 1 U is the quantity of the enzyme able to convert 1 µmol hydrogen peroxide to water in 1 minute at room temperature.

BON cell culture: BON cells (human carcinoid cell line derived from a metastasis of a pancreatic carcinoid tumor of EC cell origin; also known as a widely used model of human EC cell) were maintained in Dulbecco modified Eagle medium (DMEM)/F12 (1:1) with 10% (v/v) heat-inactivated fetal bovine serum (FBS), and penicillin/streptomycin (complete growth medium) at 37 °C in a humidified 5% COs_2 atmosphere. Briefly, cells were seeded at 10^5 cells/ml in 24-well plates and incubated for 24 hours at 37°C in the complete growth medium. The medium was replaced with serum-free media (complete growth medium without FBS) prior to treatment. Cells were treated for 24 hours at three different concentrations (1 pmol/l, 1 nmol/l, 1 µmol/l) of: Allura Red AC (Toronto Research Chemicals), Brilliant Blue (Toronto Research Chemicals), Cresidine sulfonic acid (Toronto Research Chemicals), Sunset Yellow (Toronto Research Chemicals), and Tartrazine Yellow (Toronto Research Chemicals). In separate experiments, BON cells were treated with triptolide, an inhibitor for NF-κB,

(20 nmol/l, Tocris Biosciences, Burlington, Canada), TNF-α (10 ng/ml, Peprotech, Princeton, NJ) or the medium alone. Following the treatments, the cell supernatants and RNA were collected and stored at −80 ℃ for further analysis. Intracellular ROS production detected by 2',7'-dichlorofluorescein diacetate (DCF-DA) fluorescence as previously described (Regmi et al., 2014). Briefly, cells were treated with Allura Red AC (1 µmol/l), CS (1 µmol/l), or 5-HT (10 µmol/l) for 24 hours, followed by DCF-DA treatment at a final concentration of 10 µmol/l at 37 ℃ for 30 min. The cells were washed twice with warm PBS and then imaged using a Nikon Eclipse 80i microscope.

HT-29 cell culture: Human colonic adenocarcinoma HT-29 cells (ATCC HTB-38) were maintained in DMEM/F12 (1:1) with 10% (v/v) heat-inactivated FBS, supplemented with Minimum Essential Medium (MEM) and HEPES (4-(2-hydroxyethyl)-1-piperazineethanesulfonic acid) buffer at pH 7.5 as well as penicillin/streptomycin (complete growth medium) at 37 ℃ in a humidified 5% CO_2 atmosphere. HT-29 cells were seeded in 24-well culture plates at a density of 10^5 cells/ml. Cells were allowed to attach overnight, which were then replenished with the serum-free media (complete growth medium without FBS). Cells were stimulated for 24 hours with Allura Red AC (1 µmol/l), indole-3-carboxyaldehyde (I3A) (50 or 500 µmol/l, Sigma-Aldrich), TNF-α (10 ng/ml) or the medium alone. For Allura Red AC treatment, cells were pre-treated for 1 hour with TNF-α (10 ng/ml). Following the treatments, the cell supernatants was collected and stored at −80 ℃ for further analysis.

RAW264.7 cell culture: The murine macrophage RAW264.7 cells were maintained in DMEM/F12 (1:1) with 10% (v/v) heat-inactivated FBS, and penicillin/streptomycin at 37 °C in a humidified 5% CO_2 atmosphere. Briefly, cells were seeded at 10^5 cells/ml in 24-well plates and incubated for 24 hours at 37 °C in the complete growth medium. The medium was replaced with serum-free media (complete medium minus FBS) prior to treatment. Cells were treated for 24 hours with Allura Red AC at 1 pmol/l, 1 nmol/l, and 1 µmol/l, or the medium alone. Following the treatments, the cell supernatants was collected and stored at −80 °C for further analysis.

Measurement of cell viability with PrestoBlue: Cell viability was measured in BON cells using resazurin (PrestoBlue, Life Technologies/Thermo Fisher Scientific). Cells were seeded onto a 96-well plate at a concentration of 50,000 cells per well and then treated with Allura Red AC at three different concentrations: 1 pmol/l, 1 nmol/l, and 1 µmol/l. Following treatment with Allura Red AC for different time points (1, 3, 6, and 24 hours), PrestoBlue reagent was added to each well at 10% of total well volume and incubated for 4 hours in a tissue culture incubator maintained at 37 °C with 5% CO_2 atmosphere. TNF-α (1 µg/ml) was used as a positive control. Each sample was run in triplicate on a 96-well plate. Fluorescence intensity was measured using a multi-well plate reader (SpectraMax M5 plate reader).

Generation of mouse colon organoids and maintenance: Murine colonoids were isolated as previously described (Crowley et al., 2020; Sato et al., 2009). Briefly, whole

colon was washed with cold PBS and fats were removed. Colon was then cut longitudinally (or butterfly) to remove feces and washed on a new petri dish with cold PBS. Colon was gently scraped off to remove villi, mucus, and other debris using a forceps. Next, colon was vortexed 10 times for 8 seconds with ice-cold advanced DMEM/F12 with replacing the medium to new medium after each wash. After the last wash, colon was placed in 5 ml of cell recovery solution (Cat #: 354253; Corning, Corning, NY) on a petri dish at 4 ℃ for 1 hour. After incubation, colon was gently washed with the solution and centrifuged twice at 1500 rpm for 5 minutes, followed by being diluted in Matrigel (Corning). After the Matrigel was solidified, organoid media (10 ml of base media: Advanced DMEM/F12, supplemented with penicillin/streptomycin [100 U/ml], GlutaMAX [100X], and HEPES [0.01 mol/l]) with 10 ml of 50% WRN supplemented with N2 (100X) (Invitrogen, Burlington, Canada), B27 (Invitrogen), N-acetylcystine (1 mmol/l) (Sigma-Aldrich), nicotinamide (Sigma-Aldrich), mouse epidermal growth factor (mEGF; 50 ng/ml) (Invitrogen), A83-01 (500 nmol/l) (Tocris Biosciences), SB-202190 (10 µmol/l) (Sigma-Aldrich), Y-27632 (10 µmol/l) (Abmole Biosciences, Houston, TX) were added prior to incubation at 37 ℃ with 5% CO_2 atmosphere. The medium in each well was changed every 3 days. During this time, the complete medium did not contain Y-27632. The colonoids were passaged every 7 days. Upon each passage, Y-27632 (10 µmol/l) (Abmole Biosciences) was added.

Determination of organoid cell death by counting: Organoids were counted before treatment at the budding stage after 2–3 days of culture. A minimum of 25 crypts in each quadrant (a total of 4 quadrants) were counted and macroscopically defined as viable or dead by their morphological appearance (bright or dark lumen, respectively) in the bright-field microscope. Organoids were then treated for 24 hours with or without Allura Red AC (1 μmol/l), followed by pre-treatment for 1 hour with or without TNF-α (10 ng/ml) in triplicates. Finally, the organoids were counted and scored as viable or dead. The percentage of disruption was calculated as % $viable_{after}$–% $viable_{before}$.

Colonoid-derived monolayer seeding and stimulation: Monolayers derived from colonoids were generated as previously described (Crowley et al., 2020). Briefly, the growth media was removed, and Matrigel domes were mechanically disrupted with gentle pipetting through a p200 pipette tip. Disrupted colonoids in each well were then resuspended in 150 μl TrypLE express (Gibco, Mississauga, Canada) and incubated at 37 °C with 5% CO_2 for 7.5 minutes. Colonoids were then rapidly disrupted into single cell suspensions with gentle pipetting through a p1000 tip, and an equal volume of monolayer media (base media supplemented with 50% WRN, N2 (Invitrogen), B27 (Invitrogen), mEGF (Invitrogen)) and Y-27632 (Abmole) was added. The concentrations of these supplements are the same as generating mouse colonic organoids. Cells were centrifuged at 1,500 rpm for 5 minutes, then resuspended in monolayer media and added dropwise to Geltrex (Gibco) coated coverslips in 12-well plates. Coverslips were coated with Geltrex and maintained at 37 °C with 5% CO_2

atmosphere for 24-48 hours prior to mechanical disruption of Matrigel domes. Monolayers were incubated at 37 °C with 5% CO_2 and the medium in each well was changed to the monolayer medium without Y-27362 the next day. After 5 days of culture, monolayers were pre-treated for 1 hour with or without TNF-α (10 ng/ml), followed by 24 hours with or without Allura Red AC (1 μmol/l).

Quantitative real-time polymerase chain reaction: Colonic tissues (approximately 1 cm of the mid colon), mouse colonic monolayer derived from colonoids, or cell lysates from cell lines were processed with Trizol reagent (Invitrogen, Burlington, Canada) using a Mixer Mill (MM 400, Retsch, Inc., Newtown, PA) at 30 frequency (1/s) for 5 min. Total RNA was quantified using a NanoDrop One/OneC Microvolume UV-Vis Spectrophotometer (Thermo Fisher Scientific, Mississauga, Canada). RNA purity was assessed by the ratio of absorbance at 260/280 nm, and only samples with a ratio of ~ 2.0 for RNA were considered. cDNA was prepared from 1 μg of total RNA using iScript cDNA Synthesis Kit (Bio-Rad Laboratories, Mississauga, Canada). Relative quantification of real-time polymerase chain reaction (RT-qPCR) was performed using SsoFast EvaGreen Supermix (Bio-Rad Laboratories) with the primers at a concentration of 10 μmol/l. Both human and mouse 18S were used as an internal standard. Data were analyzed according to the $2^{-\Delta\Delta CT}$ method and expressed as relative abundances (mean ± S.D. or S.E.M.). Primer sequences used in this thesis are listed in **Table S1** and **S2**.

Enzyme-Linked Immunosorbent Assay (ELISA): Colonic tissue 5-HT levels were measured by using commercially available enzyme-linked immunosorbent assay (ELISA) kits (Cat. # IM1749; Beckman Coulter, Fullerton, CA). Briefly, approximately 1 cm of colonic tissues (mid colon) were weighed, and each of the colonic sections was homogenized in 500 µl of 0.2 N perchloric acid. After centrifugation at 10,000 × g for 5 minutes, the supernatants were collected, and the pH was neutralized by adding 500 µl of 1 mol/l borate buffer. 5-HT content was expressed as a function of tissue weight (ng/mg). For measurement of 5-HT level in BON cells and mouse colonic organoids, as well as for measurement of cytokines in HT-29 and RAW264.7 cells, the culture supernatants were collected and directly assessed using the kit according to the manufacturer's instruction. For cytokines measurement in colonic tissues, 50 µl of protease inhibitor cocktail (PIC; Cat. # P8340; Sigma-Aldrich) was added to 15 ml of Tris-buffered saline. Approximately 1 cm of colonic tissues (mid colon) were homogenized in 500 µl of Tris-buffered saline containing PIC. Samples were centrifuged for 5 minutes at 3,300 × g, and the resulting supernatants were frozen at –80^{o}C before analysis. Total protein levels were quantified in the colonic homogenates by using DC Protein Assay Kit (Cat. # 5000111; Bio-Rad Laboratories). Cytokine levels (IL-1β, Cat. # SMLB00C; IL-6, Cat. # SM6000B; IL-8, Cat. # D8000C; IFN-γ, Cat. # MIF00; and TNF-α, Cat. # MTA00B) were assessed according to the manufacturer's instructions (Quantikine Murine; R&D Systems, Minneapolis, MN).

Western Blot: Total protein of tissue homogenates or cell lysates was extracted using radioimmunoprecipitation assay (RIPA) buffer containing a 1× PIC. Protein concentration of homogenized colonic tissues was determined by using DC Protein Assay Kit (Bio-Rad Laboratories). Equal amounts of protein homogenates were loaded and electrophoresed onto sodium dodecyl sulfate (SDS)–polyacrylamide gel electrophoresis and transferred to a polyvinylidene difluoride (PVDF) membrane. Membranes were blocked with 5% bovine serum albumin (BSA) in 1× tris-buffered saline tween 20 (TBST) for 1 hour at room temperature and incubated with 6 ml of primary antibodies against E-cadherin (1:1000) (Cat # 24E10; Cell Signaling Technology, Danvers, MA), $pMLC^{Ser19}$ (1:1000) (Cat # 3671; Cell Signaling Technology), total MLC (1:1000) (Cat # 3672; Cell Signaling Technology), ZO-1 (1:1000) (Cat # 40-2200; Thermo Fisher Scientific), and AhR (1:1000) (Cat # sc-133088; Santa Cruz Biotechnology) for overnight at 4 °C. Membranes were washed, incubated with 6 ml of either anti-rabbit horseradish peroxidase–linked antibody (1:5000, Cat. # 7074; Cell Signaling Technology) or anti-mouse horseradish peroxidase–linked antibody (1:5000, Cat. # 7076; Cell Signaling Technology) for 1 hour at room temperature. Proteins were visualized by use of SuperSignal West Femto Maximum Sensitivity Substrate (Thermo Fisher Scientific). β-actin (1:5000) (Cat # 4970; Cell Signaling Technology) or Lamin B1 (1:1000) (Cat # ab65986, Abcam, Cambridge, United Kingdom) was used as a loading control. All primary and secondary antibodies were diluted in 1× TBS. Densitometric analysis was performed on Western

blots with ImageJ software (version 1.48), normalized to total MLC, β-actin, or Lamin B1.

Immunofluorescence Staining: For colonic tissue immunostaining, coverslips were deparaffinized at 60 °C for 1 hour in xylenes using three changes for 5 minutes each, followed by washing through graded alcohols: wash in 100% ethanol twice for 10 minutes each, and 95% ethanol twice for 10 minutes each. Coverslips were then washed with distilled H_2O and blocked with few drops (sufficient to cover coverslips) of 0.01% Triton X-100 and 0.05% Tween 20 for 1 hour. Next, coverslips were stained with anti-mouse 5-HT antibody (1:100; Cat. # ab16007, Abcam) overnight at 4°C, followed by secondary antibody staining with Alexa Fluor-568 goat anti-mouse IgG (H+L) (1:1000) (Life Technologies A-11031) for 2 hours at room temperature. Coverslips were then washed with cold PBS three times and mounted using ProLong Gold Antifade reagent containing 4′,6-diamidino-2-phenylindole (DAPI) (Molecular Probes, Invitrogen) for DNA staining. The number of 5-HT positive cells per 10 crypts was counted in 4 different areas for each section. If the section was in poor condition (<25% damaged), one of the four sections was counted on the opposite side. If >25% of section is damaged, the section was not counted. For colonic organoids-derived monolayer staining, the monolayers grown on coverslips in 6-well plates were fixed with 4% PFA, followed by blocking for 1 hour with 2% BSA in PBS, 0.01% Triton X-100 and 0.05% Tween 20. Monolayers were stained with anti-rabbit ZO-1 antibody (1:100; Cat. # 40-2200, Thermo Fisher Scientific), followed by secondary antibody staining with Alexca

Fluor-488 donkey anti-rabbit IgG (H+L) (1:1000) (Life Technologies, A-21206) for 2 hours at room temperature. Coverslips were then washed with PBS three times and mounted using ProLong Gold Antifade reagent containing DAPI (Molecular Probes, Invitrogen) for DNA staining. Images were captured using a Nikon Eclipse 80i microscope and NIS-Elements Basic Research imaging software. Investigator was blinded to the study groups.

Bioinformatics and 16s rRNA Sequencing: Luminal contents from cecal samples were stored at -80°C. DNA was extracted and the 16s rRNA variable 3 (v3) and v4 gene region was amplified as previously described with minor modifications (Stearns et al., 2015; Szamosi et al., 2020). Samples were thawed to room temperature. Approximately 0.2-0.3 g of sample was added to 800 µl of 200 mmol/l $NaPO_4$ (pH 8), and 100 µl of guanidine thiocyanate-ethylenediaminetetraacetic acid (EDTA)–Sarkosyl along with 0.2 g of 0.1 mm glass beads (Mo Bio, Carlsbad, CA). Mechanical lysis was carried out in a Powerlyzer (Mo-Bio) at 3,000 rpm for 3 minutes. Enzymatic lysis was performed using 50 µl lysozyme (100 mg/ml), 10 µl RNase A (10 mg/ml), and incubation at 37 °C for 90 minutes. Next, 25 µl 25% SDS, 25 µl proteinase K, and 62.5 µl 5 mol/l sodium chloride were added to the sample and incubated at 65°C for 90 minutes. Following, samples were pelleted at 13,500 × g for 5 minutes by centrifugation and the supernatant was recovered. Genomic DNA was purified using a MagMAX (Thermo Fisher Scientific) as per manufacturer's instructions. The 16S rRNA v3 and v4 gene region was amplified in triplicate using 341F and 806R 16S rRNA primers modified for the

Illumina platform with adaptors containing 6-base pair unique barcodes to the reverse primer. Each sample reaction mixture contained 5 pmol of each primer, 200 μmol/l of each deoxynucleoside triphosphate (dNTP), 1.5 mmol/l magnesium chloride, and 1U *Taq* polymerase (Life Technologies, Carlsbad, CA). The PCR protocol consisted of an initial denaturation step at 95 °C for 5 minutes, 30 cycles, each step for 30 seconds, of 95 °C, 50 °C, and 72 °C, and a final extension step at 72 °C for 7 minutes. Amplification of the v3 and v4 gene region was verified by electrophoresis on a 2% agarose gel. Amplicons were then sequenced (2 x 300 paired end) using the Illumina MiSeq platform. Resulting paired-end sequences from Illumina sequencing were processed using DADA2 pipeline (Callahan et al., 2016). Cutadapt was used to filter and trim adapter sequences and PCR primers from the raw reads with a minimum quality score of 30 and a minimum read length of 100bp (Martin, 2011). Sequence variants were then resolved from the trimmed raw reads using DADA2, an accurate sample inference pipeline from 16s amplicon data (Callahan et al., 2016). DNA sequence reads were filtered and trimmed based on the quality of the reads for each Illumina run separately, error rates were learned, and sequence variants were determined by DADA2. Sequence variant tables were merged to combine all information from separate Illumina runs. Bimeras were removed and taxonomy was assigned using the SILVA database version 1.2.8. Analysis was conducted using the phyloseq (McMurdie et al., 2013) on R and using Graph Pad Prism version 5.0 (Graphpad Software, La Jolla, CA). The significance was based on the phylum and genus level, not ASV. The table was filtered to remove taxa whose mean abundance was 10 or less, samples with sampling depth

<2500, and those reads not assigned to bacteria or archaea. After filtering, the minimal number of reads per sample was 29,926, and the samples were rarified to 20,000 reads.

Statistical analysis: All data are presented as mean or mean ± S.D. or S.E.M. Where appropriate, unpaired Student's *t* test, one-way ANOVA, or two-way ANOVA. Multiple comparisons were performed by Bonferroni's test, Dunnett's test, or Mann-Whitney U test, where appropriate, using GraphPad Prism version 5.0 (GraphPad Software). $P < 0.05$ was considered statistically significant.

Table S1. RT-qPCR Mouse Primers

	Forward (5'-3')	Reverse (5'-3')
18S	GTAACCCGTTGAACCCCATT	CCATCCAATCGGTAGTAGCG
Defb3	GGATCCATTACCTTCTGTTTGC	ATTTGAGGAAAGGAACTCCAC
Il22	TGTCCGGCTCATCGGGGAGA	ACAGCAGGTCCAGTTCCCCA
Mlck	GCGTGATCAGCCTGTTCTTTCTAA	GCCCCATCTGCCCTTCTTTGACC
Muc2	CTGACCAAGAGCGAACACAA	CATGACTGGAAGCAACTGGA
Ocln	ATGTCCGGCCGATGCTCTCTC	CTTTGGCTGCTCTTGGGTCTGTAT
Pparg	CTGCTCAAGTATGGTGTCCATGA	ATGAGGACTCCATCTTTATTCA
Reg3γ	CCGTGCCTATGGCTCCTATTG	GCACAGACACAAGATGTCCTG
Tjp1	ACCCGAAACTGCTGCTGTGGATAG	AAATGGCGGGCAGAACTTGTGTA

Table S2. RT-qPCR Human Primers

	Forward (5'-3')	**Reverse (5'-3')**
18S	TCCACAGGAGGCCTACACGCC	TTTCCGCCGCCCATCGATGTT
CYP1A1	GGTCAAGGAGCACTACAAAACC	TGGACATTGGCGTTCTCAT
CYP1B1	CACTGACATCTTCGGCG	ACCTGATCCAATTCTGCCTG
MLCK	AGGCCAAGGACTTTGTTTCC	TTCAGCCACTCGTGTTTCAG
TPH1	TGCCCTTGCTAAGTTCAGCAGGA	AGCAAGAGATGGCCCAGACCTCC

—CHAPTER 3—

RESULTS

3.1 *Synthetic food colourants promote 5-HT synthesis in BON cells*

To explore whether highly common synthetic food colourants, such as AR, BB, SY, and TY, are stimuli for 5-HT biosynthesis, BON cells were used. Despite its pancreatic origin (Siddique et al., 2009), the BON cell line, which produces and secretes 5-HT (Tran et al., 2004) is the most widely used *in vitro* model of human EC cell. BON cells were treated with colourants for 24 hours at three different concentrations (1 pM, 1 nM, and 1 µM). Sodium butyrate (NaB, 1 mM) was used as a positive control for 5-HT secretion in BON cells, which has been shown to promote 5-HT biosynthesis via TPH1 (Reigstad et al., 2015). All colourants tested significantly promoted 5-HT biosynthesis (**Figure 2a**), where AR showed the most pronounced effect in inducing 5-HT secretion at the lowest 1 pM amongst dyes tested. To determine if the colourant-induced 5-HT production in BON cells is caused by stimulation of TPH1 expression, *TPH1* mRNA expression was assessed using qRT-PCR. Treatment with these colourants in BON cells resulted in significant upregulation of *TPH1* mRNA expression levels (**Figure 2b**). To further determine the lowest effective dosage of AR in 5-HT production and TPH1 expression, BON cells were treated for 24 hours with AR at 1 fM. AR at this concentration was not able to induce 5-HT and *TPH1* mRNA expression (data not shown).

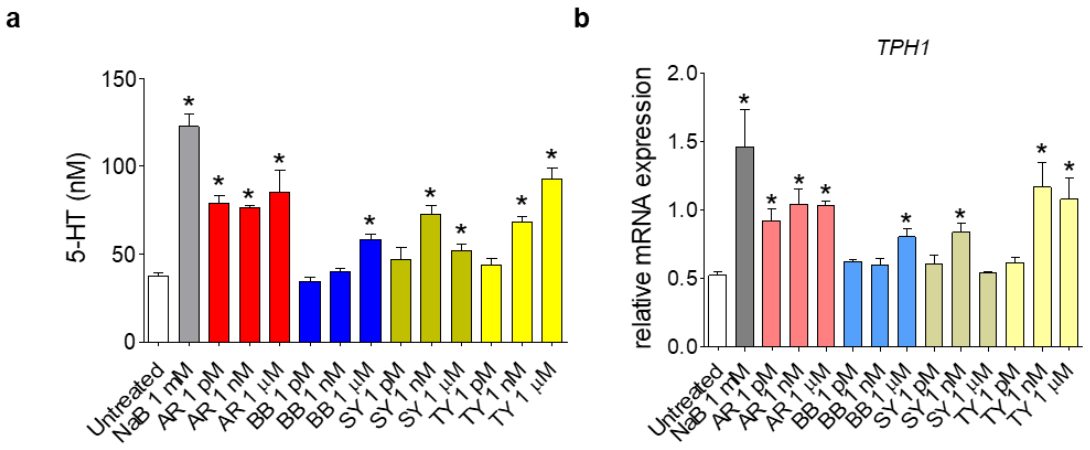

Figure 2: Synthetic colourants promote 5-HT secretion and induce *TPH1* mRNA expression in BON cells. BON cells were treated for 24 hours with synthetic colourants at three different concentrations (1 pM, 1 nM, and 1 µM). (**a**) 5-HT levels in the culture supernatant, and (**b**) *TPH1* mRNA expression. Sodium butyrate (NaB; 1 mM) was used as positive control. Values are the mean ± S.E.M. from three independent experiments. Statistical significance was measured using one-way ANOVA with Dunnett's test. **P* <0.05, compared to untreated cells.

Given that synthetic colourants are metabolized by microbial azoreductases (Zahran et al., 2019) and AR showed a pronounced increase in 5-HT levels in comparison to other synthetic dyes, the effect of AR metabolite, CS, in 5-HT biosynthesis was investigated. BON cells were treated for 24 hours with CS at three different concentrations (1 pM, 1 nM, and 1 µM). CS did not have any effects on both 5-HT secretion and *TPH1* mRNA expression (**Figure 3**).

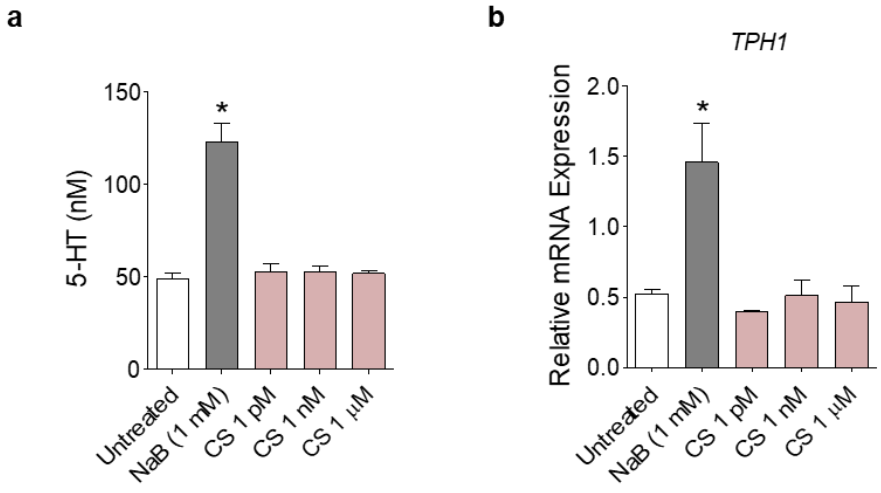

Figure 3: *p*-Cresidinesulfonic acid does not promote 5-HT secretion and induce *TPH1* mRNA expression in BON cells. BON cells were treated for 24 hours with *p*-Cresidinesulfonic acid (CS) at three different concentrations (1 pM, 1 nM, and 1 µM). (**a**) 5-HT levels in the culture supernatant, and (**b**) *TPH1* mRNA expression. Sodium butyrate (NaB; 1 mM) was used as positive control. Values are the mean ± S.E.M. from three independent experiments. Statistical significance was measured using one-way ANOVA with Dunnett's test. **P* <0.05, compared to untreated cells.

Since AR was able to promote 5-HT secretion at 1 pM, but at increasing concentrations of 1 nM and 1 µM, no relative increases in 5-HT levels were detected (**Figure 2a**), it was investigated whether these effects were due to any inherent cytotoxicity of AR using PrestoBlue assay. BON cells were treated with three different concentrations (1 pM, 1 nM, and 1 µM), and cell viability was determined at four different time points (1, 3, 6 and 24 h). TNF-α (1 µg/ml) was used as a positive control in this experiment. BON cells treated with AR at these three different concentrations did not show any reduction in cell viability compared to untreated cells, while TNF-α (1 µg/ml) treatment for 24 hours led to significant inhibition of cell viability (**Figure 4**). However, the possibility of any inherent cytotoxicity with increasing concentrations of AR (beyond 1 µM) cannot excluded. Together, these data indicate that AR but not CS, promote 5-HT synthesis and increase *TPH1* mRNA expression level *in vitro*.

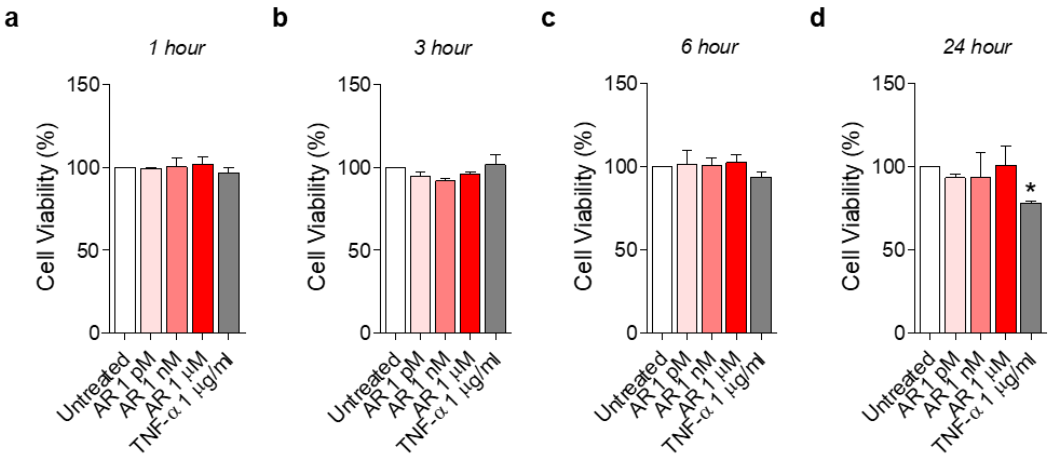

Figure 4: Effect of Allura Red AC on the viability of BON cells. BON cells were treated with Allura Red AC (AR) at three different concentrations (1 pM, 1 nM, and 1 µM), and cell viability was measured by PrestoBlue assay at 1 h (**a**), 3 h (**b**), 6 h (**c**), and 24 h (**d**). TNF-α (1 µg/ml) was used as a control for decreased cell viability. Values are the mean ± S.E.M. from three independent experiments. Statistical significance was measured using one-way ANOVA with Dunnett's test. **P* <0.05, compared to untreated cells.

3.2 *Allura Red AC induces IL-8 secretion and downregulates E-cadherin in HT-29 cells*

To elucidate whether AR increases inflammation, HT-29 cells were used. These cells are a human colorectal adenocarcinoma cell line with epithelial morphology. HT-29 cells were pre-treated for 1 hour with the pro-inflammatory cytokine, TNF-α (10 ng/ml), prior to treatment for 24 hours with three different concentrations of AR (1 pM, 1 nM, and 1 μM). Levels of IL-8 were assessed as an ideal readout candidate. IL-8 is known as a neutrophil chemotactic factor that induces migration of immune cells to the site of inflammation and is also elevated in colonic tissues of patients with IBD (Mitsuyama et al., 1994). Another unique functional characteristic of IL-8 is that it is produced early in the inflammatory response yet remains active for a prolonged period from days to weeks (DeForge et al., 1992). When HT-29 cells were treated with only AR, IL-8 was not induced. Upon pre-treatment for 1 hour with TNF-α, AR potently induced IL-8 secretion starting from 1 nM, but a significant increase was observed at 1 μM (**Figure 5a**). In contrast, the AR metabolite, CS, did not induce IL-8 secretion even when HT-29 cells were pre-treated for 1 hour with TNF-α (**Figure 5b**).

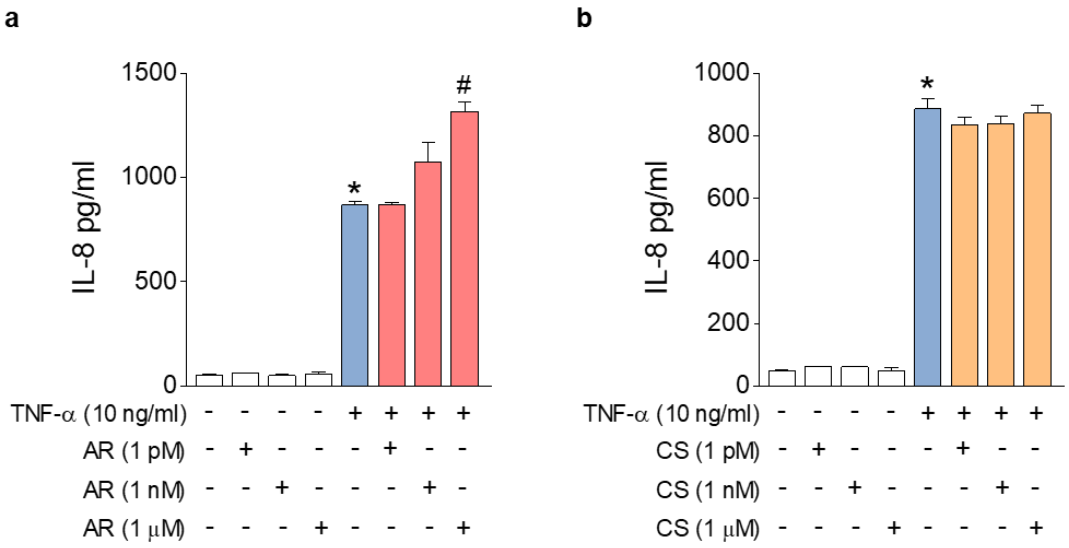

Figure 5: Allura Red AC, but not its metabolite *p*-Cresidinesulfonic acid, promotes IL-8 secretion in TNF-α-induced HT-29 cells. HT-29 cells were treated for 24 hours with Allura Red AC (AR) or *p*-Cresidinesulfonic acid (CS) with or without TNF-α pre-treatment for 1 hour. IL-8 levels from the cell culture supernatants were detected by ELISA. (**a**) IL-8 levels with AR, and (**b**) IL-8 levels with CS. Values are the mean ± S.E.M. from three independent experiments. Statistical significance was measured using Student's t-test or one-way ANOVA with Dunnett's test. **P* <0.05, compared to untreated cells. $^{\#}P$ <0.05, compared to TNF-α.

E-cadherin is a major component of adherens junctions, the impaired expression of which has been linked to pathological processes including IBD. When HT-29 cells were treated for 24 hours with AR (1 μM), there was no difference in E-cadherin expression. However, when cells were pre-treated for 1 hour with TNF-α (10 ng/ml), AR decreased E-cadherin expression (**Figure 6**).

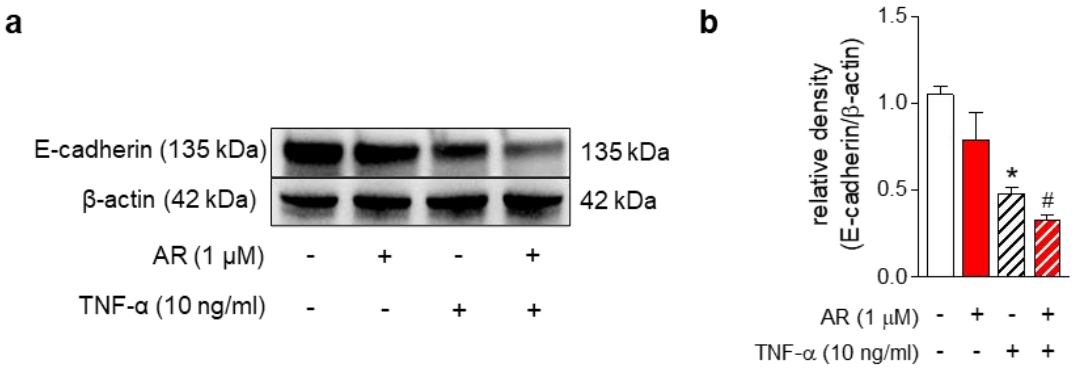

Figure 6: Allura Red AC decreases E-cadherin expression in TNF-α-induced HT-29 cells. HT-29 cells were treated for 24 hours with Allura Red AC (AR) with or without TNF-α pre-treatment for 1 hour. Proteins were extracted from HT-29 cells, and western blot was performed to detect E-cadherin level. (**a**) Representative western blot analyses of E-cadherin, and β-actin. (**b**) Relative densitometry (E-cadherin/β-actin). Values are the mean ± S.E.M. from three independent experiments. Statistical significance was measured using Student's t-test. $^{*}P$ <0.05, compared to untreated cells. $^{\#}P$ <0.05, compared to TNF-α.

3.3 *Allura Red AC potently increases the production of IL-1β, IL-6, and TNF-α in LPS-induced RAW264.7 macrophages*

To further investigate the effect of AR in inducing inflammation, a commonly used model of mouse macrophages, RAW264.7, was used. These cells were pre-treated for 1 hour with LPS (1 µg/ml), followed by 24 hours of treatment with AR (1 pM, 1 nM, and 1 µM). AR potently increased the production of pro-inflammatory cytokines, such as IL-1β (**Figure 7a**), IL-6 (**Figure 7b**), and TNF-α (**Figure 7c**), in LPS-induced RAW264.7 cells.

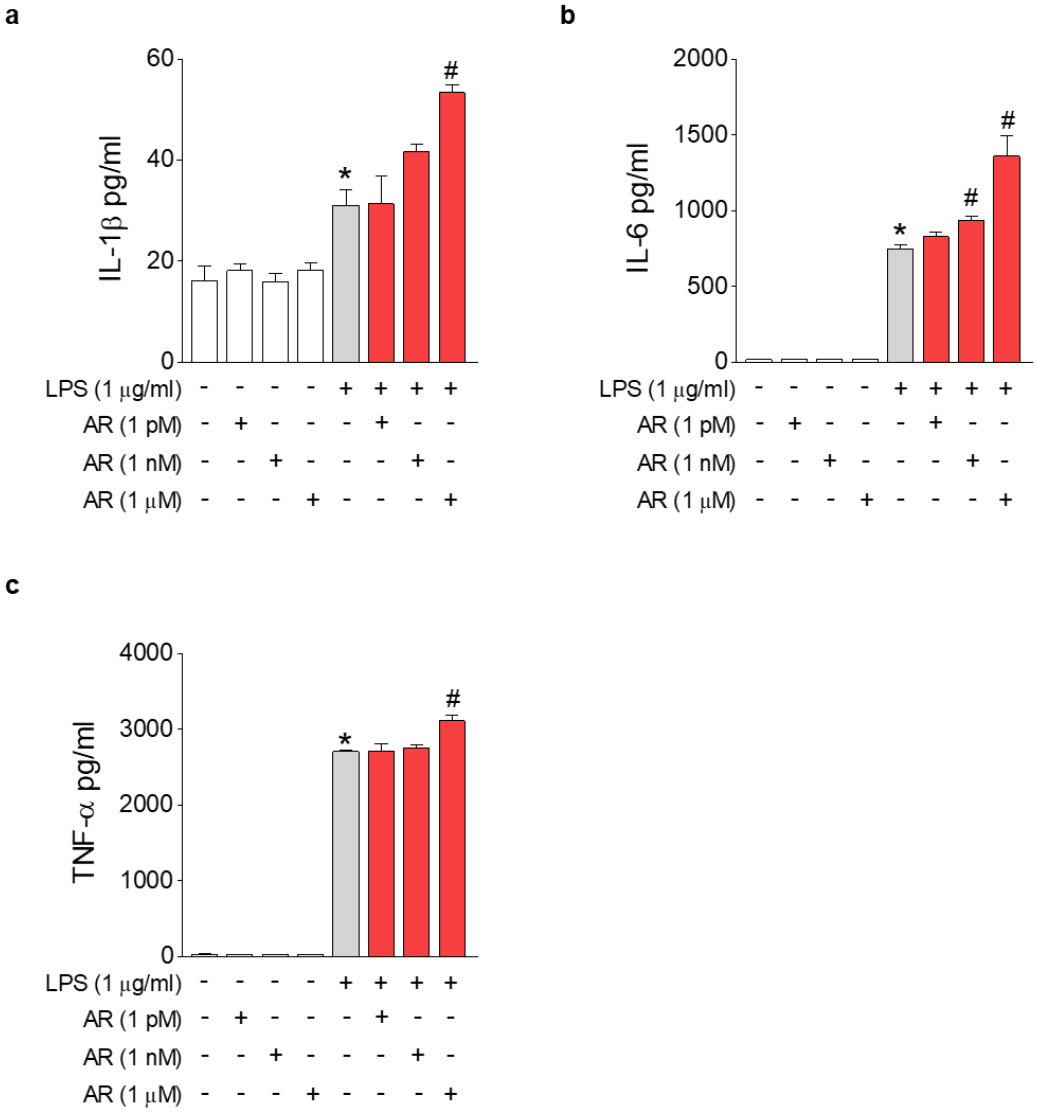
a
IL-1β pg/ml
60
40
20
0
*
#
LPS (1 μg/ml) - - - - + + + +
AR (1 pM) - + - - - + - -
AR (1 nM) - - + - - - + -
AR (1 μM) - - - + - - - +
b
IL-6 pg/ml
2000
1500
1000
500
0
*
#
#
LPS (1 μg/ml) - - - - + + + +
AR (1 pM) - + - - - + - -
AR (1 nM) - - + - - - + -
AR (1 μM) - - - + - - - +
c
TNF-α pg/ml
4000
3000
2000
1000
0
*
#
LPS (1 μg/ml) - - - - + + + +
AR (1 pM) - + - - - + - -
AR (1 nM) - - + - - - + -
AR (1 μM) - - - + - - - +

Figure. 7: Allura Red AC potently increases the production of IL-1β, IL-6, and TNF-α in LPS-induced RAW264.7 murine macrophages. RAW264.7 murine macrophages were treated for 24 hours with Allura Red AC (AR) at three different concentrations (1 pM, 1 nM, and 1 μM) with or without LPS pre-treatment for 1 hour. Cytokines from the cell culture supernatants were detected by ELISA. (**a**) IL-1β, (**b**) IL-6, and (**c**) TNF-α. Values are the mean ± S.E.M. from three independent experiments. Statistical significance was measured using Student's t-test or one-way ANOVA with Dunnett's test. **P* <0.05, compared to untreated cells. $^{\#}P$ <0.05, compared to LPS.

3.4 *Allura Red AC exacerbates DSS-induced colitis in C57BL/6 mice*

US FDA defined ADI for AR in humans is 7 mg/kg of body weight per day. Using the calculation published previously (Suez et al., 2014) as a benchmark, the formula to calculate the dosage for AR was: ADI (7 mg/kg of body weight per day) times average mouse weight (0.03 kg), divided by average daily liquid intake (2 mL). This calculation led to dosing of 0.1 mg/ml (0.01% w/v or 100 ppm) in normal drinking water or 0.1 g/kg of the red dye in normal chow diet.

To test if the effects of AR on cultured cells also occurred *in vivo*, the impact of the colourant on colitis development in mice was assessed using DSS. Briefly, naïve C57BL/6 mice were exposed to AR via normal chow diet for 12 weeks. During this period, no significant difference in the food intake was observed between the two groups during the 12-week diet intervention (**Figure 8**).

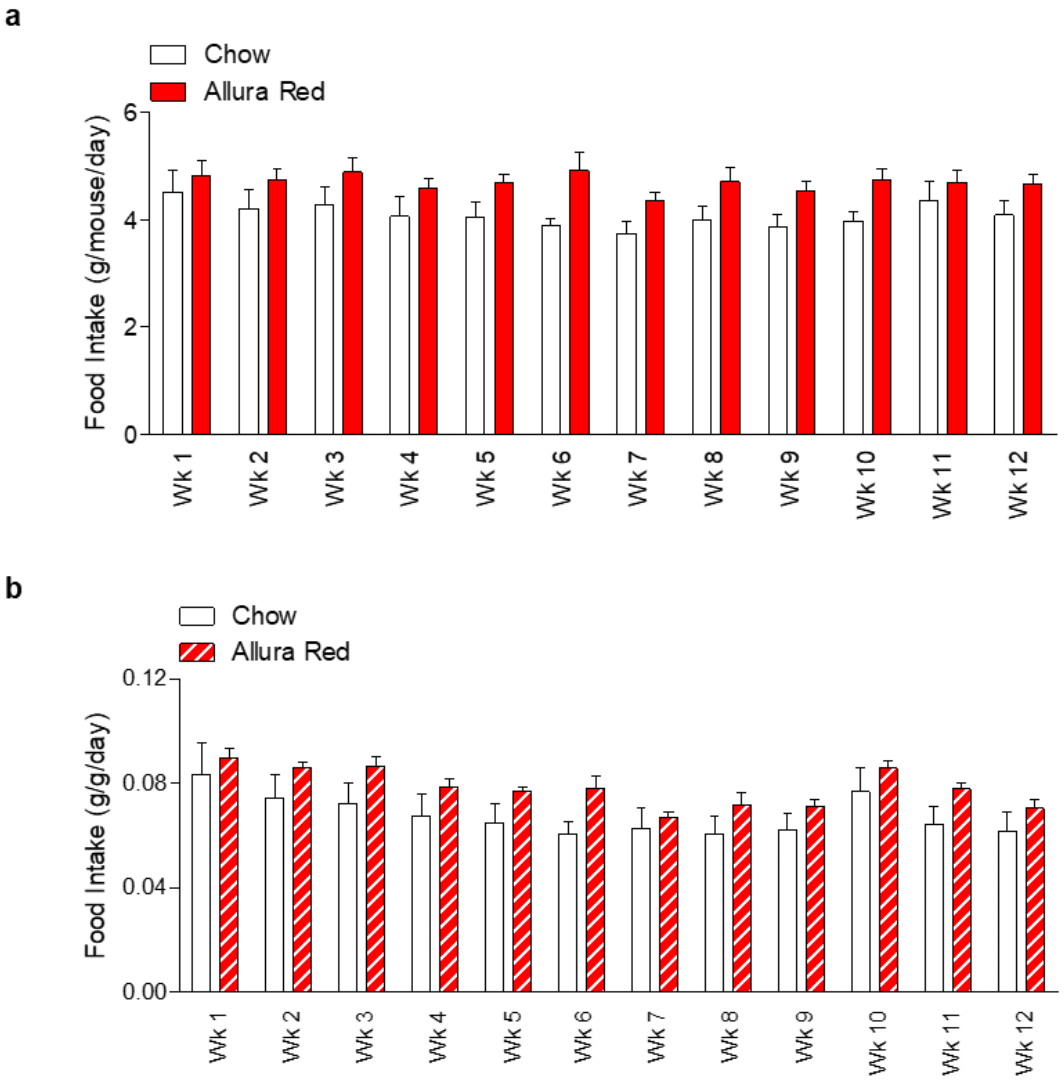

Figure 8: Measurement of food consumption in naïve C57BL/6 mice fed normal chow diet or exposed to Allura Red AC via normal chow diet for 12 weeks. (**a**) Food intake represented in g per mouse per day. (**b**) Food intake is represented in g per g of mouse per day. Values represent mean ± S.E.M. from 9 to 13 mice per group.

After 12 weeks of AR exposure, mice were subjected to acute colitis with 3.5% DSS for 7 days in the drinking water (**Figure 9a**). It should be noted that mice exposed to AR, without DSS treatment, showed body weight loss at 13 weeks. DSS treatment itself further induced a substantial weight loss in mice fed normal chow diet compared to their non-DSS counterpart (**Figure 9b**). Compared with DSS-treated mice, DSS-treated mice exposed to AR showed an elevated cumulative disease activity index (DAI) (**Figure 9c**) which was accompanied by higher macroscopic scoring (**Figure 9d**), a reduction in colonic length (**Figure 9, e** and **f**) and increased colonic weight (**Figure 9g**). Histological scores (**Figure 9, h** and **i**), and colonic MPO levels (**Figure 9j**) were also higher in DSS-treated mice exposed to AR, compared with DSS-treated counterparts. In addition, AR exposure potently increased levels of pro-inflammatory cytokines, such as IL-1β, IL-6, and TNF-α, in mice on day 7 post-DSS (**Figure 9, k-m**). Intestinal epithelial barrier function was impaired by DSS. Interestingly, a significant decrease in *Muc2* mRNA expression was observed in mice exposed to AR without DSS compared to control mice (**Figure 9n**). Higher colonic 5-HT levels in the non-DSS group of mice exposed to AR were observed, and colonic 5-HT levels were potently increased on day 7 post-DSS in mice exposed to AR compared with DSS-treated counterparts (**Figure 9o**). Similar observations were made when C57BL/6 mice were exposed to AR via normal drinking water (0.01% w/v or 0.1 mg/ml) (**Figure 10** and **11**). Together, these data indicate that AR exacerbates DSS-induced colitis in C57BL/6 mice.

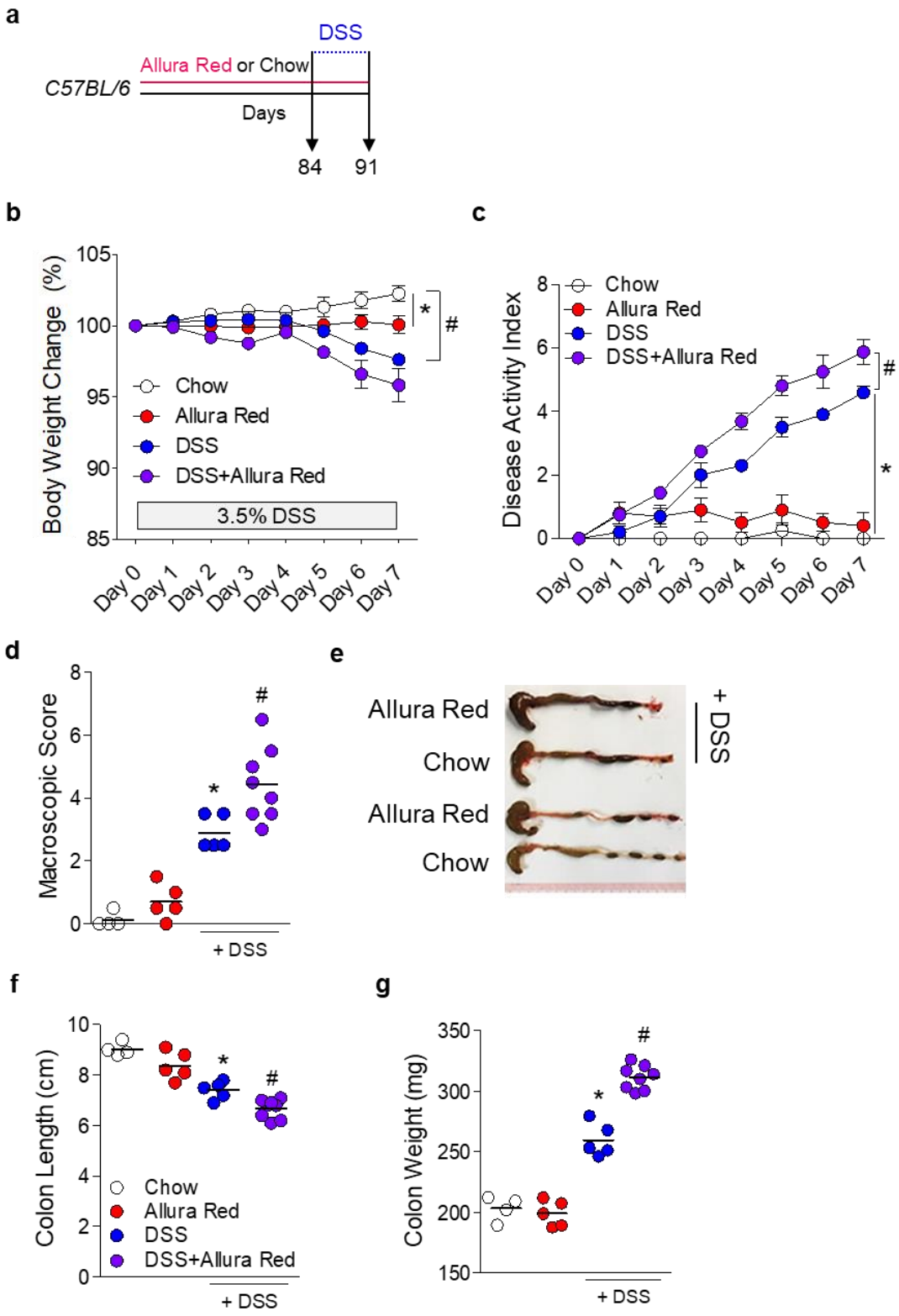
a
DSS
Allura Red or Chow
C57BL/6
Days
84
91
b
Body Weight Change (%)
105
100
95
90
85
Chow
Allura Red
DSS
DSS+Allura Red
3.5% DSS
Day 0
Day 1
Day 2
Day 3
Day 4
Day 5
Day 6
Day 7
c
Disease Activity Index
8
6
4
2
0
Chow
Allura Red
DSS
DSS+Allura Red
d
Macroscopic Score
+ DSS
e
Allura Red
Chow
Allura Red
Chow
+ DSS
f
Colon Length (cm)
10
8
6
4
2
0
Chow
Allura Red
DSS
DSS+Allura Red
+ DSS
g
Colon Weight (mg)
350
300
250
200
150
+ DSS

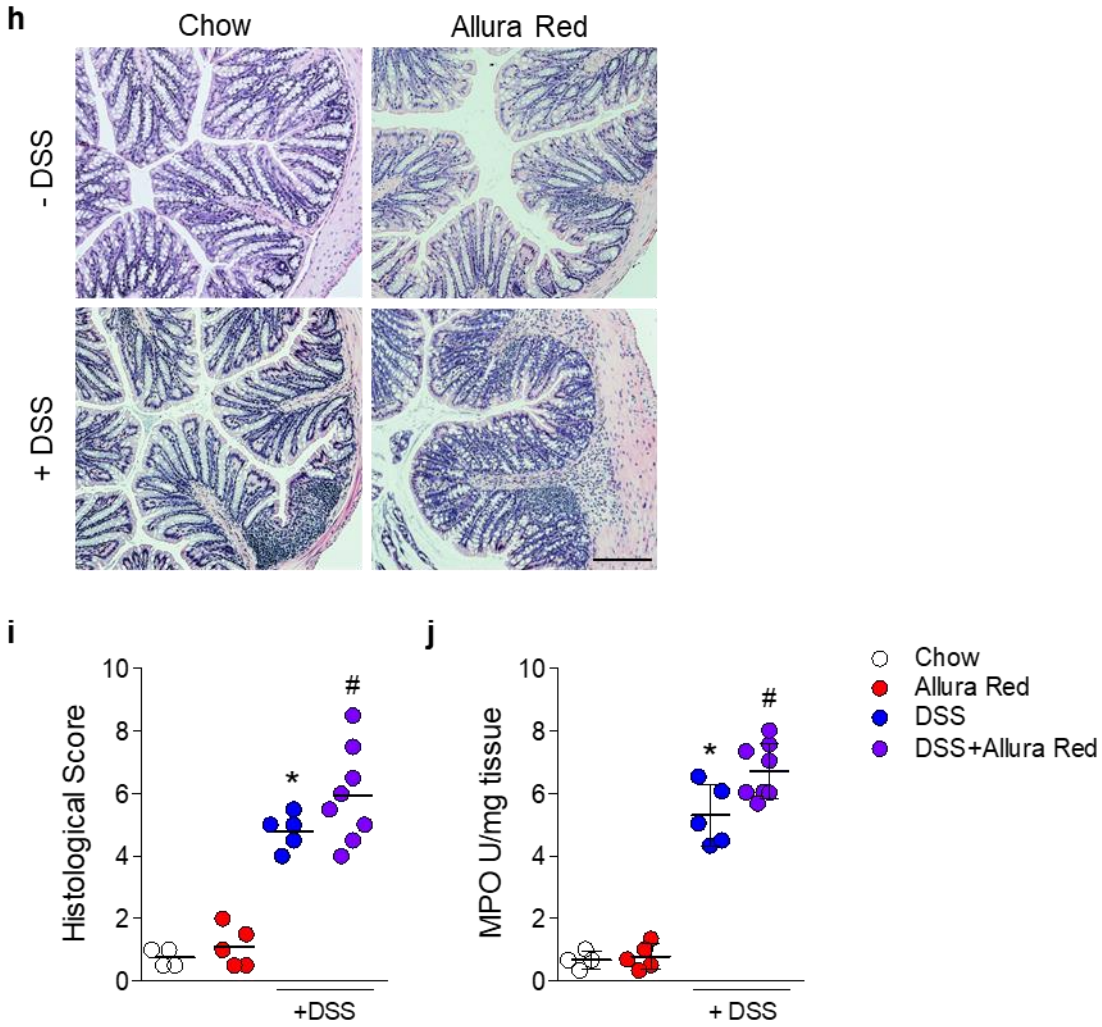
h
Chow
Allura Red
- DSS
+ DSS
i
Histological Score
10
8
6
4
2
0
*
#
+DSS
j
MPO U/mg tissue
10
8
6
4
2
0
*
#
+ DSS
Chow
Allura Red
DSS
DSS+Allura Red

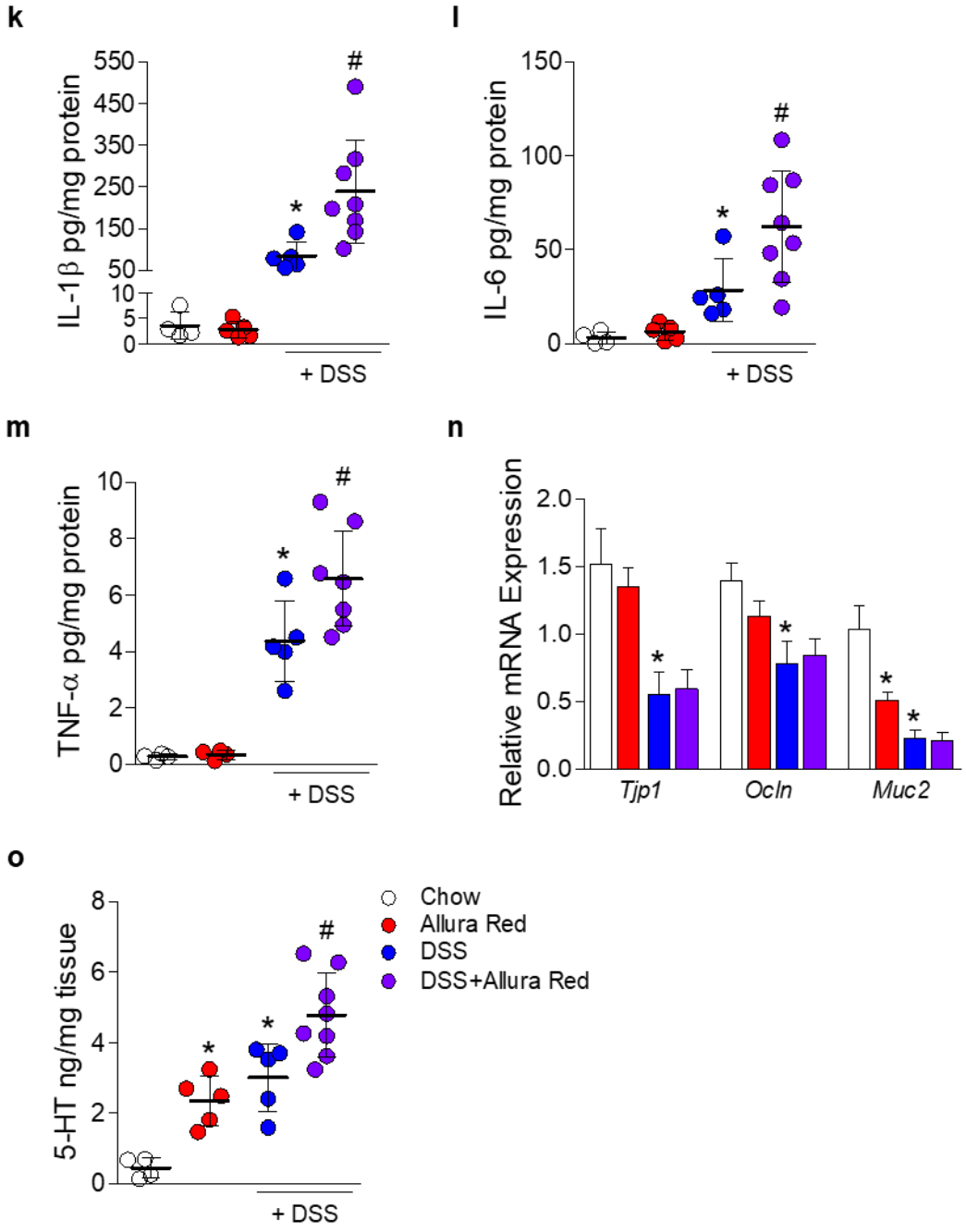
k
IL-1β pg/mg protein
550
450
350
250
150
50
10
5
0
+ DSS
l
IL-6 pg/mg protein
150
100
50
0
+ DSS
m
TNF-α pg/mg protein
10
8
6
4
2
0
+ DSS
n
Relative mRNA Expression
2.0
1.5
1.0
0.5
0.0
Tjp1
Ocln
Muc2
o
5-HT ng/mg tissue
8
6
4
2
0
+ DSS
Chow
Allura Red
DSS
DSS+Allura Red

Figure 9: Exacerbation of DSS-induced colitis by Allura Red AC in C57BL/6 mice. C57BL/6 mice were fed normal chow diet or exposed to AR via normal chow diet for 12 weeks (84 days) prior to induction of acute colitis with 3.5% DSS for 7 days. During DSS, mice were continuously exposed to AR in the corresponding groups. (**a**) Schematic illustration of the experimental design. (**b**) Body weight change during DSS. Each point represents mean ± S.E.M. (**c**) Disease activity index (DAI) during DSS. Each point represents mean ± S.E.M. (**d**) Macroscopic score. (**e**) Representative image of colons. (**f**) Colonic length (cm). (**g**) Colonic weight (mg). (**h**) Representative images of hematoxylin and eosin (H&E)-stained colonic sections on day 7 post-DSS; scale bar: 100 μm. (**i**) Histological score. (**j**) Colonic MPO level. (**k**-**m**) Colonic pro-inflammatory cytokines. (**n**) Relative mRNA expression of intestinal barrier function related genes. (**o**) Colonic 5-HT level. Values represent mean or mean ± S.D. from n = 4-8 mice/group. Statistical significance was determined by Student's *t*-test, one-way ANOVA with Bonferroni's test, or two-way ANOVA with Bonferroni's test. $^{*}P < 0.05$ versus chow. $^{\#}P < 0.05$ versus DSS.

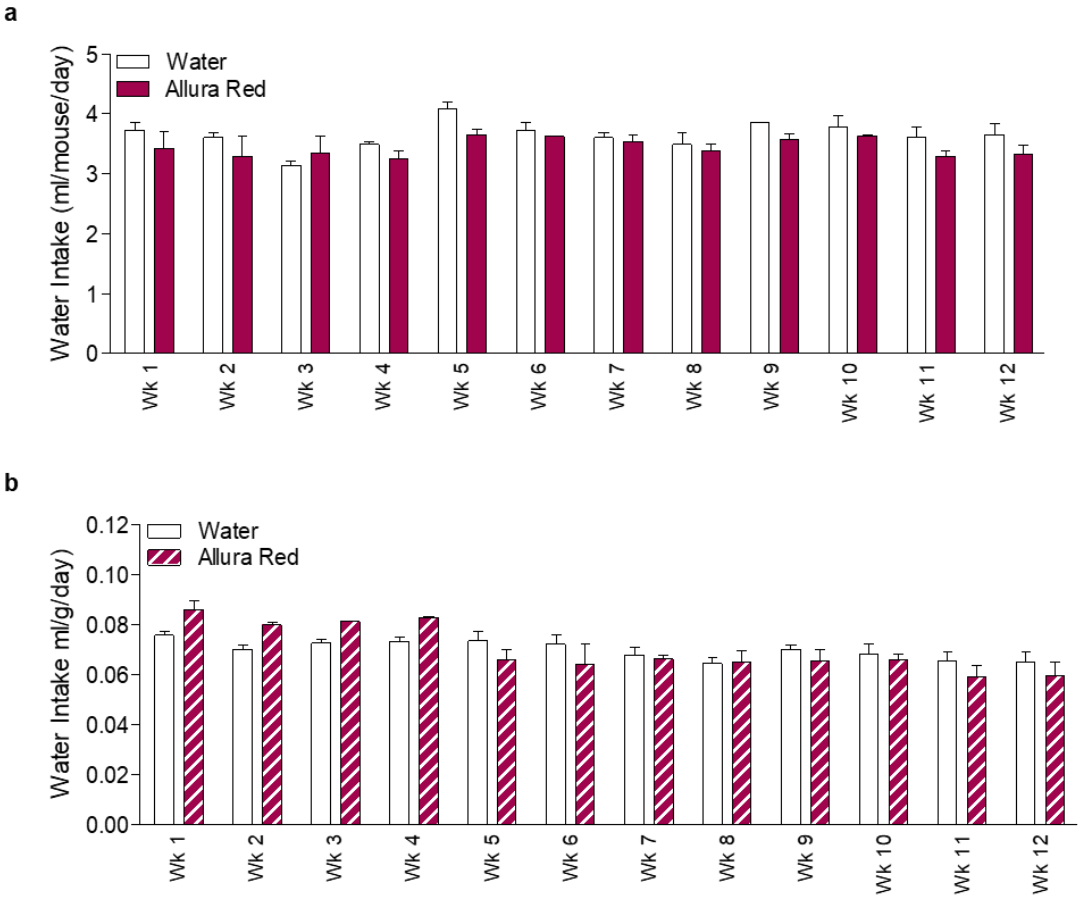

Figure 10: Water intake measurement in naïve C57BL/6 mice exposed to Allura Red AC or administered normal drinking water for 12 weeks. (**a**) Water intake represented in ml per mouse per day. (**b**) Water intake is represented in ml per g of mouse per day. Values represent mean ± S.E.M. from 10 to 12 mice per group.

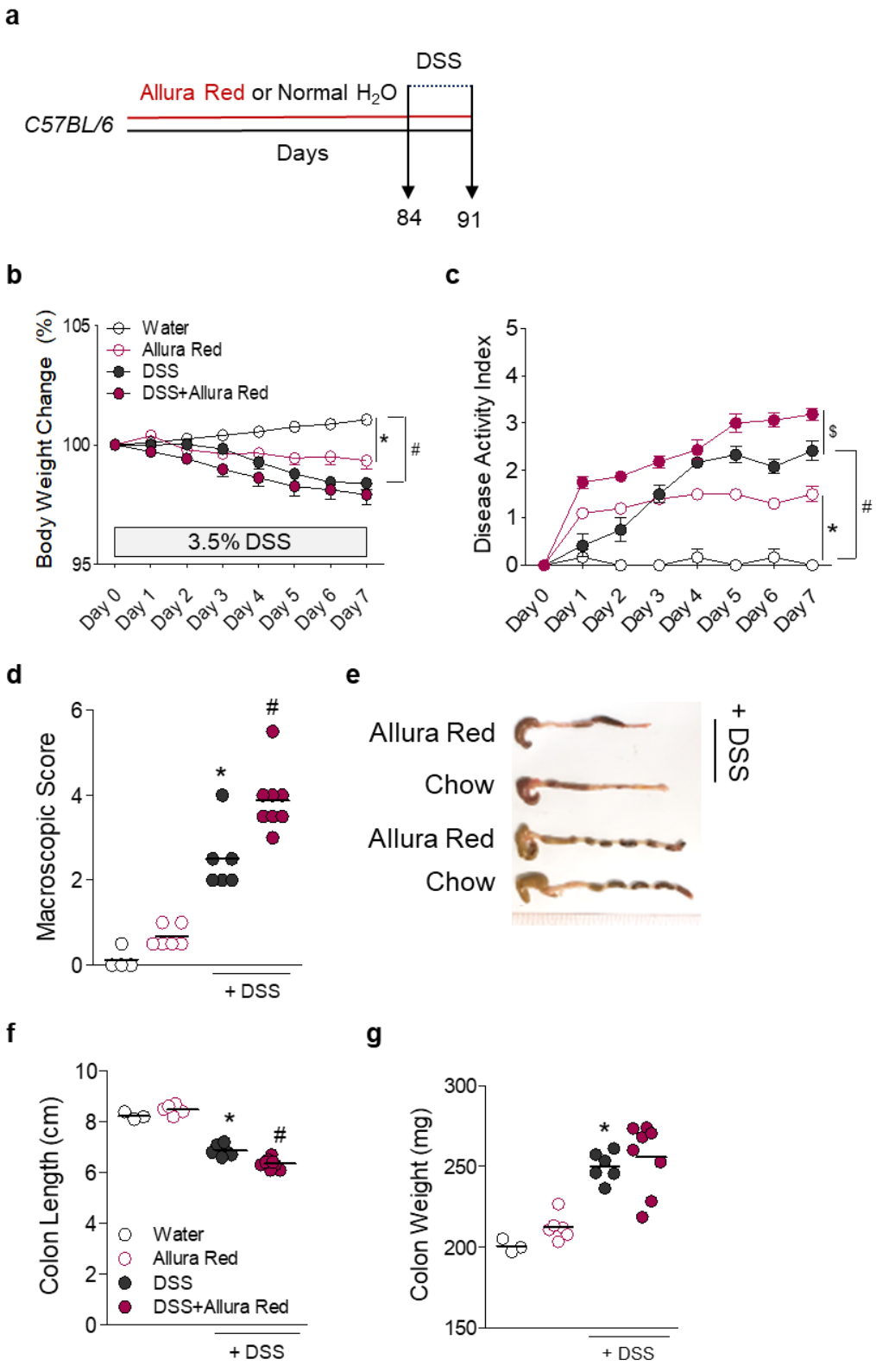
a
DSS
Allura Red or Normal H_2O
C57BL/6
Days
84
91
b
Body Weight Change (%)
105
100
95
Water
Allura Red
DSS
DSS+Allura Red
3.5% DSS
Day 0
Day 1
Day 2
Day 3
Day 4
Day 5
Day 6
Day 7
c
Disease Activity Index
d
Macroscopic Score
+ DSS
e
Allura Red
Chow
Allura Red
Chow
+ DSS
f
Colon Length (cm)
g
Colon Weight (mg)

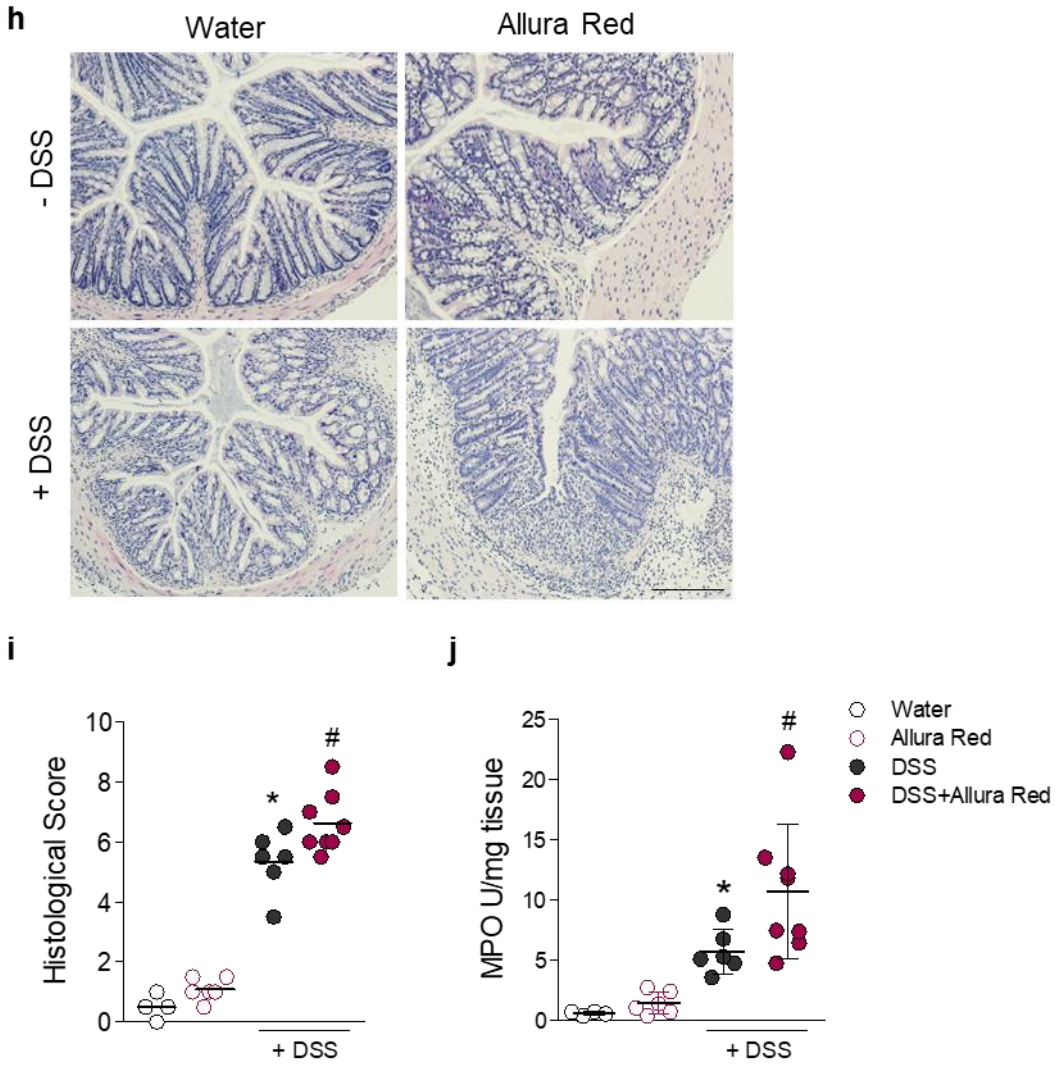
h
Water
Allura Red
- DSS
+ DSS
i
Histological Score
10
8
6
4
2
0
*
#
+ DSS
j
MPO U/mg tissue
25
20
15
10
5
0
*
#
+ DSS
Water
Allura Red
DSS
DSS+Allura Red

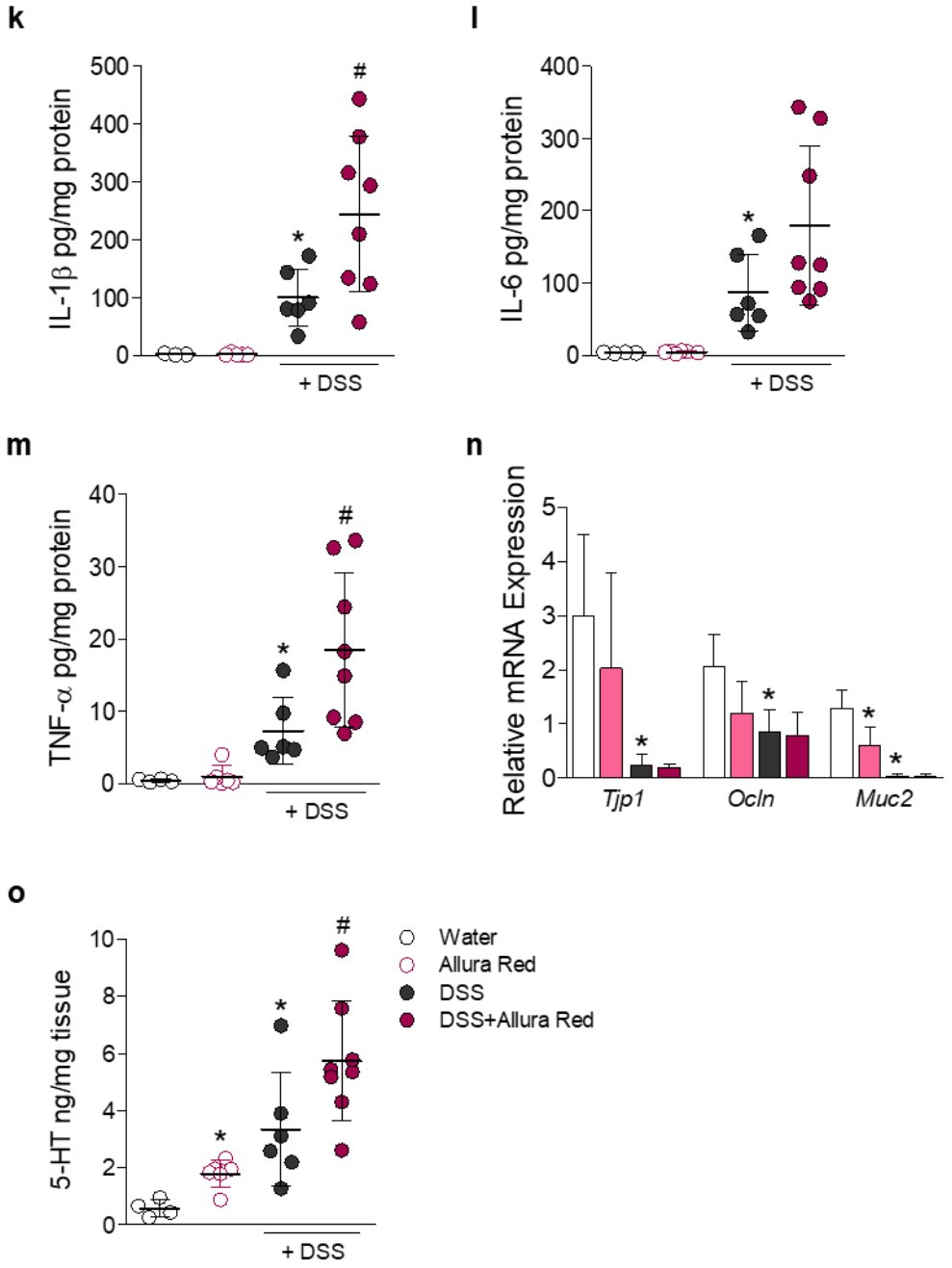
k
IL-1β pg/mg protein
500
400
300
200
100
0
+ DSS
l
IL-6 pg/mg protein
400
300
200
100
0
+ DSS
m
TNF-α pg/mg protein
40
30
20
10
0
+ DSS
n
Relative mRNA Expression
5
4
3
2
1
0
Tjp1
Ocln
Muc2
o
5-HT ng/mg tissue
10
8
6
4
2
0
+ DSS
Water
Allura Red
DSS
DSS+Allura Red

Figure 11: Allura Red AC in drinking water exacerbates DSS-induced colitis in C57BL/6 mice. C57BL/6 mice were administered normal drinking water or exposed to AR via normal drinking water for 12 weeks (84 days) prior to induction of acute colitis with 3.5% DSS for 7 days. During DSS, mice were continuously exposed to AR in the corresponding groups. (**a**) Schematic illustration of the experimental design. (**b**) Body weight change during DSS. Each point represents mean ± S.E.M. (**c**) Disease activity index (DAI) during DSS. Each point represents mean ± S.E.M. (**d**) Macroscopic score. (**e**) Representative image of colons. (**f**) Colonic length (cm). (**g**) Colonic weight (mg). (**h**) Representative images of H&E-stained colonic sections on day 7 post-DSS; scale bar: 100 μm. (**i**) Histological score. (**j**) Colonic MPO level. (**k-m**) Colonic pro-inflammatory cytokines. (**n**) Relative mRNA expression of intestinal barrier function related genes. (**o**) Colonic 5-HT level. Values represent as mean or mean ± S.D. from n = 4-8 mice/group. Statistical significance was determined by Student's *t*-test, one-way ANOVA with Bonferroni's test, or two-way ANOVA with Bonferroni's test. $^{*}P < 0.05$ versus chow. $^{\#}P < 0.05$ versus DSS.

3.5 *Intermittent exposure to Allura Red AC does not alter the susceptibility to DSS-induced colitis*

In the previous experiments, C57BL/6 mice were continuously exposed to AR every day for 12 weeks before the induction of acute colitis by 3.5% DSS for 7 days. In a separate experiment, C57BL/6 mice were intermittently exposed to AR for one day per week for 12 weeks before the induction of acute colitis by 3.5% DSS for 7 days (**Figure 12a**). The body weight change and DAI were not different between chow-fed mice and AR exposed mice on day 7 post-DSS (**Figure 12, b** and **c**). Macroscopic and histological scores were not different between the two groups (**Figure 12, d-f**). Also, colonic MPO levels and pro-inflammatory cytokine levels were not different between the two groups on day 7 post-DSS (**Figure 12, g** and **h**).

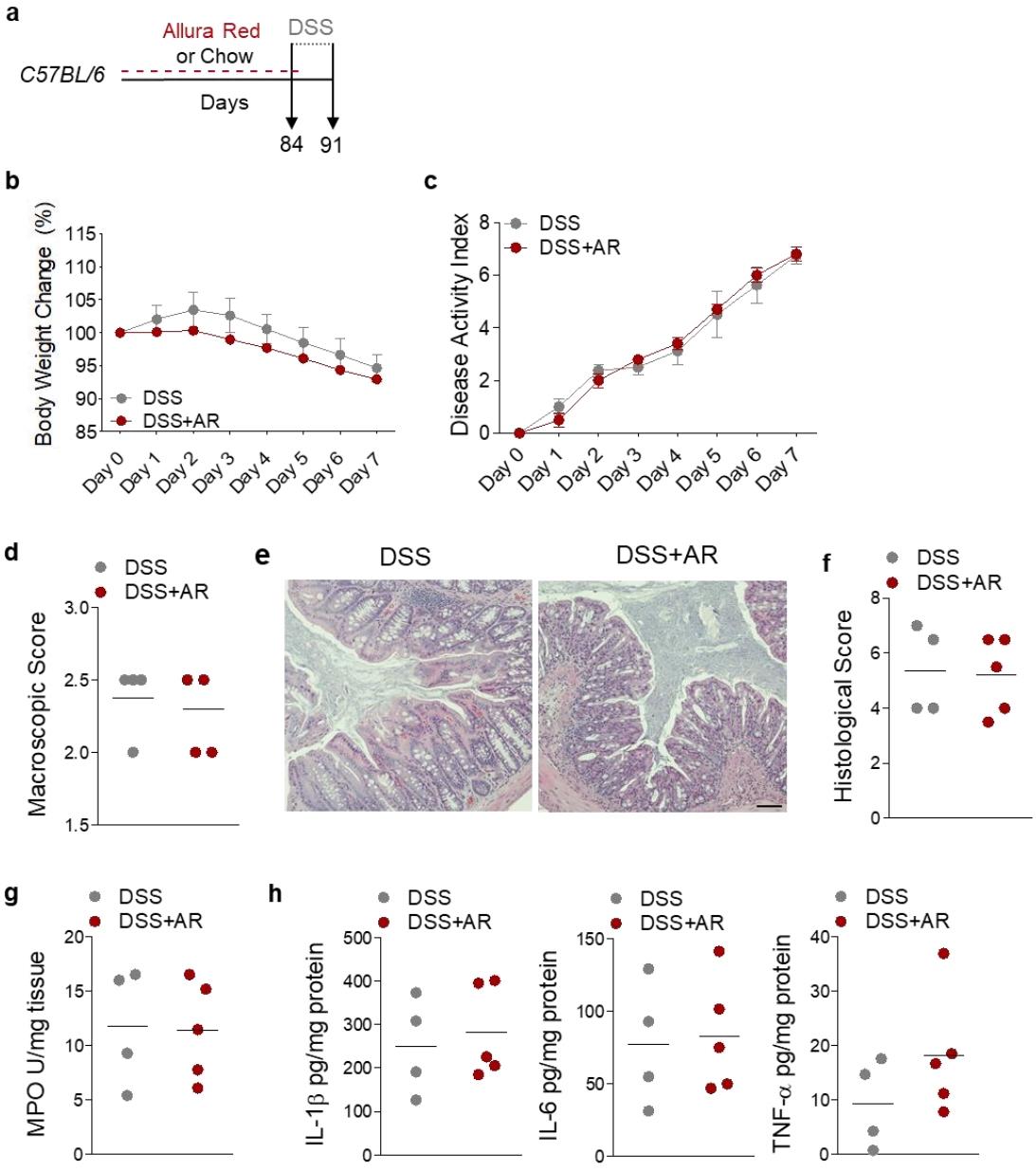
a
Allura Red
or Chow
DSS
C57BL/6
Days
84
91
b
Body Weight Change (%)
DSS
DSS+AR
Day 0
Day 1
Day 2
Day 3
Day 4
Day 5
Day 6
Day 7
c
Disease Activity Index
DSS
DSS+AR
d
Macroscopic Score
DSS
DSS+AR
e
DSS
DSS+AR
f
Histological Score
DSS
DSS+AR
g
MPO U/mg tissue
DSS
DSS+AR
h
IL-1β pg/mg protein
IL-6 pg/mg protein
TNF-α pg/mg protein
DSS
DSS+AR

Figure 12: Intermittently exposing C57BL/6 mice with AR does not enhance susceptibility to DSS-induced colitis. C57BL/6 mice were fed normal chow diet or intermittently exposed to AR via normal chow diet for one day per week for 12 weeks (84 days) prior to induction of acute colitis with 3.5% DSS for 7 days. During DSS, mice were exposed to AR on the first day of DSS. (**a**) Schematic illustration of the experimental design. (**b**) Body weight change during DSS. Each point represents mean ± S.E.M. (**c**) Disease activity index (DAI) during DSS. Each point represents mean ± S.E.M. (**d**) Macroscopic score. (**e**) Representative images of H&E-stained colonic sections on day 7 post-DSS; scale bar: 100 µm. (**f**) Histological score. (**g**) Colonic MPO level. (**h**) Colonic pro-inflammatory cytokines. Values represent as mean or mean ± S.D. from n = 4-5 mice/group. Statistical significance was determined by Student's *t*-test, one-way ANOVA with Bonferroni's test, or two-way ANOVA with Bonferroni's test.

3.6 *Early life exposure to Allura Red AC enhances susceptibility to the later development of DSS-induced colitis*

Early life is an important period of influencing the susceptibility for IBD development in later life (Agrawal et al., 2021). Four-week-old C57BL/6 mice were exposed to AR via normal chow diet for 4 weeks prior to the induction of acute colitis by 3.5% DSS for 7 days. To examine whether early life exposure to AR primes mice to enhanced susceptibility to DSS-induced colitis in adulthood, exposure of AR was stopped during DSS (**Figure 13a**). Mice exposed to AR during early life showed increased body weight loss compared to the vehicle group on day 7 post-DSS (**Figure 13b**). Compared with DSS-treated mice, DSS-treated mice which were pre-exposed to AR showed higher disease activity index (DAI) (**Figure 13c**). This increased DAI was accompanied by higher macroscopic scores (**Figure 13d**), reduction in colonic length (**Figure 13, e** and **f**). Histological scores (**Figure 13, g** and **h**), and colonic MPO levels (**Figure 13i**) were also higher in DSS-treated mice which were pre-exposed to AR, compared with DSS-treated counterparts. In addition, the exposure to AR potently increased levels of pro-inflammatory cytokines, such as IL-1β, IL-6, and TNF-α, in mice on day 7 post-DSS, compared with DSS-treated counterparts (**Figure 13j**). These data indicate that early life exposure to AR can prime mice to the later development of DSS-induced colitis.

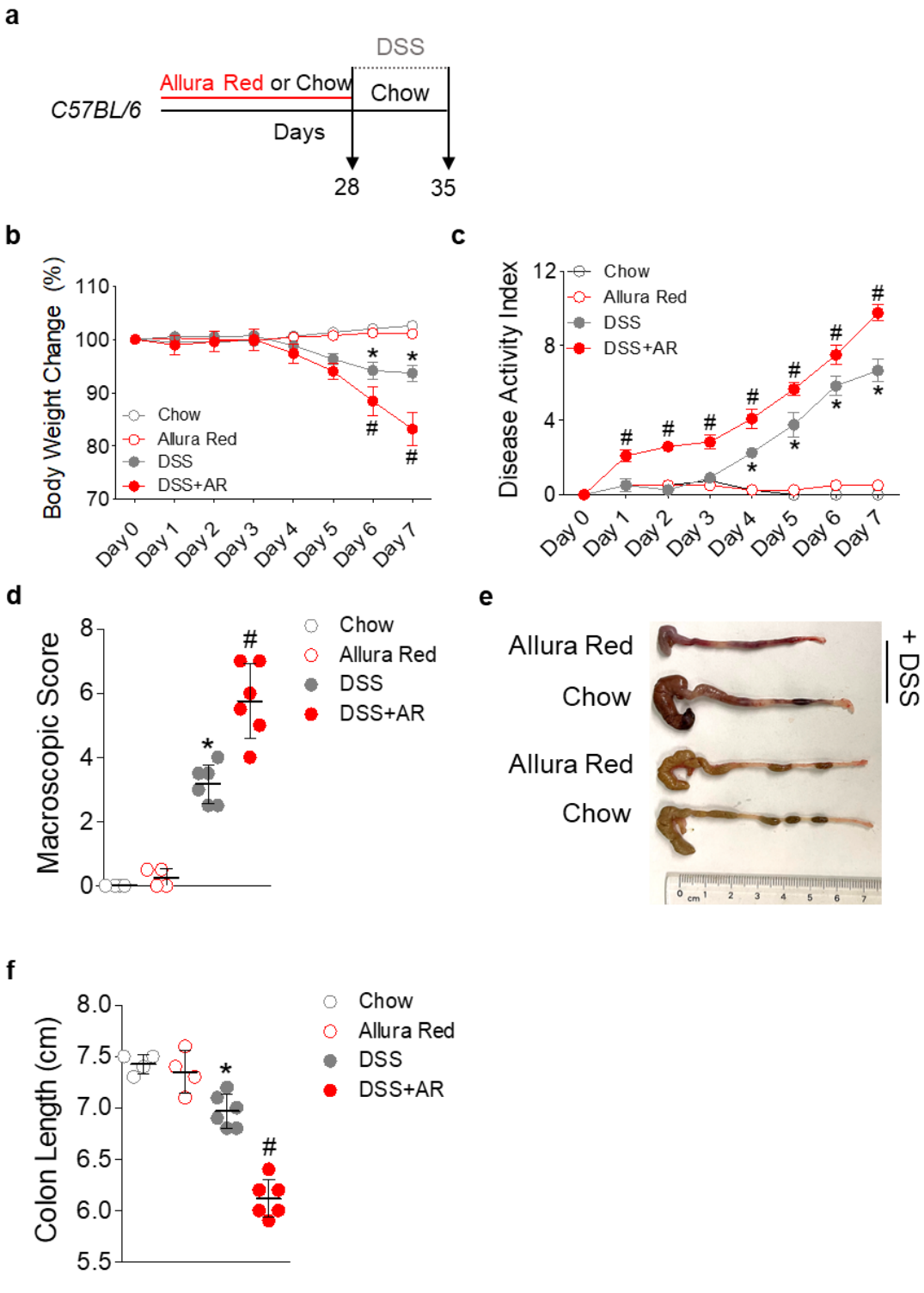
a
DSS
Allura Red or Chow
Chow
C57BL/6
Days
28
35
b
Body Weight Change (%)
110
100
90
80
70
Chow
Allura Red
DSS
DSS+AR
Day 0
Day 1
Day 2
Day 3
Day 4
Day 5
Day 6
Day 7
c
Disease Activity Index
12
8
4
0
Chow
Allura Red
DSS
DSS+AR
d
Macroscopic Score
8
6
4
2
0
Chow
Allura Red
DSS
DSS+AR
e
Allura Red
Chow
Allura Red
Chow
+ DSS
f
Colon Length (cm)
8.0
7.5
7.0
6.5
6.0
5.5
Chow
Allura Red
DSS
DSS+AR

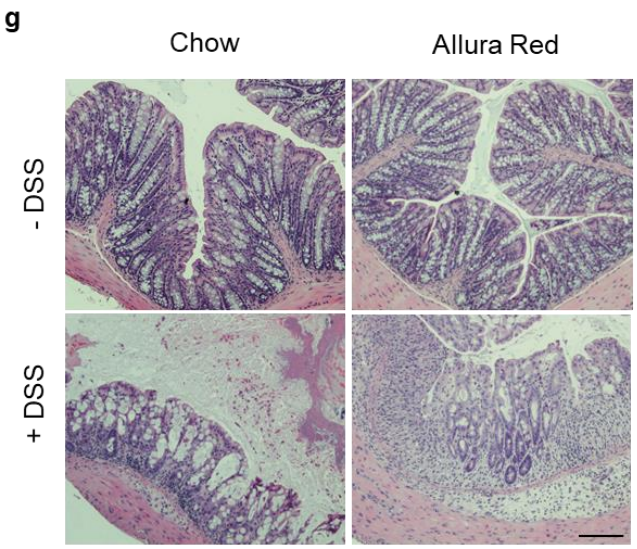
g
Chow
Allura Red
- DSS
+ DSS

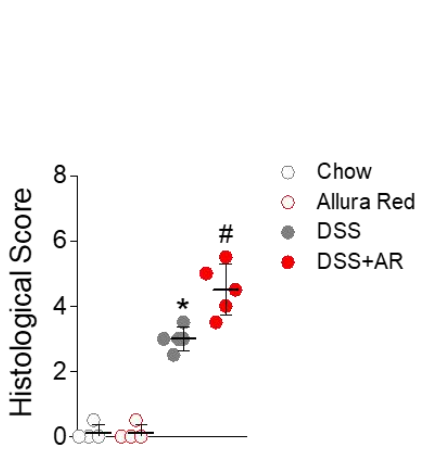
h
Histological Score
0
2
4
6
8
*
#
Chow
Allura Red
DSS
DSS+AR

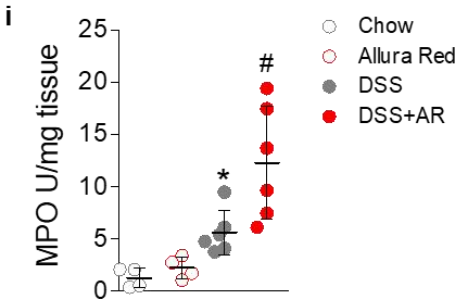
i
MPO U/mg tissue
0
5
10
15
20
25
*
#
Chow
Allura Red
DSS
DSS+AR

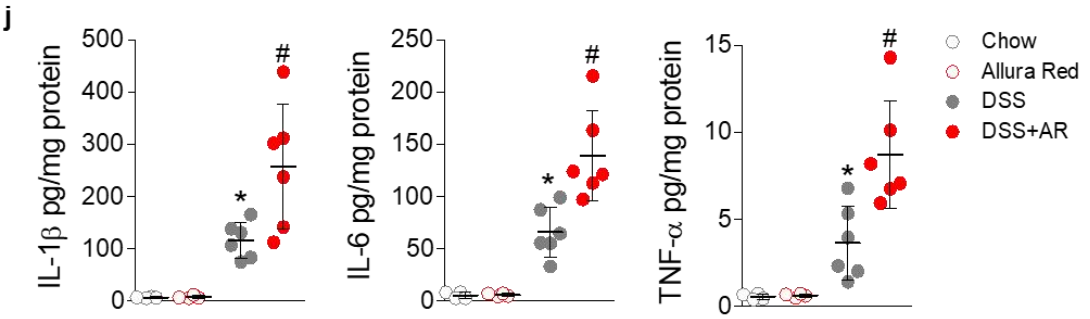
j
IL-1β pg/mg protein
0
100
200
300
400
500
IL-6 pg/mg protein
0
50
100
150
200
250
TNF-α pg/mg protein
0
5
10
15
*
#
Chow
Allura Red
DSS
DSS+AR

Figure 13: Exposure of AR during early life exacerbates the severity of DSS-induced colitis in later life. Four-week-old C57BL/6 mice were fed normal chow diet or exposed to AR via normal chow diet for 4 weeks (28 days) prior to induction of acute colitis by 3.5% DSS for 7 days. During DSS, mice were not exposed to AR, but fed normal chow diet. (**a**) Schematic illustration of the experimental design. (**b**) Body weight change during DSS. Each point represents mean ± S.E.M. (**c**) Disease activity index (DAI) during DSS. Each point represents mean ± S.E.M. (**d**) Macroscopic score. (**e**) Representative image of colons. (**f**) Colonic length (cm). (**g**) Representative images of H&E-stained colonic sections on day 7 post-DSS; scale bar: 100 μm. (**h**) Histological score. (**i**) Colonic MPO level. (**j**) Colonic pro-inflammatory cytokines. Values represent as mean or mean ± S.D. from n = 4-6 mice/group. Statistical significance was determined by Student's *t*-test, one-way ANOVA with Bonferroni's test, or two-way ANOVA with Bonferroni's test. $^{*}P < 0.05$ versus chow. $^{\#}P < 0.05$ versus DSS.

3.7 *Allura Red AC triggers an early development of $CD4^+CD45RB^{high}$ T cell-induced colitis*

To further probe the role of AR in the development of colitis, $CD4^+CD45RB^{high}$ T cell transfer model of chronic colitis was utilized. Briefly, FACS-sorted WT $CD4^+CD45RB^{high}$ T cells (naïve CD4+ T cells) were adoptively transferred into lymphopenic *Rag1*$^{-/-}$ mice, and at the time of reconstitution, mice were exposed to AR via normal chow diet for 5 weeks (**Figure 14a**). Starting from week 2 post-AR exposure, increased hair loss was observed in *Rag1*$^{-/-}$ mice exposed to AR with or without reconstitution of T cells, an effect more profound in mice reconstituted with T cells (**Figure 15**). However, *Rag1*$^{-/-}$ mice without AR exposure did not show any signs of hair loss.

Rag1$^{-/-}$ mice with T cell reconstitution ($CD45RB^{hi}$) showed increased body weight loss compared to naïve *Rag1*$^{-/-}$ mice at week 5 (**Figure 14b**). However, there was no significant difference in body weight loss between $CD45RB^{hi}$ and *Rag1*$^{-/-}$ mice with T cell reconstitution and AR exposure ($CD45RB^{hi}$-AR) (**Figure 14b**). $CD45RB^{hi}$-AR showed significantly higher DAI compared to $CD45RB^{hi}$ (**Figure 14c**). In addition, $CD45RB^{hi}$-AR had higher macroscopic scores (**Figure 14d**) along with reduced colon lengths compared to $CD45RB^{hi}$ (**Figure 14, e** and **f**). Cross-sections of colonic tissues stained with H&E from $CD45RB^{hi}$-AR also showed higher histological scores than $CD45RB^{hi}$ (**Figure 14, g** and **h**). Furthermore, colonic MPO levels (**Figure 14i**) and pro-inflammatory cytokines (IL-1β, IL-6, TNF-α, and IFN-γ) were potently increased

in CD45RB^{hi}-AR compared to CD45RB^{hi} (**Figure 14j-m**). These findings indicate that AR can also promote colitis via CD4+ T cells in *Rag1*$^{-/-}$ mice.

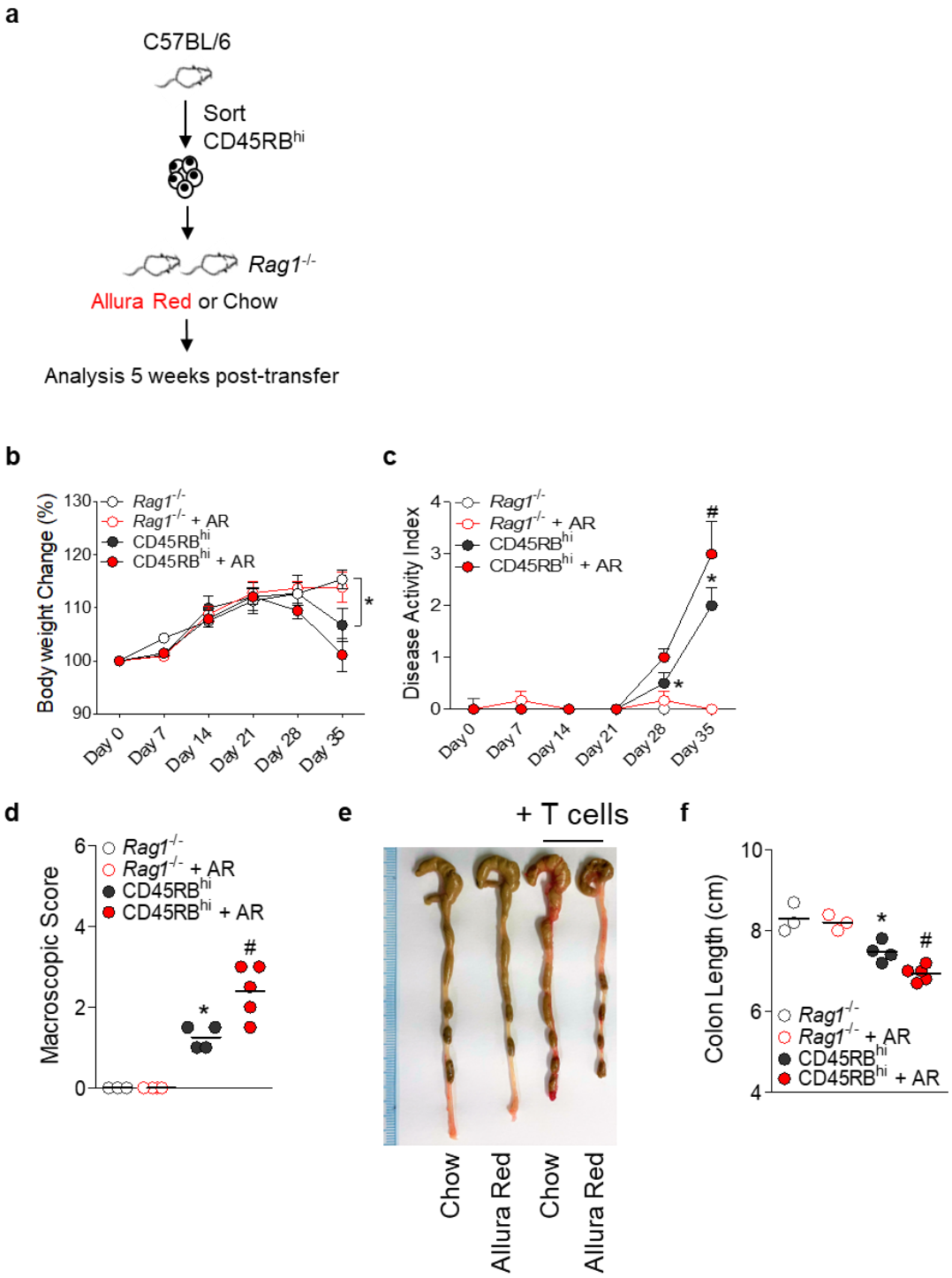
a
C57BL/6
Sort
CD45RBhi
Rag1-/-
Allura Red or Chow
Analysis 5 weeks post-transfer
b
Body weight Change (%)
Rag1-/-
Rag1-/- + AR
CD45RBhi
CD45RBhi + AR
Day 0
Day 7
Day 14
Day 21
Day 28
Day 35
c
Disease Activity Index
d
Macroscopic Score
e
+ T cells
Chow
Allura Red
Chow
Allura Red
f
Colon Length (cm)

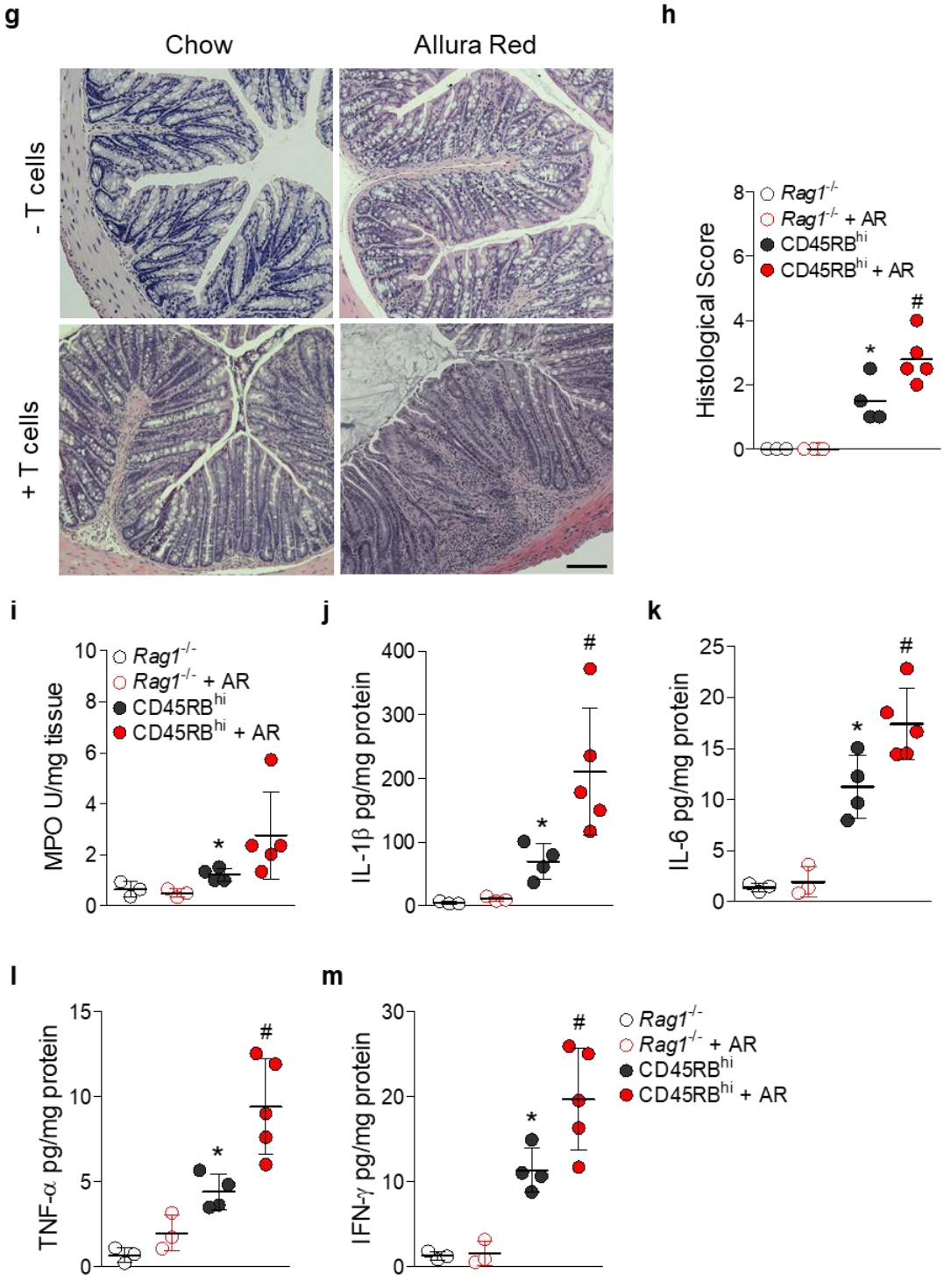
g
Chow
Allura Red
- T cells
+ T cells
h
Histological Score
Rag1-/-
Rag1-/- + AR
CD45RBhi
CD45RBhi + AR
i
MPO U/mg tissue
j
IL-1β pg/mg protein
k
IL-6 pg/mg protein
l
TNF-α pg/mg protein
m
IFN-γ pg/mg protein

Figure 14: Allura Red AC exacerbates the development of T cell-induced colitis model. (**a**) Experimental design. Briefly, *Rag*1$^{-/-}$ mice were reconstituted with FACS-sorted 5.0 x 10^5 $CD4^+CD45RB^{hi}$ T cells harvested from spleens of C57BL/6 mice. Mice were exposed to AR via normal chow diet or fed normal chow diet at the time of reconstitution. (**b**) Body weight change. Each point represents mean ± S.E.M. (**c**) Disease activity index (DAI). Each point represents mean ± S.E.M. (**d**) Macroscopic score. (**e**) Representative image of colons. (**f**) Colonic length (cm). (**g**) Representative images of H&E-stained colonic sections; scale bar: 100 μm. (**h**) Histological score. (**i**) Colonic MPO levels. (**j**-**m**) Colonic IL-1β, IL-6, TNF-α, and IFN-γ levels. Values represent mean or mean ± S.D. from n = 3-5 mice/group. Statistical significance was determined by Student's *t*-test, one-way ANOVA, or two-way ANOVA with Bonferroni's test. $^*P < 0.05$ versus *Rag1*$^{-/-}$. $^{\#}P < 0.05$ versus $CD45RB^{hi}$.

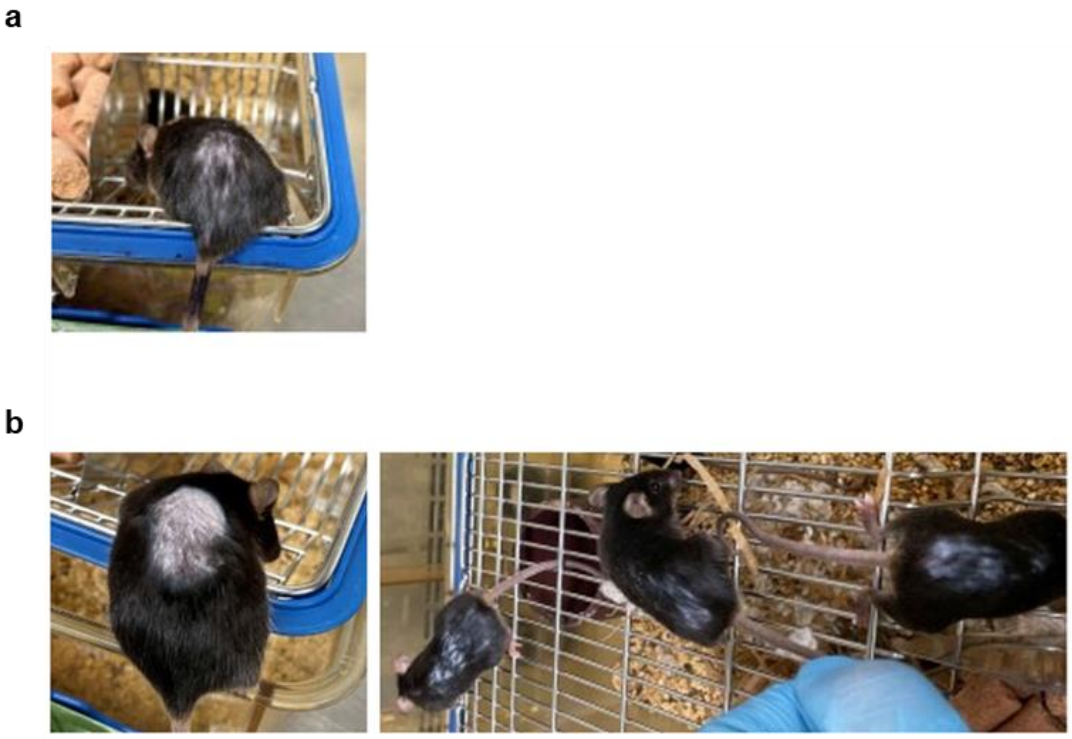

Figure 15: Representative images of alopecia in *Rag1*$^{-/-}$ mice exposed to AR with or without reconstitution with CD4^{+}CD45RB^{high} T cells. (**a**) *Rag1*$^{-/-}$ mice exposed to AR via normal chow diet. (**b**) *Rag1*$^{-/-}$ mice reconstituted with T cells and exposed to AR via normal chow diet.

3.8 *Allura Red AC induces low-grade colon inflammation in naïve C57BL/6 mice*

In the first *in vivo* experiment, the body weight (**Figure 9b**) and *Muc2* mRNA expression was reduced (**Figure 9n**), while colonic 5-HT levels were increased (**Figure 9o**), in mice exposed to AR without DSS. To further test these observations, it was examined whether AR promotes low-grade colon inflammation without inducing colitis with DSS (**Figure 16a**). Food intake was not different between the groups during the 14 weeks of AR exposure (**Figure 17**). Fecal lipocalin 2 (Lcn2) is a sensitive and broadly dynamic marker of intestinal inflammation in mice. Mice exposed to AR via normal chow diet showed elevated fecal Lcn2 levels at week 14 (**Figure 16b**). Mice exposed to AR also showed higher macroscopic (**Figure 16c**) and histological scores (**Figure 16, d** and **e**), which were accompanied by increased colonic MPO levels (**Figure 16f**). Additionally, there were significantly higher numbers of 5-HT–positive cells in the colons of AR exposed mice (**Figure 16, g** and **h**), and increased colonic 5-HT levels compared with control mice (**Figure 16i**). Moreover, genes related to host defense, such as peroxisome proliferator activated receptor gamma (*Pparg*), β-defensin 3 (*Defb3*), IL-22 (*Il22*), and regenerating islet-derived protein (REG) 3 gamma (*Reg3g*), were all down-regulated in the colons of mice exposed to AR compared to control mice (**Figure 16j**).

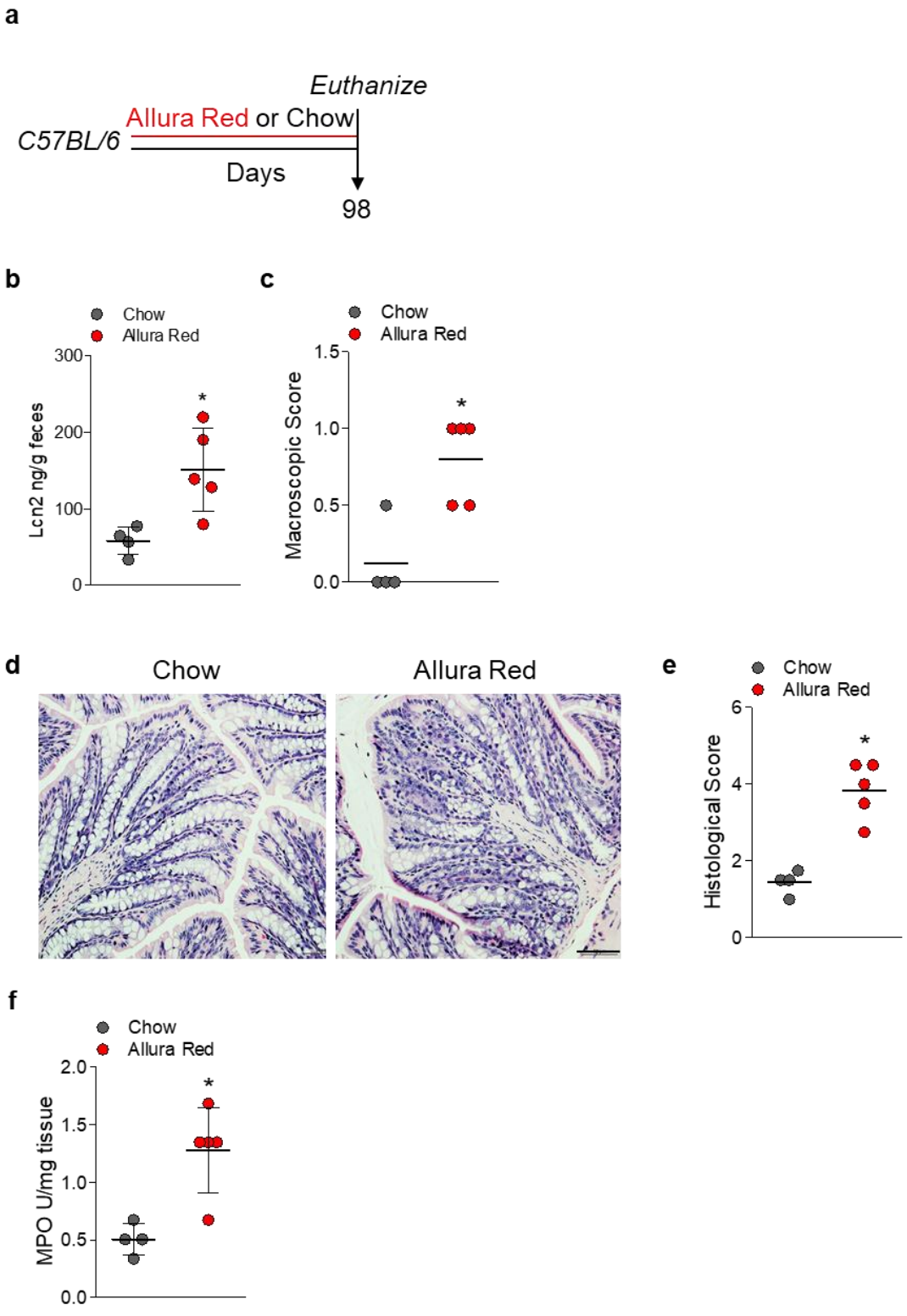
a
Euthanize
Allura Red or Chow
C57BL/6
Days
98
b
Chow
Allura Red
Lcn2 ng/g feces
300
200
100
0
*
c
Chow
Allura Red
Macroscopic Score
1.5
1.0
0.5
0.0
*
d
Chow
Allura Red
e
Chow
Allura Red
Histological Score
6
4
2
0
*
f
Chow
Allura Red
MPO U/mg tissue
2.0
1.5
1.0
0.5
0.0
*

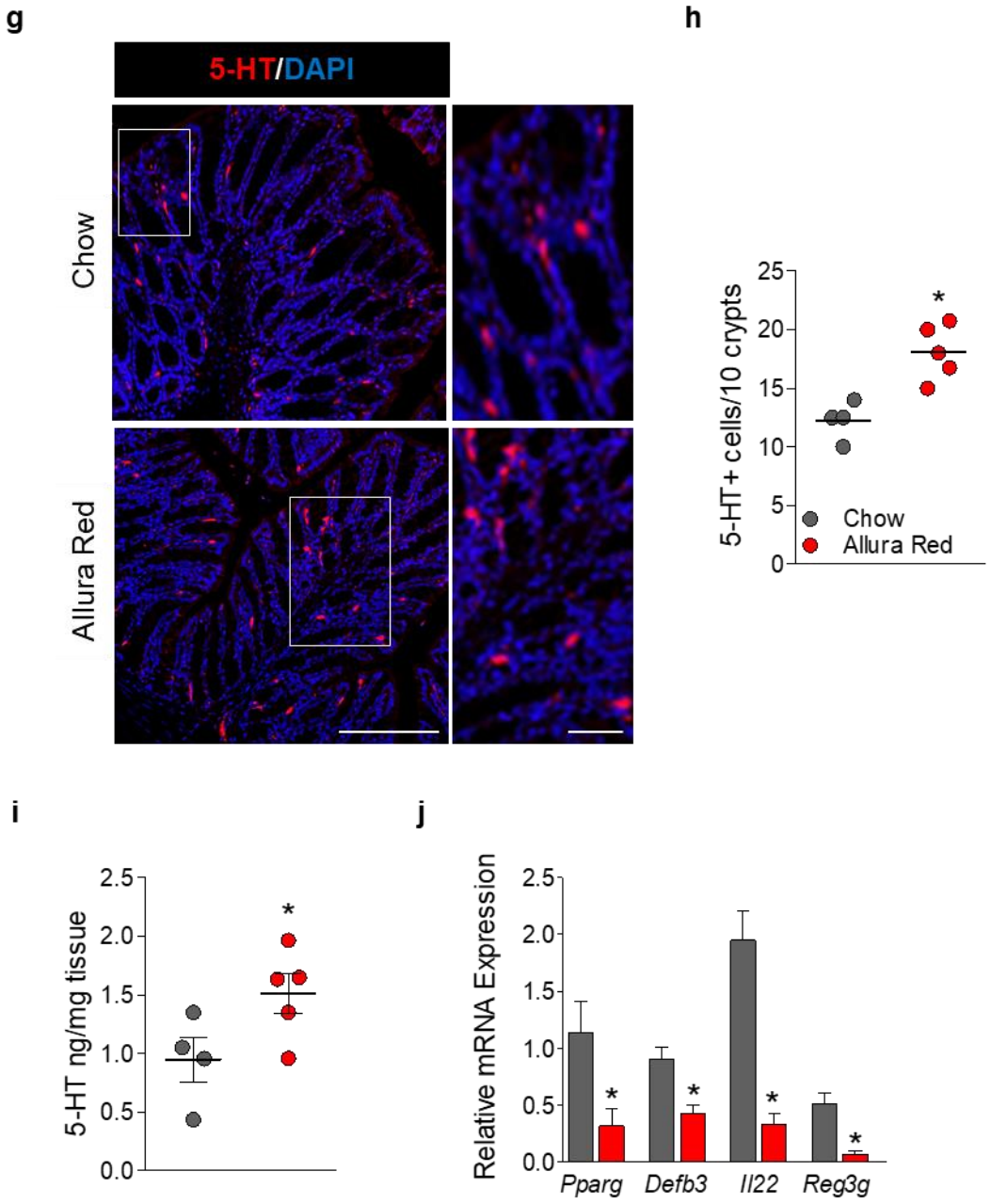
g
5-HT/DAPI
Chow
Allura Red
h
5-HT+ cells/10 crypts
25
20
15
10
5
0
*
Chow
Allura Red
i
5-HT ng/mg tissue
2.5
2.0
1.5
1.0
0.5
0.0
*
j
Relative mRNA Expression
2.5
2.0
1.5
1.0
0.5
0.0
*
*
*
*
Pparg
Defb3
Il22
Reg3g

Fig. 16: Allura Red AC promotes low-grade inflammation and increases colon 5-HT level in naïve C57BL/6 mice. Naïve C57BL/6 mice were fed normal chow diet or exposed to AR via normal chow diet for 14 weeks (98 days). (**a**) Schematic illustration of the experimental design (**b**) Fecal Lcn2 level at week 14. (**c**) Macroscopic score. (**d**) Representative images of H&E-stained colonic sections; scale bar: 50 μm. (**e**) Histological score. (**f**) Colonic MPO level. (**g**) Representative images of immunofluorescence (IF) staining for 5-HT (red) in the colon; scale bar: 50 μm. (**h**) Number of 5-HT–positive cells per 10 crypts. (**i**) Colonic 5-HT level. (**j**) Relative mRNA expression of genes related to antimicrobial response. Values represent as mean or mean ± S.D. from n = 4-5 mice/group. Statistical significance was determined by Student's *t*-test. **P* < 0.05 versus chow.

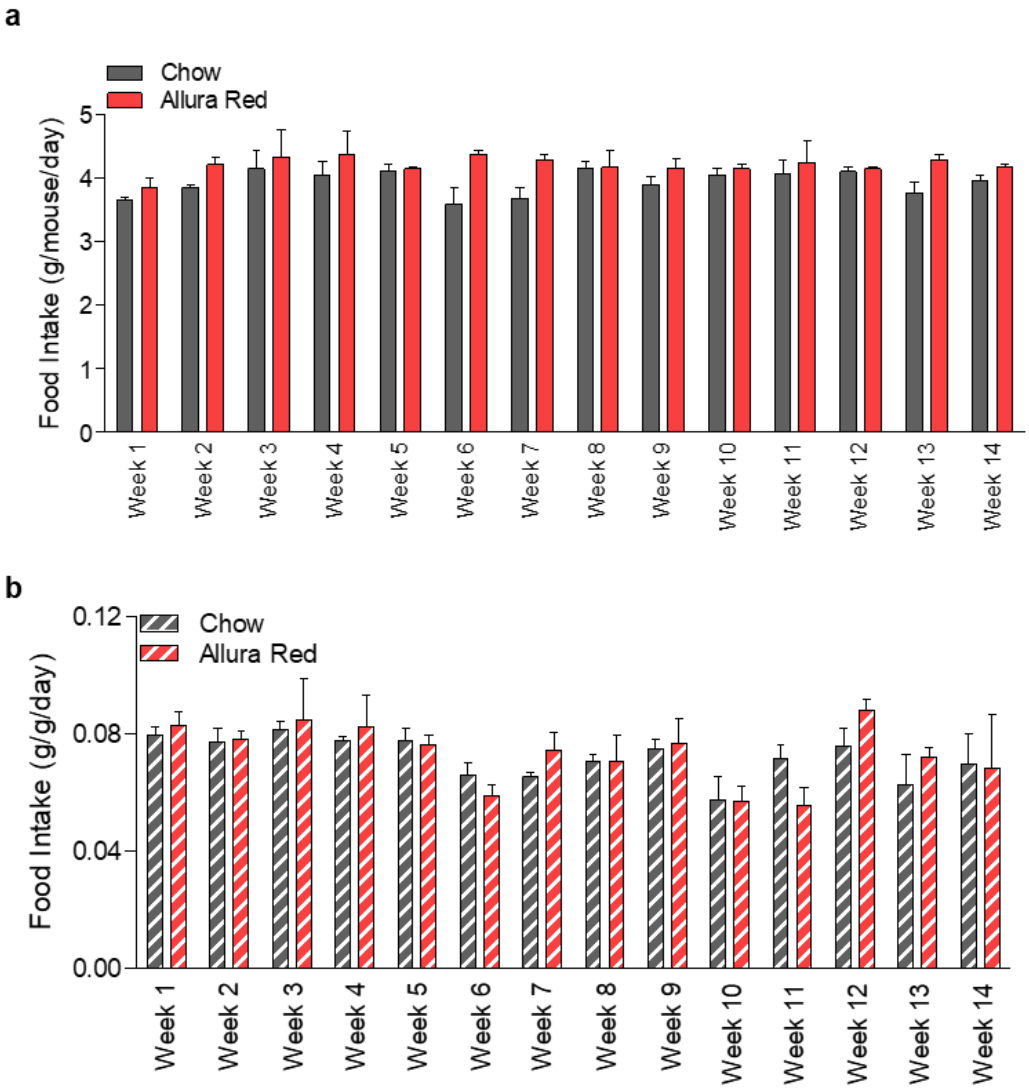

Figure 17: Measurement of food consumption in naïve C57BL/6 mice fed with normal chow diet or exposed to Allura Red AC via normal chow diet for 14 weeks. (**a**) Food intake represented in g per mouse per day. (**b**) Food intake is represented in g per g of mouse per day. Values represent mean ± S.E.M. from 4 to 5 mice per group.

3.9 *Allura Red AC activates MLCK signaling pathway and alters the intestinal barrier function in naïve C57BL/6 mice and mouse intestinal organoids*

The myosin light chain kinase (MLCK) pathway regulates intestinal barrier function, and MLCK is necessary for TNF-α induced barrier loss by phosphorylating myosin II regulatory light chain (MLC) (Cunningham et al., 2012). MLCK-dependent regulation is observed in mice with colitis and in inflamed colonic tissues of patients with IBD, where increased MLCK phosphorylates MLC protein at Serine (Ser) 19 (Blair et al., 2006). When C57BL/6 mice were exposed to AR for 14 weeks (**Figure 16**), there was significantly higher *Mlck* mRNA expression level (**Figure 18a**) and $pMLC^{Ser19}$ (**Figure 18, b** and **c**). In addition, ZO-1 (*Tjp1*) expression levels were significantly decreased in mice exposed to AR (**Figure 18, d-f).** Protective mucus layers generated by goblet cells are essential for maintaining a healthy intestinal barrier, the impairment of which correlates with increased microbiota-induced colitis. Mice exposed to AR showed depletion of colonic goblet cell numbers and lower *Muc2* mRNA expression levels (**Figure 18, g-i**).

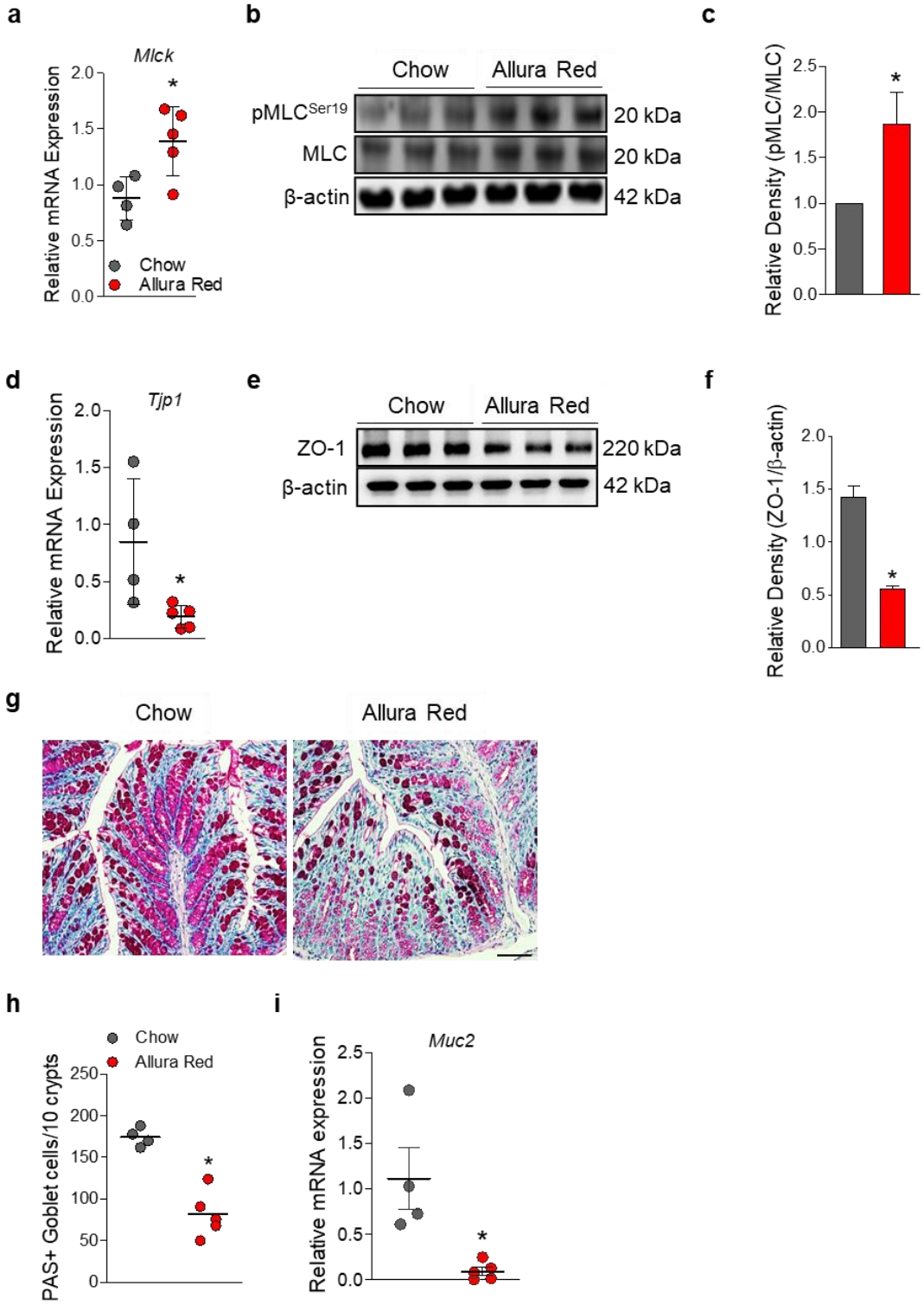
a
Mlck
Relative mRNA Expression
2.0
1.5
1.0
0.5
0.0
*
Chow
Allura Red
b
Chow
Allura Red
pMLC^Ser19
20 kDa
MLC
20 kDa
β-actin
42 kDa
c
Relative Density (pMLC/MLC)
2.5
2.0
1.5
1.0
0.5
0.0
*
d
Tjp1
Relative mRNA Expression
2.0
1.5
1.0
0.5
0.0
*
e
Chow
Allura Red
ZO-1
220 kDa
β-actin
42 kDa
f
Relative Density (ZO-1/β-actin)
2.0
1.5
1.0
0.5
0.0
*
g
Chow
Allura Red
h
Chow
Allura Red
PAS+ Goblet cells/10 crypts
250
200
150
100
50
0
*
i
Muc2
Relative mRNA expression
2.5
2.0
1.5
1.0
0.5
0.0
*

Figure 18: Allura Red AC activates MLCK signaling pathway and alters intestinal barrier function in naïve C57BL/6 mice. (**a**) *Mlck* mRNA expression. (**b**) Representative western blot analyses of $pMLC^{Ser19}$, MLC, and β-actin. (**c**) Relative densitometry (pMLC/MLC). (**d**) *Tjp1* mRNA expression. (**e**) Representative western blot analyses of ZO-1 and β-actin. (**f**) Relative densitometry (ZO-1/β-actin). (**g**) Representative images of Periodic acid-Schiff (PAS)-stained for Muc2 (violet) in the colon; scale bar: 50 μm. (**h**) Number of PAS–positive colonic goblet cells per 10 crypts. (**i**) *Muc2* mRNA expression. Values represent as mean or mean ± S.D. from n = 4-5 mice/group. Statistical significance was determined by Student's *t*-test. **P* < 0.05 versus chow.

The cytochrome P450 (CYP) family 1 enzymes are responsible for metabolizing various xenobiotics (Koppel et al., 2017). CYPs are mainly controlled by the aryl hydrocarbon receptor (AhR), which is involved in phase I xenobiotic metabolism in the intestine (Mescher et al., 2018). In addition, induction of CYP1A1 and CYP1B1 enhances inflammatory responses and alters intestinal barrier function (Alhouayek et al., 2018; Tian et al., 2020), and notably, azo dyes induce CYP1 enzymes (Johnson et al., 2010). To elucidate the underlying mechanism by which AR alters intestinal barrier function, HT-29 cells were treated for 24 hours with AR (1 μM). AhR activation by AR was observed as indicated by nuclear translocation of AhR (**Figure 19, a** and **b**). Also, there were significantly higher *CYP1A1* and *CYP1B1* mRNA levels after 24 hours of AR treatment compared to untreated cells (**Figure 19, c** and **d**); I3A (50 and 500 μM) was used as a positive control. Similarly, both *MLCK* mRNA expression (**Figure 19e**) and $pMLC^{Ser19}$ were increased (**Figure 19, f** and **g**) when HT-29 cells were treated for 24 hours with AR (1 μM) following pre-treatment for 1 hour with TNF-α (10 ng/ml).

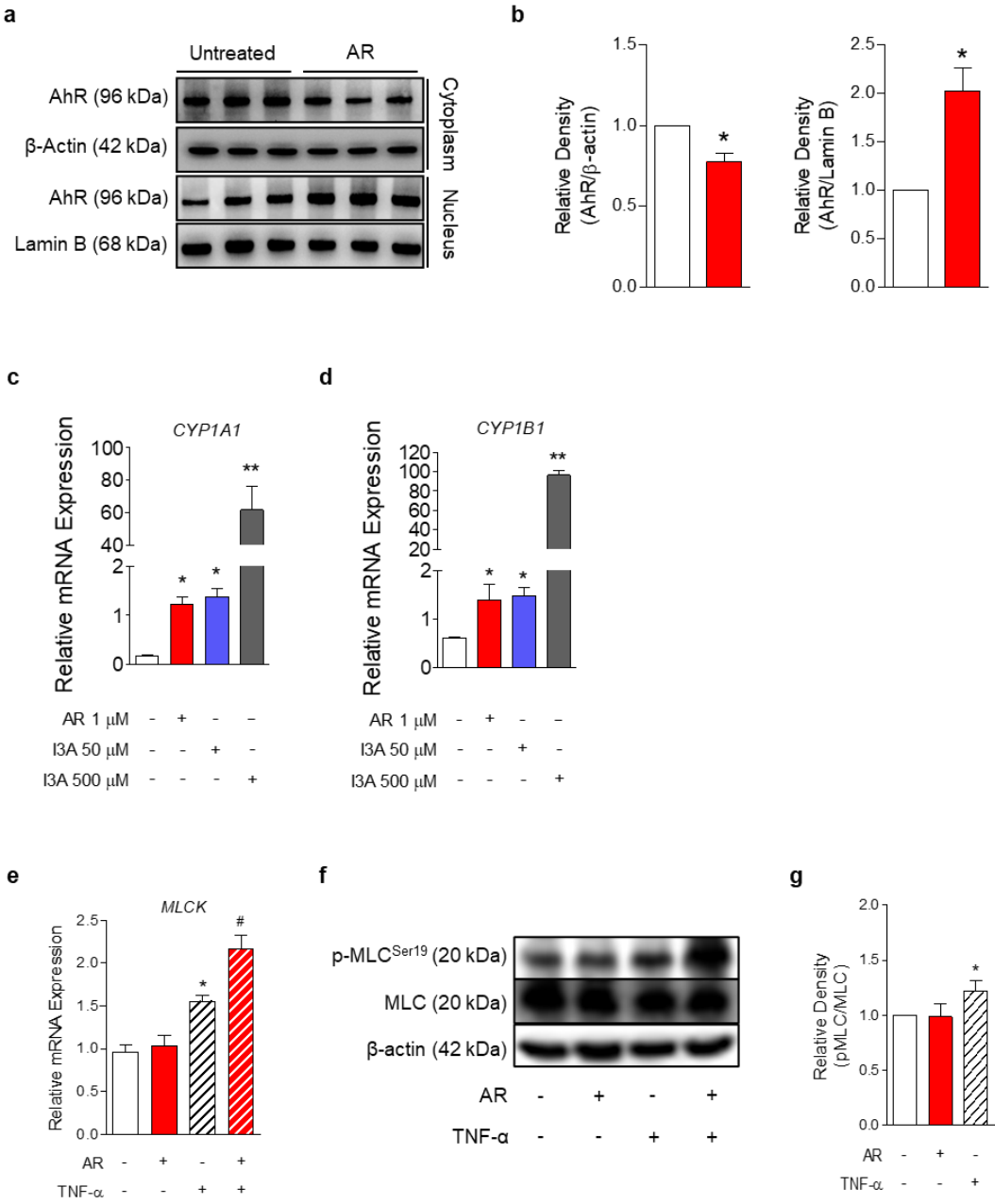
a
Untreated
AR
AhR (96 kDa)
β-Actin (42 kDa)
AhR (96 kDa)
Lamin B (68 kDa)
Cytoplasm
Nucleus
b
Relative Density (AhR/β-actin)
Relative Density (AhR/Lamin B)
c
CYP1A1
Relative mRNA Expression
AR 1 μM
I3A 50 μM
I3A 500 μM
d
CYP1B1
Relative mRNA Expression
AR 1 μM
I3A 50 μM
I3A 500 μM
e
MLCK
Relative mRNA Expression
AR
TNF-α
f
p-MLC^Ser19 (20 kDa)
MLC (20 kDa)
β-actin (42 kDa)
AR
TNF-α
g
Relative Density (pMLC/MLC)
AR
TNF-α

Figure 19: Allura Red AC up-regulates *CYP1A1*/*CYP1B1* mRNA expression and activates MLCK pathway in HT-29 cells. HT-29 cells were treated for 24 hours with AR (1 μM). Indole-3-carboxaldehyde (I3A) was used as a positive control. (**a**) Representative western blot analysis of nuclear translocation of AhR. β-actin was used for quantifying cytoplasmic proteins. Lamin B was used for quantifying nuclear proteins. (**b**) Relative density of nuclear and cytoplasmic AhR. (**c**) *CYP1A1* mRNA expression. (**d**) *CYP1B1* mRNA expression. In another experiment, HT-29 cells were pre-treated for 1 hour with TNF-α (10 ng/ml), followed by 24 hours of AR treatment (1 μM). (**e**) *MLCK* mRNA expression. (**f**) Representative western blot analysis of $pMLC^{Ser19}$, MLC and β-actin. (**g**) Relative density of $pMLC^{Ser19}$/MLC. Values represent as mean ± S.E.M. from three independent experiments. Statistical significance was determined by Student's *t*-test or one-way ANOVA with Dunnett's test. $^{*}P < 0.05$ or $^{**}P < 0.01$ versus untreated. $^{\#}P < 0.05$ versus TNF-α.

Next, whole colon-derived crypt organoids were cultured to mimic a more physiological microenvironment. Prior to treatment with AR (1 µM), whole colon organoids were exposed to TNF-α (10 ng/ml). When organoids were exposed to AR for 24 hours following 1 hour of TNF-α pre-treatment, there was reduction in the relative number of organoids with altered morphology and increase in dead cells in the lumen (indicated by dark lumen) (**Figure 20, a** and **b**). As a sphere-like geometry prevents access of AR to the apical side of the epithelium, 2D monolayers from 3D organoids were established as described previously (Crowley et al., 2020). In a functional 2D monolayer evidenced by accumulated ZO-1 at the intercellular membrane (**Figure 20, c** and **d**), there was no difference in *Mlck* mRNA expression levels when organoids were treated for 24 hours with AR compared to untreated organoids (**Figure 20e**). In contrast, when the monolayer was pre-treated for 1 hour with TNF-α prior to treatment for 24 hours with AR, *Mlck* mRNA expression levels were potently increased compared to those treated with TNF-α alone (**Figure 20e**). Collectively, these findings corroborate with *in vivo* findings that AR induces low-grade inflammation and impairs intestinal barrier function by activating MLCK pathway.

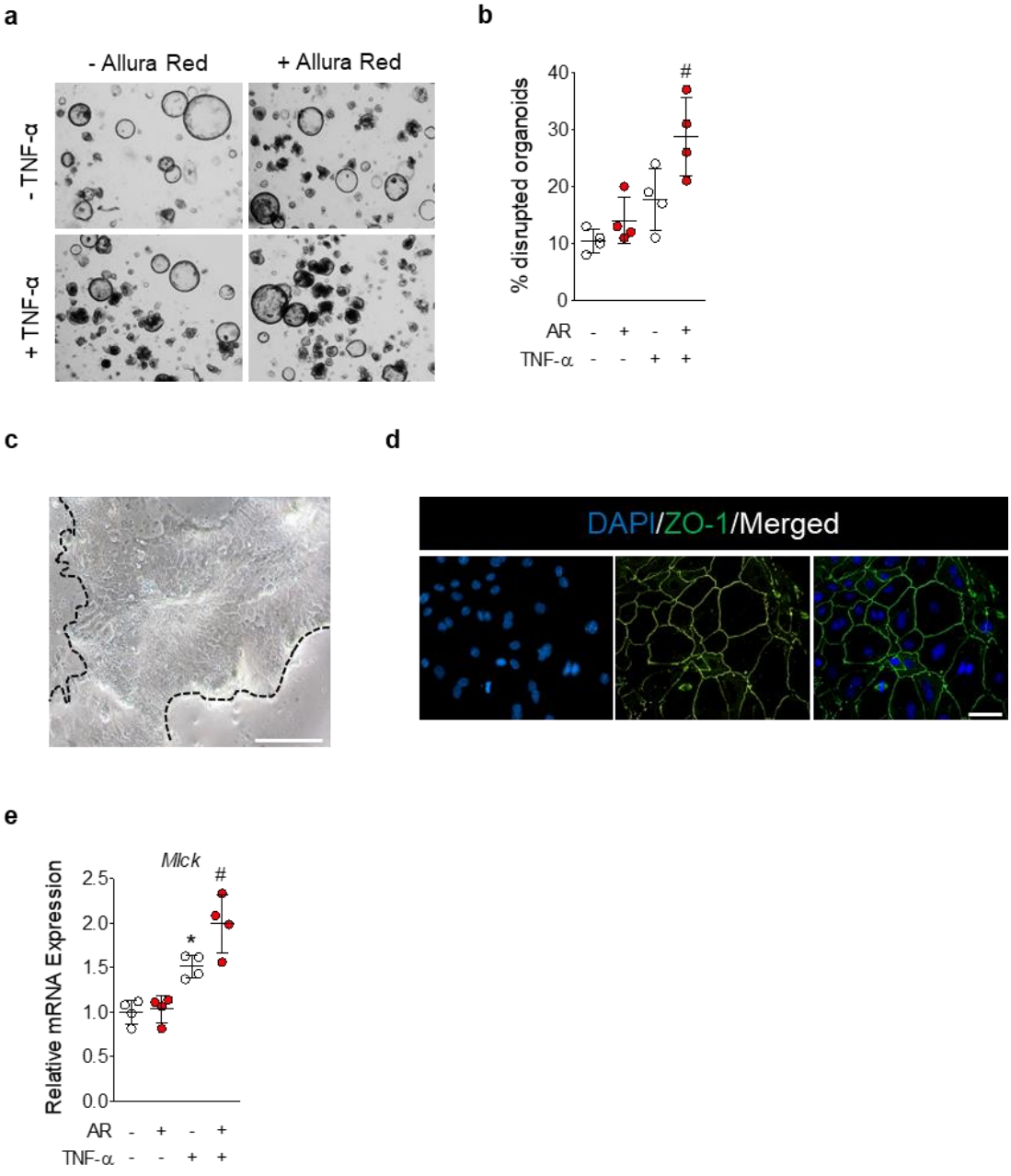
a
- Allura Red
+ Allura Red
- TNF-α
+ TNF-α
b
% disrupted organoids
40
30
20
10
0
#
AR - + - +
TNF-α - - + +
c
d
DAPI/ZO-1/Merged
e
Mlck
Relative mRNA Expression
2.5
2.0
1.5
1.0
0.5
0.0
*
#
AR - + - +
TNF-α - - + +

Figure 20: Allura Red AC up-regulates *CYP1A1*/*CYP1B1* mRNA expression and activates MLCK pathway in HT-29 cells. (**a**) Representative bright field (BF) images of mouse colonic organoids treated for 24 hours with or without AR (1 μM), followed by pre-treatment for 1 hour with or without TNF-α (10 ng/ml). (**b**) Percentage of disrupted organoids. A functional 2D monolayer derived from mouse colonic organoids. (**c**) Representative BF image of 2D monolayer derived from mouse colonic organoids. (**d**) Representative IF image of a functional 2D monolayer stained for ZO-1 (green) and DAPI (blue). Scale bar: 50 μm. (**e**) *Mlck* mRNA expression in 2D monolayer derived from mouse colonic organoids. Statistical significance was determined by Student's *t*-test. $^{*}P < 0.05$ versus untreated organoids/monolayer. $^{\#}P < 0.05$ versus organoids or monolayer treated with TNF-α.

3.10 *Colonic 5-HT is essential to enhancing the susceptibility to colitis by Allura Red AC*

To delineate the role of 5-HT in mediating the effect of AR, *Tph1*$^{-/-}$ mice were exposed to AR via normal chow diet for 12 weeks prior to induction of acute colitis with 3.5% DSS in drinking water for 7 days (**Figure 21a**). Similar food intake (**Figure 22**) and colitis assessment, namely body weight change, DAI, macroscopic score, colon length, and colon weight were observed in AR exposed DSS-treated mice compared to their DSS counterparts (**Figure 21, b-g**). Histological scores (**Figure 21, h** and **i**) and colonic MPO levels (**Figure 21j**) were also similar between AR exposed DSS-treated mice and their DSS counterparts. Additionally, the levels of colonic pro-inflammatory cytokines were not different between the two DSS groups (**Figure 21, k-m**). Similarly, when *Tph1*$^{-/-}$ mice were exposed to AR via normal drinking water for 12 weeks prior to induction of acute colitis with 3.5% DSS in drinking water for 7 days, there was no significant difference in the severity of DSS-induced colitis (**Figure 23** and **24**).

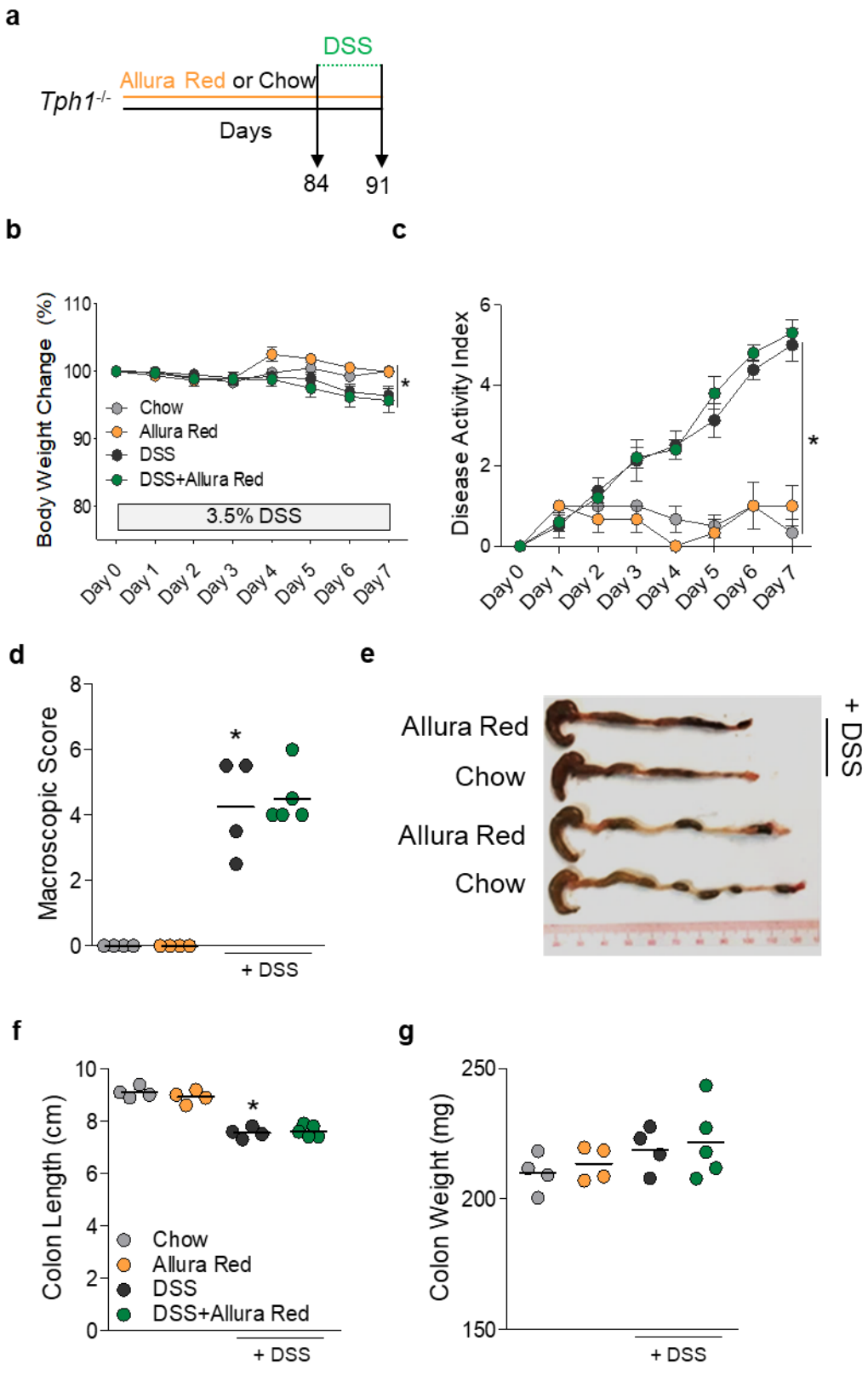
a
DSS
Allura Red or Chow
Tph1-/-
Days
84
91
b
Body Weight Change (%)
110
100
90
80
Chow
Allura Red
DSS
DSS+Allura Red
3.5% DSS
*
Day 0
Day 1
Day 2
Day 3
Day 4
Day 5
Day 6
Day 7
c
Disease Activity Index
6
4
2
0
*
Day 0
Day 1
Day 2
Day 3
Day 4
Day 5
Day 6
Day 7
d
Macroscopic Score
8
6
4
2
0
*
+ DSS
e
Allura Red
Chow
Allura Red
Chow
+ DSS
f
Colon Length (cm)
10
8
6
4
2
0
*
Chow
Allura Red
DSS
DSS+Allura Red
+ DSS
g
Colon Weight (mg)
250
200
150
+ DSS

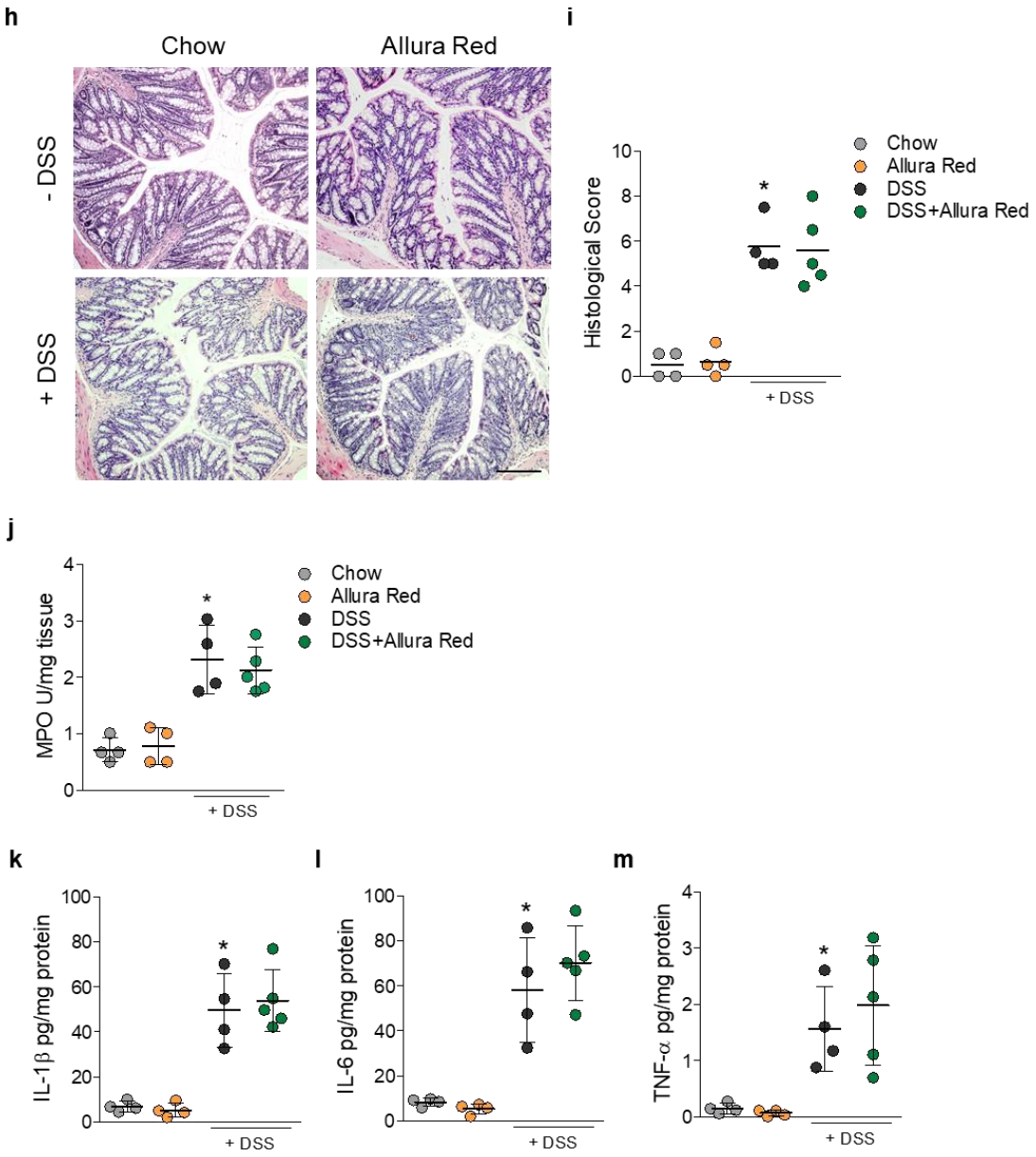
h
Chow
Allura Red
- DSS
+ DSS
i
Histological Score
Chow
Allura Red
DSS
DSS+Allura Red
+ DSS
j
MPO U/mg tissue
Chow
Allura Red
DSS
DSS+Allura Red
+ DSS
k
IL-1β pg/mg protein
+ DSS
l
IL-6 pg/mg protein
+ DSS
m
TNF-α pg/mg protein
+ DSS

Figure 21: Allura Red AC does not exacerbate DSS-induced colitis in Tph1-deficient mice. *Tph1*$^{-/-}$ mice were exposed to AR via normal chow diet or fed normal chow diet for 12 weeks (84 days) prior to induction of acute colitis by 3.5% DSS for 7 days. During DSS, mice were continuously exposed to AR in the corresponding groups. (**a**) Schematic illustration of the experimental design. (**b**) Body weight change during DSS. Each point represents mean ± S.E.M. (**c**) DAI during DSS. Each point represents mean ± S.E.M. (**d**) Macroscopic score. (**e**) Representative image of colons. (**f**) Colonic length (cm). (**g**) Colon weight (mg). (**h**) Representative images of H&E-stained colonic sections on day 7 post-DSS; scale bar: 100 μm. (**i**) Histological score. (**j**) Colonic MPO level. (**k-m**) Colonic pro-inflammatory cytokines. Values represent mean or mean ± S.D. from n = 4-5 mice/group. Statistical significance was determined by Student's *t*-test, one-way ANOVA with Bonferroni's test, or two-way ANOVA with Bonferroni's test. *$P < 0.05$ versus chow.

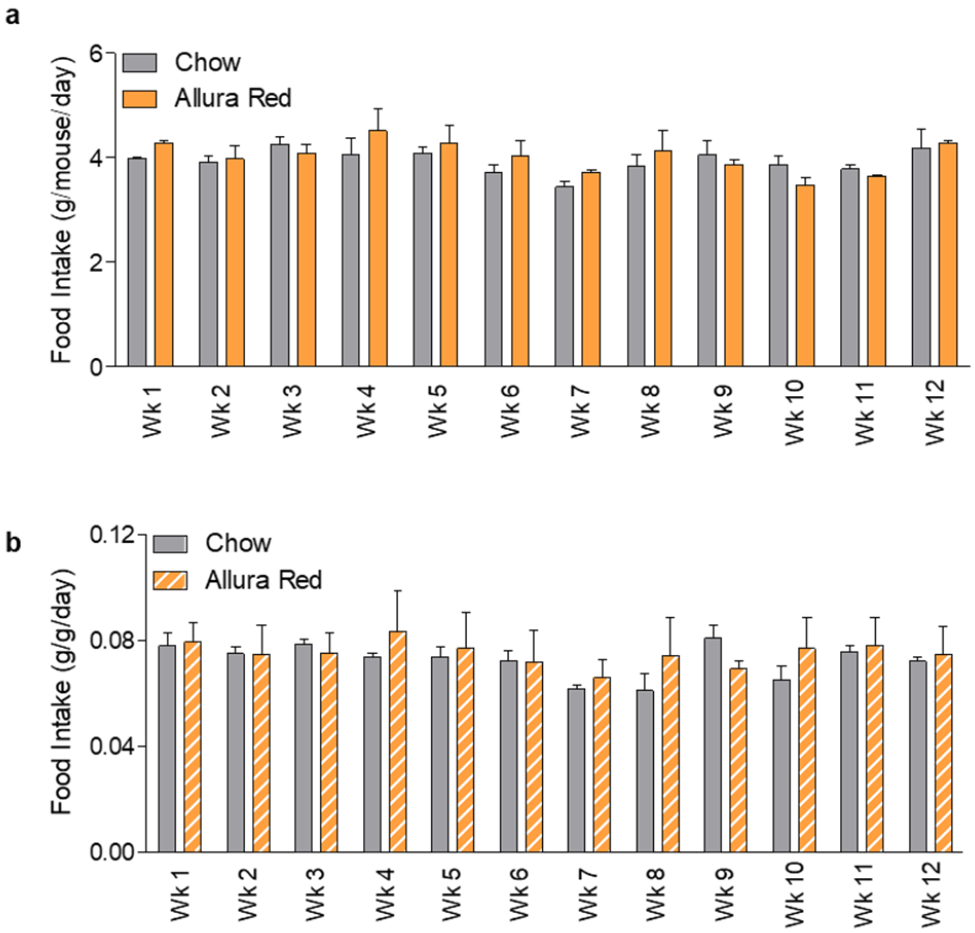

Figure 22: Food intake measurement in Tph1-deficient mice exposed to Allura Red AC via normal chow diet or fed with normal chow diet for 12 weeks. (**a**) Food intake represented in g per mouse per day. (**b**) Food intake is represented in g per g of mouse per day. Values represent mean ± S.E.M. from 8 to 9 mice per group.

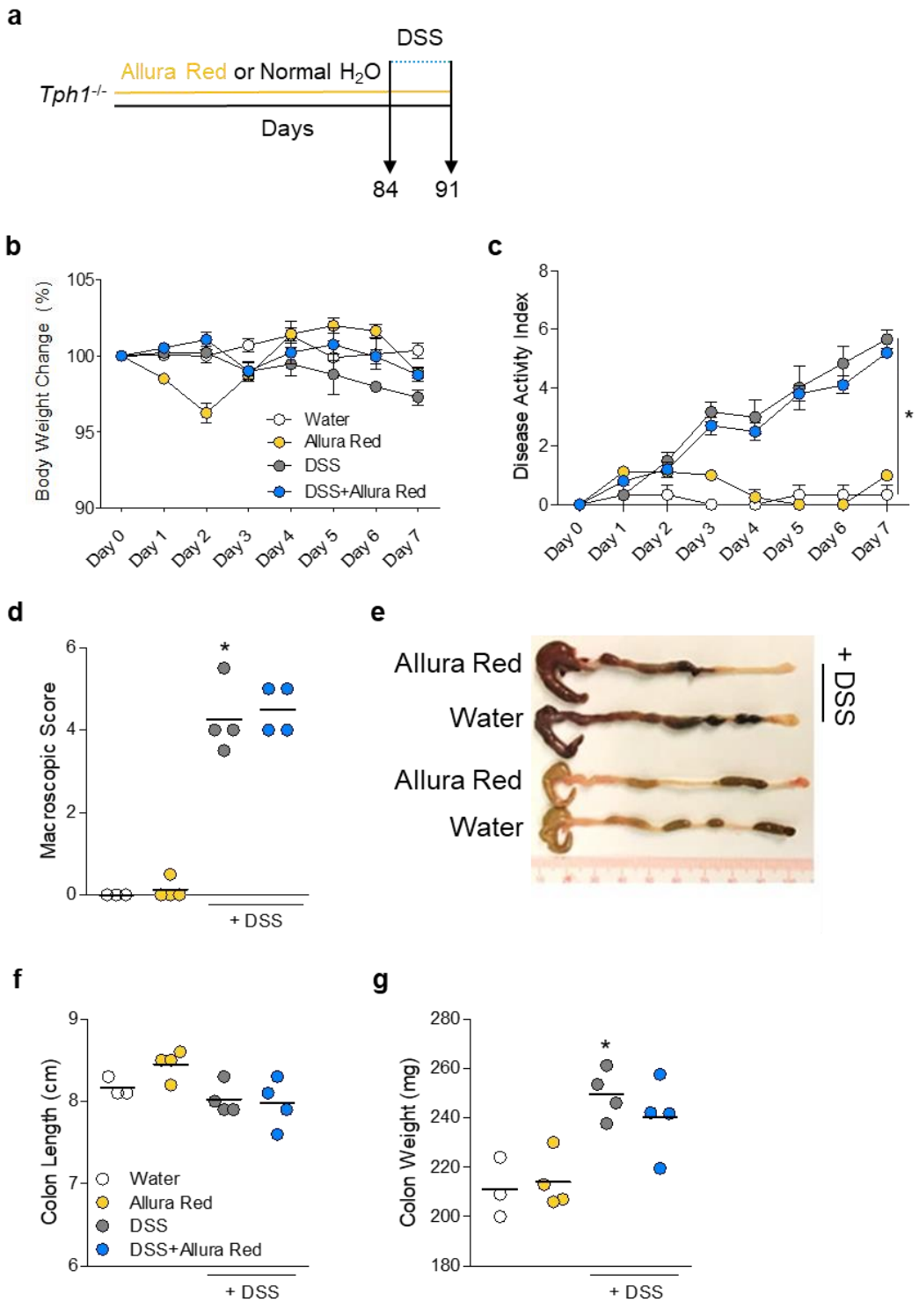
a
DSS
Allura Red or Normal H_2O
Tph1-/-
Days
84
91
b
Body Weight Change (%)
105
100
95
90
Water
Allura Red
DSS
DSS+Allura Red
Day 0
Day 1
Day 2
Day 3
Day 4
Day 5
Day 6
Day 7
c
Disease Activity Index
8
6
4
2
0
*
d
Macroscopic Score
6
4
2
0
*
+ DSS
e
Allura Red
Water
Allura Red
Water
+ DSS
f
Colon Length (cm)
9
8
7
6
Water
Allura Red
DSS
DSS+Allura Red
+ DSS
g
Colon Weight (mg)
280
260
240
220
200
180
*
+ DSS

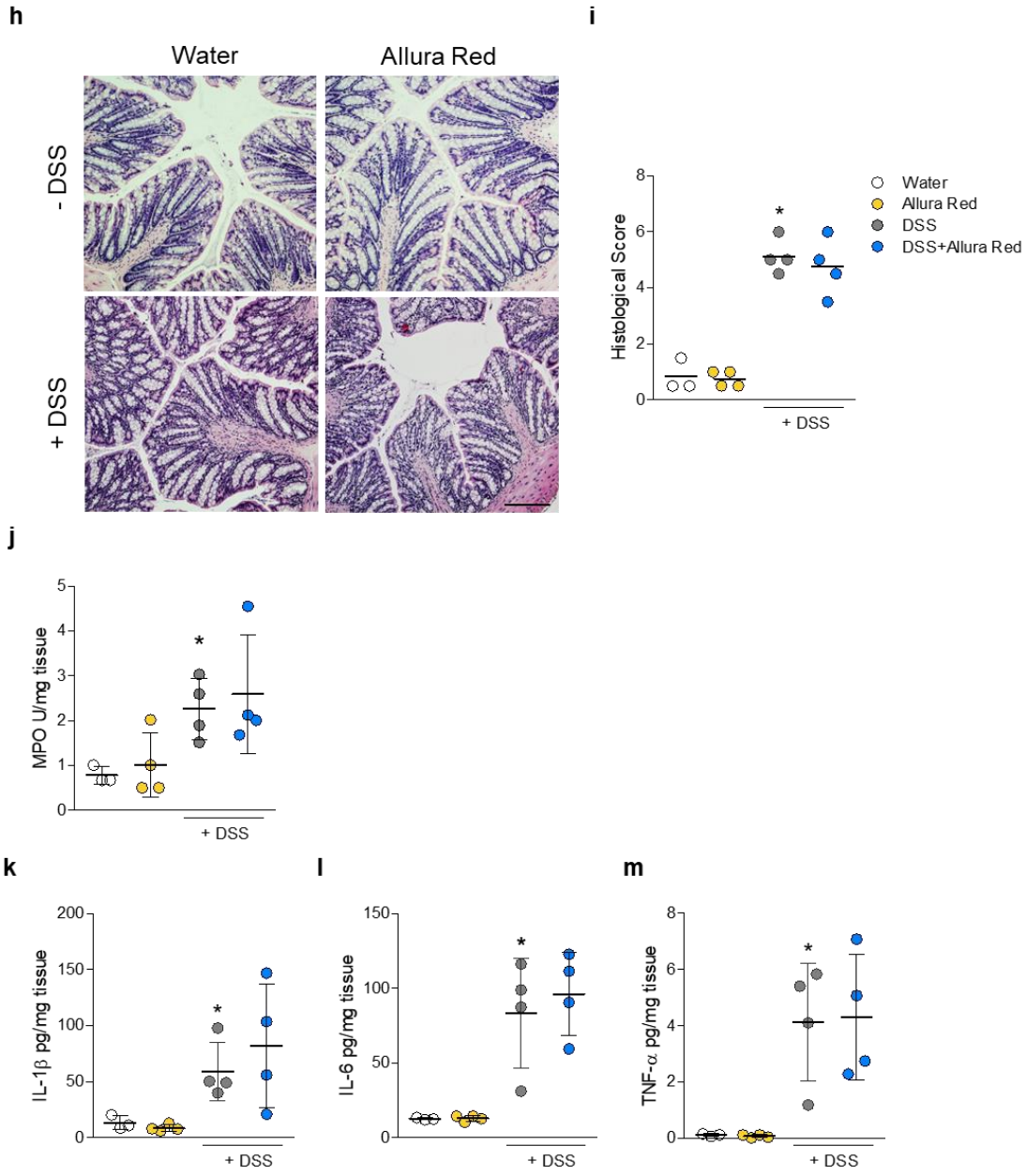
h
Water
Allura Red
- DSS
+ DSS
i
Histological Score
Water
Allura Red
DSS
DSS+Allura Red
+ DSS
j
MPO U/mg tissue
+ DSS
k
IL-1β pg/mg tissue
+ DSS
l
IL-6 pg/mg tissue
+ DSS
m
TNF-α pg/mg tissue
+ DSS

Figure 23: Allura Red AC in drinking water does not increase the severity of DSS-induced colitis in Tph1-deficient mice. *Tph1*$^{-/-}$ mice were exposed to AR via normal drinking water or administered with normal drinking water for 12 weeks (84 days) prior to induction of acute colitis by 3.5% DSS for 7 days. During DSS, mice were continuously exposed to AR in the corresponding groups. (**a**) Schematic illustration of the experimental design. (**b**) Body weight change during DSS. Each point represents mean ± S.E.M. (**c**) DAI during DSS. Each point represents mean ± S.E.M. (**d**) Macroscopic score. (**e**) Representative image of colons. (**f**) Colonic length (cm). (**g**) Colon weight (mg). (**h**) Representative images of H&E-stained colon sections on day 7 post-DSS; scale bar: 100 µm. (**i**) Histological score. (**j**) Colonic MPO level. (**k-m**) Colonic pro-inflammatory cytokines. Values represent mean or mean ± S.D. from n = 4 mice/group. Statistical significance was determined by Student's *t*-test, one-way ANOVA with Bonferroni's test, or two-way ANOVA with Bonferroni's test. **P* < 0.05 versus water.

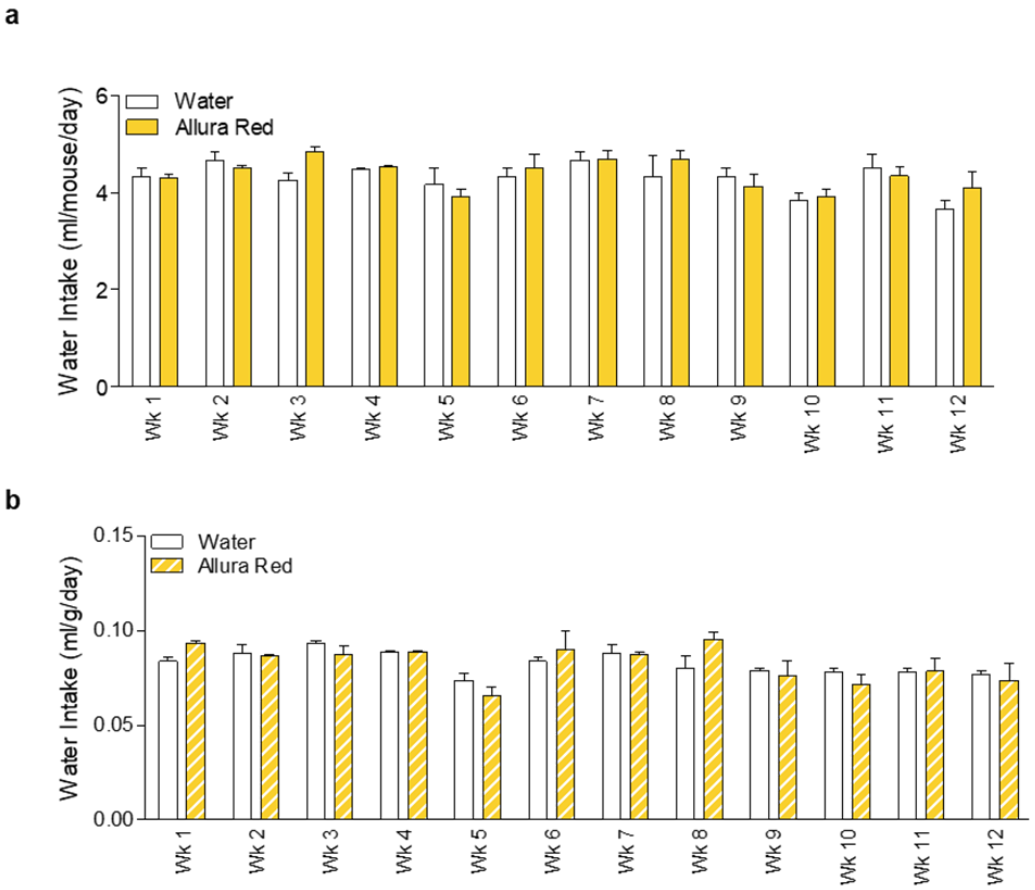

Figure 24: Water intake measurement in Tph1-deficient mice exposed to Allura Red AC via normal drinking water or administered with normal drinking water for 12 weeks. (**a**) Water intake represented in ml per mouse per day. (**b**) Water intake is represented in ml per g of mouse per day. Values represent mean ± S.E.M. from 7 to 8 mice per group.

Next, the underlying mechanism by which AR promotes 5-HT secretion was examined using BON cells. ROS is a well-characterized driver of colitis pathogenesis, (Blaser et al., 2016) and NF-κB activity is regulated by intracellular ROS level (Morgan et al., 2011). Elevation of intracellular ROS levels were detected by 2',7'-dichlorofluorescein diacetate (DCF-DA) fluorescence after 24 hours of AR treatment (1 μM) (**Figure 25a**); 5-HT (10 μM) was used as a positive control (Regmi et al., 2014). However, the effect of modulating 5-HT secretion and ROS production was absent when BON cells were treated for 24 hours with CS (**Figure 25b**). To further investigate the relationship between AR and 5-HT, BON cells were pre-treated for 1 hour with triptolide (20 nM), a potent NF-κB inhibitor, followed by 24 hours of AR treatment (1 μM). Triptolide attenuated the effect of AR on *TPH1* mRNA expression and 5-HT secretion (**Figure 25, c** and **d**). Similarly, 5-HT secretion was increased when the monolayer derived from whole mouse colonic organoids was treated for 24 hours with AR (1 μM) (**Figure 25e**). Taken together, these data indicate that AR induces ROS production, activates NF-κB, and promotes 5-HT secretion *in vitro*, while AR does not influence susceptibility to DSS-induced colitis in the absence of Tph1 *in vivo*.

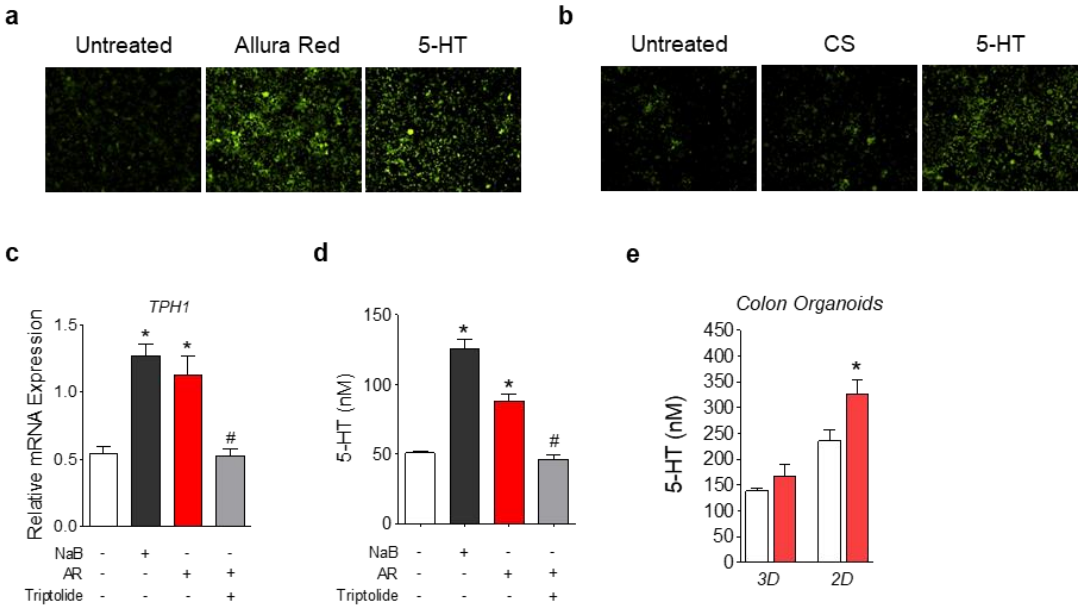
a
Untreated
Allura Red
5-HT
b
Untreated
CS
5-HT
c
TPH1
Relative mRNA Expression
1.5
1.0
0.5
0.0
NaB - + - -
AR - - + +
Triptolide - - - +
d
5-HT (nM)
150
100
50
0
NaB - + - -
AR - - + +
Triptolide - - - +
e
Colon Organoids
5-HT (nM)
450
400
350
300
250
200
150
100
50
0
3D
2D

Figure 25: Allura Red AC induces ROS production and activates NF-κB to increase 5-HT secretion *in vitro*. (**a)** Representative fluorescence image of intracellular reactive oxygen species (ROS) detected using 2',7'-dichlorofluorescin diacetate (DCF-DA) in BON cells treated for 24 hours with AR (1 µM) or 5-HT (10 µM). (**b**) Representative fluorescence image of intracellular ROS detected using DCF-DA in BON cells treated for 24 hours with CS (1 µM) or 5-HT (10 µM). 5-HT was used as a positive control for ROS induction. (**c**) *TPH1* mRNA expression and (**d**) 5-HT level in the cell culture supernatant of BON cells pre-treated for 1 hour with triptolide (20 nM), followed by AR treatment (1 µM). NaB (1 mM) was used as a positive control. (**e**) 5-HT level in 2D monolayer derived from colon organoids. Data represent 3 independent experiments. Values represent mean ± S.E.M. Statistical significance was determined by Student's *t*-test or one-way ANOVA with Bonferroni's test. $^{*}P < 0.05$ versus untreated. $^{\#}P < 0.05$ versus AR.

3.11 *Perturbed gut microbiota by Allura Red AC enhances colitis susceptibility*

To explore whether the increased susceptibility to colitis by AR is mediated through regulation of the gut microbiota composition, bacterial profiling in cecal luminal contents was performed to elucidate whether the low-grade colon inflammation observed in naïve C57BL/6 mice (**Figure 16** and **18**) was associated with disruption of the gut microbiota composition. Analysis of β-diversity using Bray-Curtis dissimilarity revealed a markedly distinct clustering pattern between the two groups along the PCoA1 axis (**Figure 26a**). At the phylum level, the composition of microbiota was changed between the two groups. Relative abundance of Proteobacteria, *Deferribacteres* bloomed in mice exposed to AR (**Figure 26b**). At the genus level, the relative abundance of *Roseburia* was decreased while that of *Desulfovibrio, Muribaculum, Mucispirillum*, and *Turicibacter* was increased in AR exposed mice (**Figure 26c**).

To substantiate the observation that perturbed gut microbiota enhanced colitis susceptibility by AR exposure, GF mice were inoculated by gavage with an equally weighted pool of cecal contents derived from mice exposed to AR or control for 3 days (once per day), followed by 21 days of colonization prior to 2.0% DSS in drinking water for 7 days (**Figure 26d**). During the experiment, all mice were fed normal chow diet. GF mice, which were inoculated with cecal contents from mice previously exposed to AR (GF-AR), showed increased severity of colitis compared with GF mice inoculated with cecal contents of control mice (GF-NC). Although the body weight loss was similar between the two groups (**Figure 26e**), DAI was significantly higher in GF-AR (**Figure 26f**). This increased DAI was associated with higher macroscopic scores

(**Figure 26g**) and reduced colonic lengths (**Figure 26h**). Additionally, histological scores (**Figure 26, i** and **j**) and colonic MPO levels (**Figure 26k**) were elevated along with increased colonic 5-HT levels in GF-AR compared with GF-NC (**Figure 26l**). Furthermore, colonic pro-inflammatory cytokines, such as IL-1β, IL-6, and TNF-α, were significantly elevated in GF-AR compared with GF-NC (**Figure 26, m-o**). These findings show that perturbed gut microbiota induced by AR exposure exacerbates DSS-induced colitis.

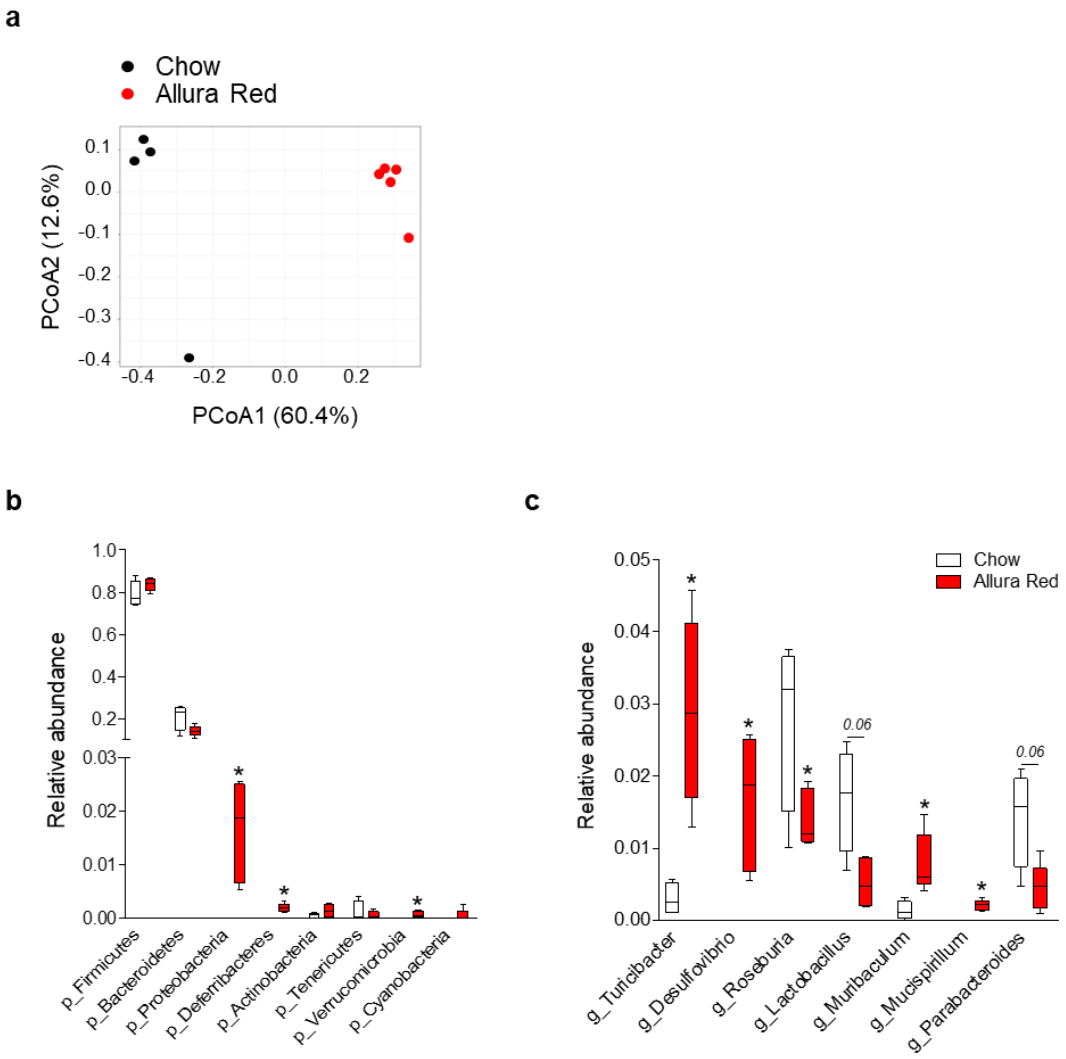
a
Chow
Allura Red
PCoA2 (12.6%)
PCoA1 (60.4%)
b
Relative abundance
p_Firmicutes
p_Bacteroidetes
p_Proteobacteria
p_Deferribacteres
p_Actinobacteria
p_Tenericutes
p_Verrucomicrobia
p_Cyanobacteria
c
Chow
Allura Red
Relative abundance
0.06
0.06
g_Turicibacter
g_Desulfovibrio
g_Roseburia
g_Lactobacillus
g_Muribaculum
g_Mucispirillum
g_Parabacteroides

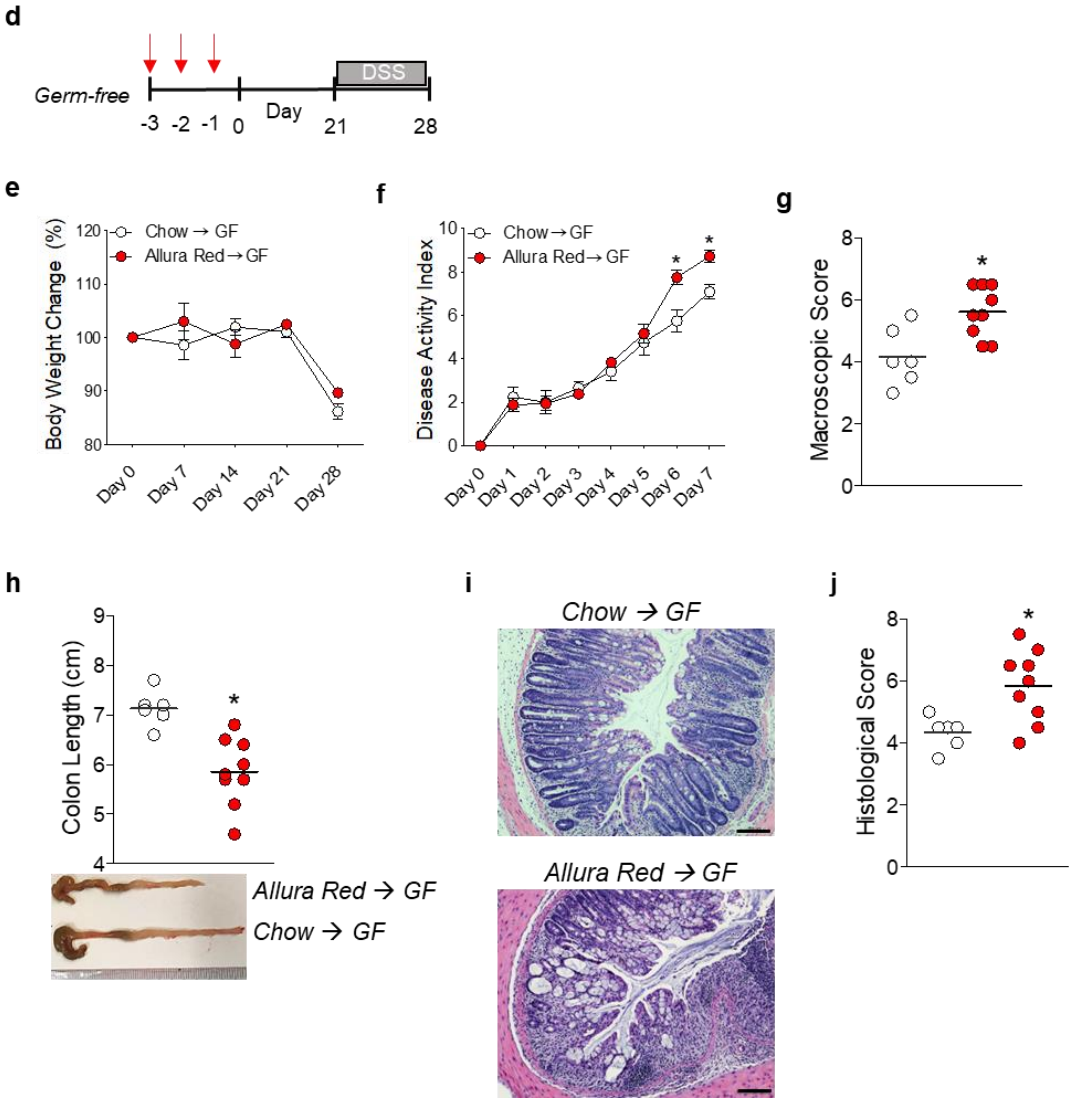
d
Germ-free
DSS
-3 -2 -1 0
Day
21
28
e
Body Weight Change (%)
Chow → GF
Allura Red → GF
Day 0
Day 7
Day 14
Day 21
Day 28
f
Disease Activity Index
Chow → GF
Allura Red → GF
Day 0
Day 1
Day 2
Day 3
Day 4
Day 5
Day 6
Day 7
g
Macroscopic Score
h
Colon Length (cm)
Allura Red → GF
Chow → GF
i
Chow → GF
Allura Red → GF
j
Histological Score

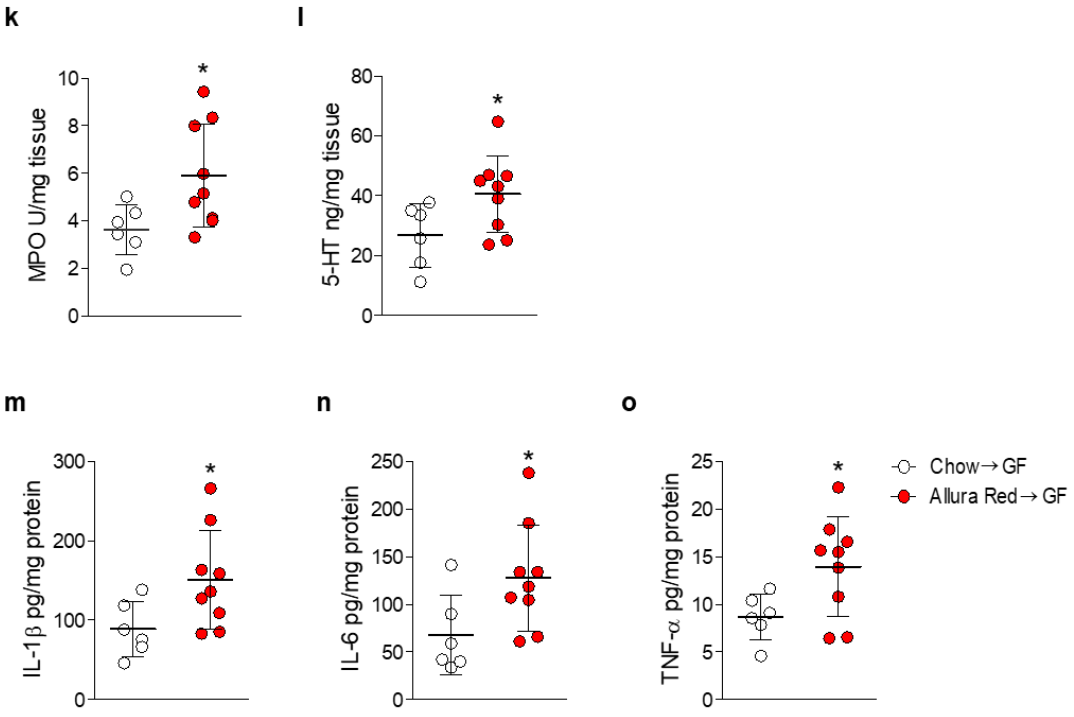
k
MPO U/mg tissue
10
8
6
4
2
0
*
l
5-HT ng/mg tissue
80
60
40
20
0
*
m
IL-1β pg/mg protein
300
200
100
0
*
n
IL-6 pg/mg protein
250
200
150
100
50
0
*
o
TNF-α pg/mg protein
25
20
15
10
5
0
*
Chow→GF
Allura Red→GF

Figure 26: Transplantation of Altered Gut Microbiome from Allura Red AC exposed mice into GF mice exacerbates DSS-induced colitis. 16S rRNA bacterial profiling at the v3-v4 region using cecal contents was carried out. (**a**) Bray-Curtis dissimilarity revealed each group of mice possessed distinct microbiota. Boxplots of phylum (**b**) and genus (**c**) level abundance showing lower and upper quartiles along with median value for relative abundance. Fresh cecal samples were obtained and pooled at equal amounts from naïve C57BL/6 mice exposed to AR via normal chow diet or fed normal chow diet. A 200 μl inoculum was orally administered to each GF mouse once per day for 3 consecutive days, followed by 3 weeks of colonization period prior to 2.0% DSS treatment for 7 days. All mice received normal chow diet during experiment. (**d**) Schematic illustration of the experimental design. Red arrow indicates daily inoculation. (**e**) Body weight change from day 0 to day 28. (**f**) Disease activity index during 7 days of 2.0% DSS. (**g**) Macroscopic score. (**h**) Colonic length (cm) (*top*); a representative image of colons (*bottom*) (**i**) Representative images of H&E-stained colonic sections on day 7 post-DSS; scale bar: 100 μm. (**j**) Histological score. (**k**) Colonic MPO level (**l**) Colonic 5-HT level. (**m-o**) Colonic pro-inflammatory cytokines. Values represent mean or mean ± S.D. from n = 4-9 mice/group. Statistical significance was determined by Mann-Whitney U test, Student's *t*-test, or two-way ANOVA with Bonferroni's test. $*P < .05$ versus Chow or Chow → GF.

3.12 *Allura Red AC promotes 5-HT synthesis in germ-free mice*

To further discern whether increased colitis susceptibility by AR exposure is dependent on the gut microbiota, GF mice were exposed to AR via normal chow diet for 14 weeks (**Figure 27a**). There was no difference in colonic lengths (**Figure 27b**). Colonic MPO levels were increased (**Figure 27c**), and histological scores were higher in mice exposed to AR (**Figure 27, d** and **e**). In addition, the numbers of 5-HT–positive cells were significantly increased (**Figure 27, f** and **g**), and colonic 5-HT levels were also elevated, in mice exposed to AR (**Figure 27h**). Thought not significantly increased, there was also a trend for high colonic IL-1β levels (**Figure 27i**). These findings indicate that AR can promote 5-HT synthesis and inflammatory signals via the gut microbiota-independent pathway.

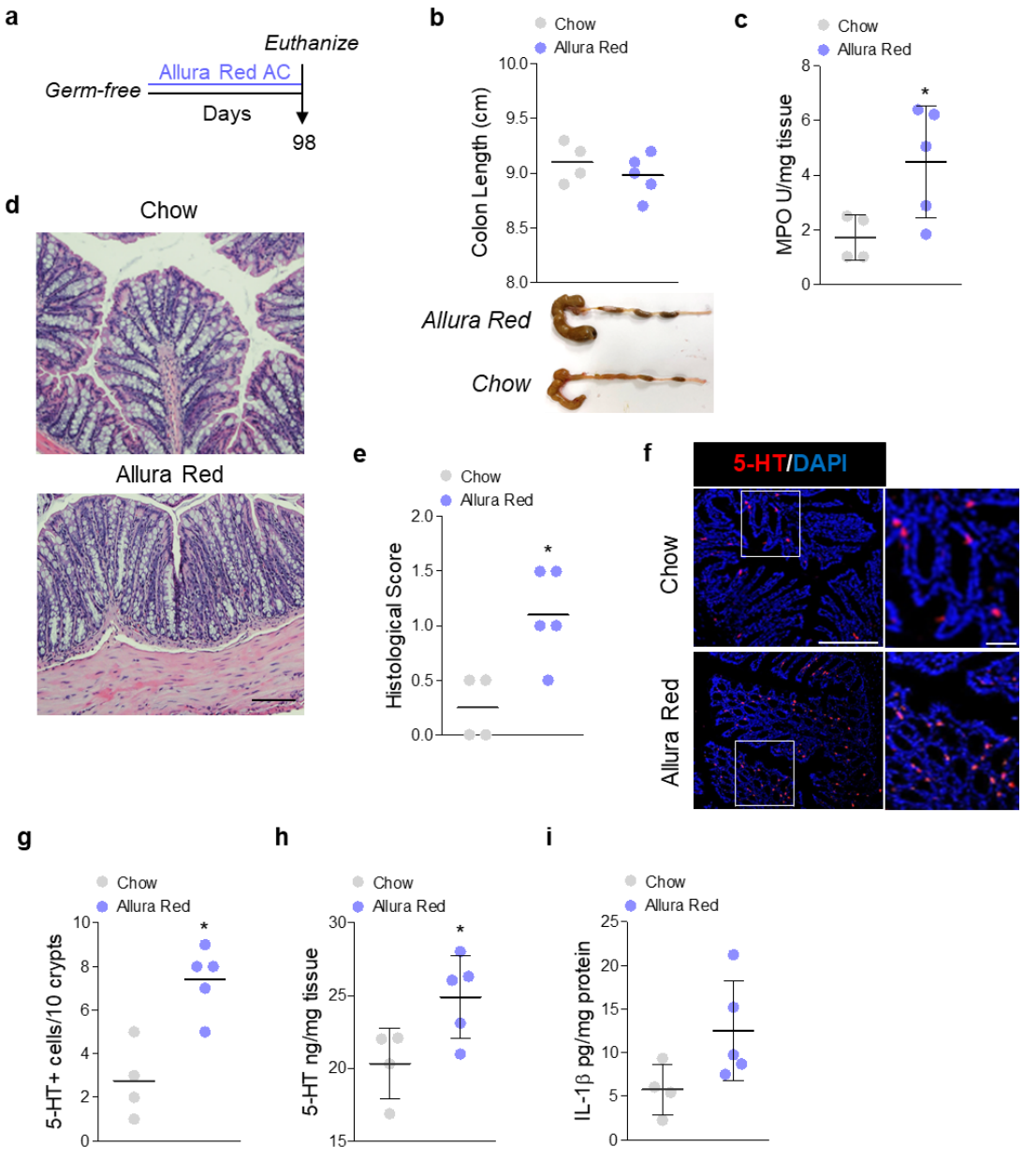
a
Euthanize
Allura Red AC
Germ-free
Days
98
b
Chow
Allura Red
Colon Length (cm)
10.0
9.5
9.0
8.5
8.0
Allura Red
Chow
c
Chow
Allura Red
MPO U/mg tissue
8
6
4
2
0
*
d
Chow
Allura Red
e
Chow
Allura Red
Histological Score
2.0
1.5
1.0
0.5
0.0
*
f
5-HT/DAPI
Chow
Allura Red
g
Chow
Allura Red
5-HT+ cells/10 crypts
10
8
6
4
2
0
*
h
Chow
Allura Red
5-HT ng/mg tissue
30
25
20
15
*
i
Chow
Allura Red
IL-1β pg/mg protein
25
20
15
10
5
0

Figure 27: Allura Red AC increases colonic 5-HT level in the absence of microbial signals. GF mice were exposed to AR via normal chow diet or fed with normal chow diet for 14 weeks (98 days). (**a**) Schematic illustration of the experimental design. (**b**) Colonic length (cm); a representative image of colons (*bottom*). (**c**) Colonic MPO level. (**d**) Representative images of H&E-stained colon sections; scale bar: 100 μm. (**e**) Histological score. (**f**) Representative images of IF staining for 5-HT (red) in the colon; scale bar: 50 μm. (**g**) Number of 5-HT–positive cells per 10 crypts. (**h**) Colonic 5-HT level. (**i**) Colonic IL-1β level. Values represent mean or mean ± S.D. from n = 4-5 mice/group. Statistical significance was determined by Student's *t*-test. **P* < .05 versus chow.

—CHAPTER 4—

DISCUSSION

Every day, humans are exposed to different chemical substances through a variety of pathways, including dietary intake. The Western diet, which has permeated cultures around the world due to taste and convenience, is largely composed of ready-to-eat or ready-to-heat processed foods that are typically high in salt, and invert sugar and low in fibre, vitamins, and minerals (Moubarac et al., 2017). Notably, this dietary pattern may comprise nearly two-thirds, of the total caloric intake of youths (weight mean age, 10.7 years) in the United States (Wang et al., 2021). As previously noted, diet shapes the microbial ecology of the gut, and changes in microbial composition are strongly associated not only with metabolic and neurological disorders but also with numerous intestinal disorders, including IBD (Backhed et al., 2005; Manichanh et al., 2006). Recently, a prospective cohort study involving approximately 120,000 participants from low- to high-income countries found that higher intake of ultra-processed foods (e.g., processed meats, soft drinks, snacks, and refined sweetened foods) was positively associated with the risk of developing IBD (Narula et al., 2021). Though often overlooked, the Western diet is also especially rich in food additives and synthetic colourants that enhance the flavour and appearance of foods. While several risk factors tied with the Western diet have been associated with chronic inflammatory diseases (Furman et al., 2019), the current knowledge of the role of these dietary components in IBD pathogenesis is still modest. This thesis provides evidence that the widely used synthetic colourant, Allura Red AC, promotes colitis by influencing Tph1-derived 5-HT biosynthesis in both gut microbiota-dependent and -independent pathways.

Across several *in vitro* experiments, the ability of AR to enhance 5-HT biosynthesis and elicit inflammatory effects was examined. In BON cells, a widely used model of human EC cells, AR, even a low concentration (1 pM) showed a pronounced increase in 5-HT levels in comparison to other synthetic dyes. This was correlated with increased *Tph1* mRNA expression. The metabolite of AR, CS, did not elicit these effects. When pre-treated with TNF-α, AR promoted IL-8 secretion and the diminishment of E-cadherin in HT-29 cells. The pro-inflammatory nature of AR was also observed in LPS-induced RAW264.7 macrophages, where the levels of the cytokines, IL-1β, IL-6 and TNF-α, were also potently increased compared with LPS treatment alone. Taken together, these *in vitro* findings suggest that in the presence of inflammatory mediators such as TNF-α and LPS, AR is a potent driver that can exacerbate inflammatory signals and may diminish intestinal epithelial barrier function *in vivo*.

Expanding upon the aforementioned *in vitro* work, the relationship between AR and intestinal inflammation was investigated across two mouse models. AR exposure over the course of 12 weeks, either via drinking water or dye-laden normal chow diet, exacerbated DSS-induced colitis. C57BL/6 mice exposed to AR showed elevated DAI, histological and macroscopic scoring, colonic MPO, and levels of the pro-inflammatory cytokines in the colon, such as IL-1β, IL-6, and TNF-α, compared to their naïve counterparts, on day 7 post-DSS. Studies using cultured monolayers and animal models of colitis have provided evidence that inflammatory cytokines, such as IL-1β and TNF-α, trigger tight junction barrier dysfunction via MLCK activation (Clayburgh et al.,

2005; Zolotarevsky et al., 2002). Here, in DSS studies involving C57BL/6 mice, markers of intestinal epithelial barrier function including ZO-1 (*Tjp1*), *Ocln* and *Muc2* expression, were impaired. These findings corroborate the *in vitro* observations where inflammatory mediators in combination with AR potently induced immune responses and impaired the barrier function. Though not explicitly touched on here, it should also be noted that mode of delivery (i.e., food or water-based consumption) does not alter the ability of AR to exacerbate colitis.

MLCK activation is associated with intestinal epithelial dysfunction and hyperpermeability (Yao et al., 2020), which is correlated with enhanced clinical activity in patients with IBD (Blair et al., 2006). MLCK-mediated tight junction disruption in the intestinal epithelium leads to apoptosis-mediated intestinal epithelial barrier loss and the induction of experimental colitis (Günther et al., 2013). These findings are further consistent with previous studies where the loss of intestinal epithelial barrier mediated by hyperpermeability precedes the onset of colitis in clinically healthy first-degree relatives of those with CD or in individuals with familial risk (Irvine et al., 2000; Turpin et al., 2020). Here, in naïve C57BL/6 mice, AR induced low-grade colonic inflammation even in the absence of DSS by impairing the intestinal epithelial barrier function via MLCK. The effects of AR on MLCK activation were also observed in both *in vitro* (HT-29 cells) and *ex vivo* (mouse colonic organoids) systems.

Host defense peptides are also important in mucosal defense; the lower levels of these peptides are observed IBD patients (Wehkamp et al., 2005). These peptides directly induce the expression of MUC2 and tight junction proteins *in vitro* (Otte et al.,

2008; Tai et al., 2008). Moreover, a deficiency of PPAR-γ which is an important regulator of antimicrobial factor that maintains constitutive expression of the antimicrobial peptides, β-defensins, in the colon, leads to defective killing activity against major groups of commensal bacteria (Peyrin-Biroulet et al., 2010). Here, the observed low-grade colonic inflammation induced by AR was associated with reduced markers of host defense, including *Pparg*, *mdefb3* and *Reg3g* in the colon. Previously, high levels of *mdefb3* and *Pparg* expression were found in *Tph1*$^{-/-}$ mice, which was further confirmed using HT-29 cells that 5-HT directly inhibits *Pparg* and human β-defensin 2 (hBD-2; a human ortholog of mouse β-defensin 3) expression (Kwon et al., 2019). Thus, higher numbers of 5-HT–positive cells along with increased colonic 5-HT levels by AR exposure during low-grade colonic inflammation may account for this reduction in antimicrobial factors.

In conjunction with findings in the DSS model, AR also triggered an early onset of CD4^{+}CD45RB^{high} T cell-induced colitis with CD45RB^{hi}-AR mice displaying significantly higher macroscopic and histological scoring, DAI, and colonic pro-inflammatory cytokines, IL-1β, IL-6, TNF-α, and IFN-γ levels in comparison to CD45RB^{hi} mice. IFN-γ, a Th1 cytokine, plays an essential role in IBD and in the development of experimental colitis across both DSS and CD4^{+}CD45RB^{high} T cell models (Ito et al., 2006). In synergy with TNF-α, IFN-γ promotes intestinal epithelial barrier defects by disrupting the tight junctional complexes via MLCK, contributing to the pathology of IBD (Wang et al., 2005; Youakim et al., 1999). This evidence parallels with the findings in this thesis that, in addition to the effect of AR on direct activation

of MLCK, increased levels of colonic IFN-γ and TNF-α can trigger immune-mediated intestinal epithelial barrier dysfunction.

It was recently shown that AR consumption at a dosage under the threshold of what is considered safe in humans (0.025% w/v) promoted colitis in transgenic mice overexpressing IL-23 (He et al., 2021); the signaling pathway of which is strongly linked with IBD (Dotan et al., 2007; Duerr et al., 2006). These mice were intermittently exposed to AR via normal chow diet or normal drinking water for 7 days, followed by 7 days of vehicle, for a total of 4 cycles. It is reasonable that the intermittent exposure at this dosage (2.5 times higher than the one used in this thesis) was sufficient to induce colitis in genetically susceptible mice. In this thesis, when C57BL/6 mice were intermittently exposed to AR (24 hours per week) for 12 weeks before DSS-induced colitis, there was no difference in the colitis severity. It appears that the exposure level in the intermittent exposure experiment was not sufficient to promote colitis compared to the level being exposed every day.

The immunopathogenic mechanisms induced by AR in the transgenic mice overexpressing IL-23 were dependent on IFN-γ-producing $CD4^+$ T cells (similar to those found in patients with IBD), which contributed to intestinal epithelial damage through marked IEC apoptosis; this effect was abrogated by genetically ablating IFN-γ in transgenic mice overexpressing IL-23 (Chen et al., 2022; He et al., 2021). In this thesis, when *Rag1*$^{-/-}$ mice reconstituted with T cells were exposed to AR for 5 weeks, higher levels of colonic TNF-α and IFN-γ were found. It has previously been shown that IFN-γ, in synergy with TNF-α, significantly decreases SERT expression in IECs

(Foley et al., 2007), while IFN-γ from $CD4^+$ T cells increased Trp uptake and promoted 5-HT secretion from T cells (Finocchiaro et al., 1988).

The importance of Tph1-derived 5-HT in the pathogenesis of colitis is supported by previous work that suggested pharmacologically inhibiting mucosal 5-HT synthesis uncouples the positive linkage of colonic 5-HT to colitis (Kim et al., 2015; Margolis et al., 2014). Since both *in vitro* and *in vivo* experiments involved in this thesis established a connection between 5-HT, AR exposure and inflammation, *Tph1*$^{-/-}$ mice were used to elucidate if the ability of AR to promote colitis was predicated on the expression of Tph1. Indeed, *Tph1*$^{-/-}$ mice were not more susceptible to DSS-induced colitis after exposure to AR. Additionally, AR promoted mild colitis, which was associated with increased colonic 5-HT levels and elevated numbers of 5-HT–positive cells in the colon of naïve C57BL/6 mice. Furthermore, when GF mice were exposed to AR, colonic 5-HT levels were increased. Together, these findings illustrate that any direct effects of AR on the gut microbiota do not influence colitis susceptibility if Tph1-derived 5-HT production is inhibited, suggesting that the indirect effect of AR via the host's serotonergic system on the gut microbiota contributes to a greater extent. Similarly, an increased 5-HT secretion via NF-κB through direct induction of ROS generation by AR suggests that a positive feedback cycle is in play and drives 5-HT biosynthesis. Given that high 5-HT levels promote NADPH oxidase 2 (NOX2)-derived ROS production and prime colonic epithelial cells toward inflammation (Regmi et al., 2014), as well as alter host tolerance to commensal *E. coli*, promoting adherent-invasive colonization through impaired intestinal epithelial cell junctions (Banskota et al., 2017), it is thus reasonable

to state that AR exposure primes colonic epithelial cells towards inflammatory responses through Tph1-derived 5-HT.

Low-grade inflammation in naïve C57BL/6 mice exposed to AR was associated with an increased abundance of *Turicibacter*. *T. sanguinis* expresses a neurotransmitter sodium symporter-related protein with sequence and structural homology to mammalian SERT (Fung et al., 2019). In this way, *T. sanguinis* signals nearby EC cells and imports 5-HT through a mechanism that is inhibited by the selective serotonin reuptake inhibitor (SSRI), fluoxetine (Fung et al., 2019). Previously, mice lacking TNF-α (*Tnfa*$^{-/-}$) showed decreased severity of TNBS-induced colitis with a lower abundance of *Turicibacter* compared to WT mice (Jones-Hall et al., 2015). The data from this study as well as a past study positing that *Turicibacter* may play a role in the development of IBD (Bernstein et al., 2017) suggest that further investigation is warranted to precisely determine the role of *Turicibacter* in colitis.

Across several *in vivo* experiments involving naïve C57BL/6 mice, reductions in *Muc2* expression were consistently observed. In the colon, defects in the inner mucus layer, normally devoid of microorganisms, can lead to exaggerated immune responses by the invasion of microbes and thus instigate intestinal inflammation (Johansson, 2014). In this thesis, the presence of AR was associated with reduced *Muc2* expression and the depletion in the number of PAS+ goblet cells, indicating that AR exposure can have a direct impact on the mucus layer in the colon. Defects in the mucus layer may be further attributed to the microbial composition found in AR-exposed C57BL/6 mice, which harboured increased levels of the mucin-degrading, Gram-negative commensal

bacteria, *Mucispirillum*. These bacteria are mucus-dwelling pathobionts which act as one of the several indicator phylotypes for active colitis (Berry et al., 2012; Rooks et al., 2014). For instance, *M. schaedleri*, which express systems for scavenging ROS *in vivo*, localize close to the mucosa and expand during inflammation (Loy et al., 2017). Consistent with this evidence, the development of spontaneous colitis with the classical pathological hallmarks of CD was triggered by the presence of *M. schaedleri* in mice lacking two CD-related genes, namely NOD2 and the cytochrome b-245 beta chain (CYBB) subunit of phagocyte NOX2 (Caruso et al., 2019). This study suggests *Mucispirillum* is a microbial trigger for colitis, and that expansion of *Mucispirillum* in mice exposed to AR, in this thesis, may play a role in incitement of colitis. As noted earlier, the gut microbiota is known to play a critical role in the development of colitis. For instance, IL-10-deficient mice, which typically develop spontaneous colitis under SPF conditions, do not develop colitis under GF condition (Sellon et al., 1998). Perturbation of the gut microbiota by AR exposure led to increased severity of DSS-induced colitis in GF mice upon transfer of the microbiota from AR exposed SPF mice. These findings further support the concept that disruption of the gut microbiota composition is an important factor involved in the pathogenesis of colitis.

The current data suggests that AR enhances the susceptibility to colitis. It should be mentioned that in this study, the effect of the AR's microbially-derived metabolite, CS, was not further tested *in vivo* as CS did not promote 5-HT secretion *in vitro*. Likewise, CS did not have any effects on the production of IL-8 *in vitro*. This finding is consistent with previous findings that CS did not induce colitis in transgenic mice

overexpressing IL-23 (He et al., 2021). Previously, it has been postulated that bacterial azoreductase activity can be saturated at a high concentration of AR, which would ultimately lead to accumulation of the parent compound in the lumen even in the presence of azo dye-metabolizing strains (Zou et al., 2020). This is further supported with previous findings that when the dye concentration increased beyond a certain threshold, there were changes in the decolorization rate from first to zero-order; the reaction rate was no longer affected above certain substrate concentration (Birkett, 1994; Zahran et al., 2019). The possibility of saturation of the enzyme by the chronic administration of the AR in this thesis, therefore, cannot be excluded.

The rising incidence of IBD in individuals who are less than 5 years of age is increasingly reported (Benchimol et al., 2017). In this thesis, findings that the exposure of AR during early life primes the host to the later development of colitis support the notion that early life is increasingly considered as a crucial period that influences susceptibility to IBD development in later life (Agrawal et al., 2021). Synthetic colourants are a convenient and low-cost alternative for food manufacturers to make foods even brighter and more appealing to the customer, particularly young children. The amount of synthetic colourants have increased 500% from 1950 (12 mg/capita/day) to 2012 (68 mg/capita/day) (Stevens et al., 2014). In the same vein, approximately 43% of synthetic colourants including AR are found in food products marketed to children (Batada et al., 2016). More importantly, the levels of synthetic colourants found in these consumables were present at much higher levels than the amounts tested in randomized control studies investigating dye-related reactions and behaviours in children (McCann

et al., 2007; Stevens et al., 2014). It is thus likely that children are exposed to these chemicals on a more consistent and higher basis than adults.

Conclusion and Future Directions

The data encompassed in this thesis provide evidence that chronic consumption of AR enhances the susceptibility to colitis and that colonic 5-HT derived from Tph1 is a key mediator for the observed phenotype. In addition, AR enhanced the susceptibility to colitis in both microbiota-dependent and -independent manner (**Figure 28**). Given that the synthetic colourants, SY and TY also promote 5-HT biosynthesis *in vitro* and have similar chemical structures to AR, exploring whether these colourants promote colitis by similar mechanisms is thus of the utmost importance. As many dietary products contain multiple synthetic colourants, investigating whether any synergistic actions between these colourants influence the susceptibility to colitis will be a key direction for future work. The knowledge of the association between the gut microbiota and IBD continues to expand, and the influence of environmental factors, such as dietary components, becomes increasingly crucial. This thesis investigated the cumulative effects of AR, which are relevant to individuals regularly consuming (intentionally or unintentionally) foods rich in synthetic colourants. To some extent, this work may not recapitulate the average exposure humans encounter in daily life. Thus, population-based studies on AR consumption by individuals, including IBD patients, are necessary to ascertain if the intake of synthetic colourants is associated with the later development, or exacerbation, of colitis. Moreover, with an emerging interest in food-

based exclusion diets (i.e., exclusive enteral nutrition) (Boneh et al., 2021; Levine et al., 2019), the findings herein have potential important role for managing IBD as well as in enhancing public knowledge on the harmful effects of food dyes, such as AR. With a dramatic spread of the Western diet, the effects of synthetic colourants, which are often overlooked as potentially harmful food components, are increasingly becoming a public health concern. Thus, this thesis not only prompts scrutiny of the use of synthetic colourants across industries but may, in the future, provide the foundation of research that may impact global health.

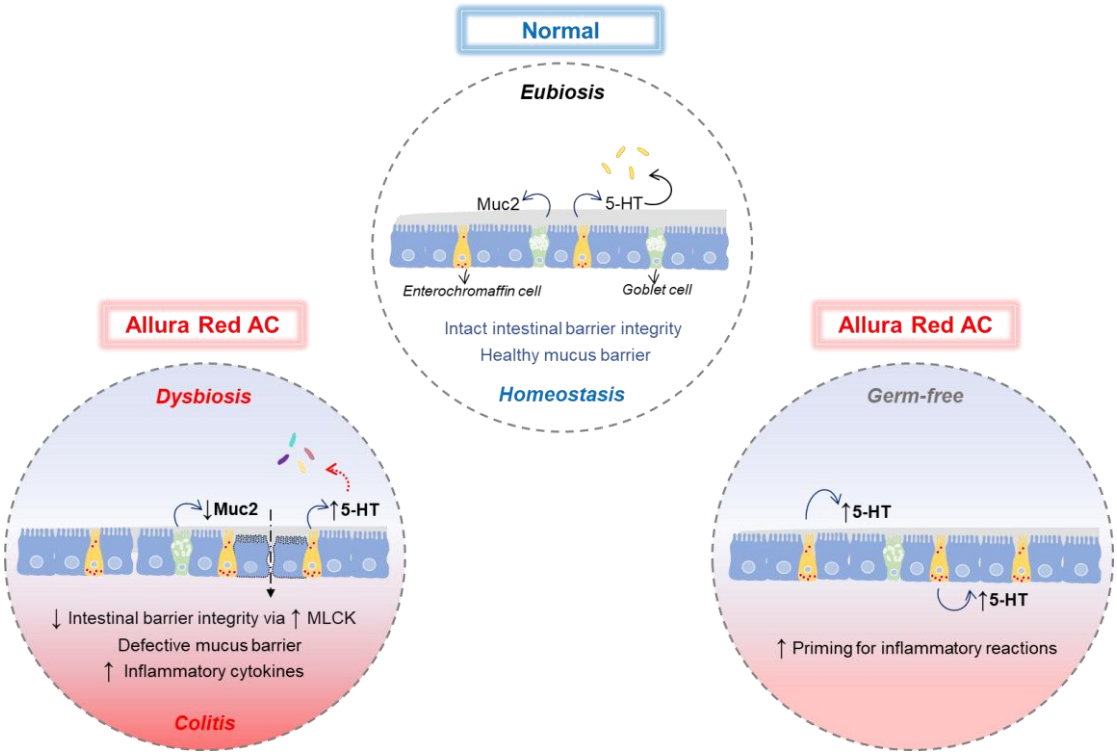
Normal
Eubiosis
Muc2
5-HT
Enterochromaffin cell
Goblet cell
Intact intestinal barrier integrity
Healthy mucus barrier
Homeostasis
Allura Red AC
Dysbiosis
↓Muc2
↑5-HT
↓ Intestinal barrier integrity via ↑ MLCK
Defective mucus barrier
↑ Inflammatory cytokines
Colitis
Allura Red AC
Germ-free
↑5-HT
↑5-HT
↑ Priming for inflammatory reactions

Figure 28: Graphical summary of the effects of Allura Red on colitis. Under the normal condition, the intestinal epithelial cells (IECs) constantly interact with commensal bacteria in the gut and maintain mucosal homeostasis by finely tuning the immune network. Chronic exposure to Allura Red AC (AR) disrupts intestinal epithelial barrier integrity via myosin light chain kinase (MLCK) activation. The mucus layer maintained by Muc2 is also impaired by exposure to AR. Additionally, colonic pro-inflammatory cytokines are increased, which can further aggravate the impairment of the epithelial barrier function. AR exposure also increases colonic serotonin (5-hydroxytryptamine; 5-HT) levels, while perturbing the gut microbiota composition, in which the microbes are also influenced by increased luminal 5-HT levels. Furthermore, the effect of AR exposure is also mediated by the gut microbiota-independent pathway as evidenced by using germ-free mice. AR exposure in these mice increased colonic 5-HT levels, which can prime IECs and immune cells for exaggerated inflammatory responses.

REFERENCES

Acovic, A., Simovic Markovic, B., Gazdic, M., et al. (2018). Indoleamine 2, 3-dioxygenase-dependent expansion of T-regulatory cells maintains mucosal healing in ulcerative colitis. *Therapeutic Advances in Gastroenterology, 11*, 1756284818793558.

Adolph, T. E., Tomczak, M. F., Niederreiter, L., et al. (2013). Paneth cells as a site of origin for intestinal inflammation. *Nature, 503*(7475), 272-276.

Agrawal, M., Sabino, J., Frias-Gomes, C., et al. (2021). Early life exposures and the risk of inflammatory bowel disease: systematic review and meta-analyses. *EClinicalMedicine, 36*, 100884.

Agus, A., Planchais, J., & Sokol, H. (2018). Gut microbiota regulation of tryptophan metabolism in health and disease. *Cell host & microbe, 23*(6), 716-724.

Ahern, G. P. (2011). 5-HT and the immune system. *Current opinion in pharmacology, 11*(1), 29-33.

Ahern, P. P., Schiering, C., Buonocore, S., et al. (2010). Interleukin-23 drives intestinal inflammation through direct activity on T cells. *Immunity, 33*(2), 279-288.

Alam, A., Leoni, G., Quiros, M., et al. (2016). The microenvironment of injured murine gut elicits a local pro-restitutive microbiota. *Nature microbiology, 1*(2), 1-8.

Alcaino, C., Knutson, K. R., Treichel, A. J., et al. (2018). A population of gut epithelial enterochromaffin cells is mechanosensitive and requires Piezo2 to convert force into serotonin release. *Proceedings of the national academy of sciences, 115*(32), E7632-E7641.

Alex, P., Zachos, N. C., Nguyen, T., et al. (2009). Distinct cytokine patterns identified from multiplex profiles of murine DSS and TNBS-induced colitis. *Inflammatory bowel diseases, 15*(3), 341-352.

Alhouayek, M., Gouveia-Figueira, S., Hammarström, M. L., et al. (2018). Involvement of CYP1B1 in interferon γ-induced alterations of epithelial barrier integrity. *British journal of pharmacology, 175*(6), 877-890.

Alkhalaf, L. M., & Ryan, K. S. (2015). Biosynthetic manipulation of tryptophan in bacteria: pathways and mechanisms. *Chemistry & Biology, 22*(3), 317-328.

Altay, G., Larrañaga, E., Tosi, S., et al. (2019). Self-organized intestinal epithelial monolayers in crypt and villus-like domains show effective barrier function. *Scientific reports, 9*(1), 1-14.

Amchova, P., Kotolova, H., & Ruda-Kucerova, J. (2015). Health safety issues of synthetic food colorants. *Regulatory toxicology and pharmacology, 73*(3), 914-922.

Ananthakrishnan, A. N., Bernstein, C. N., Iliopoulos, D., et al. (2018). Environmental triggers in IBD: a review of progress and evidence. *Nature reviews Gastroenterology & hepatology, 15*(1), 39-49.

Arthur, J. C., Perez-Chanona, E., Mühlbauer, M., et al. (2012). Intestinal inflammation targets cancer-inducing activity of the microbiota. *science, 338*(6103), 120-123.

Aune, T., McGrath, K., Sarr, T., et al. (1993). Expression of 5HT1a receptors on activated human T cells. Regulation of cyclic AMP levels and T cell proliferation by 5-hydroxytryptamine. *The Journal of Immunology, 151*(3), 1175-1183.

Ayres, J. S., Trinidad, N. J., & Vance, R. E. (2012). Lethal inflammasome activation by a multidrug-resistant pathobiont upon antibiotic disruption of the microbiota. *Nature medicine, 18*(5), 799-806.

Azmitia, E. C. (2020). Evolution of serotonin: sunlight to suicide *Handbook of behavioral neuroscience* (Vol. 31, pp. 3-22): Elsevier.

Backhed, F., Ley, R. E., Sonnenburg, J. L., et al. (2005). Host-bacterial mutualism in the human intestine. *science, 307*(5717), 1915-1920.

Bansal, T., Englert, D., Lee, J., et al. (2007). Differential effects of epinephrine, norepinephrine, and indole on Escherichia coli O157: H7 chemotaxis, colonization, and gene expression. *Infection and immunity, 75*(9), 4597-4607.

Banskota, S., Ghia, J.-E., & Khan, W. I. (2019). Serotonin in the gut: Blessing or a curse. *Biochimie, 161*, 56-64.

Banskota, S., Regmi, S. C., Gautam, J., et al. (2017). Serotonin disturbs colon epithelial tolerance of commensal E. coli by increasing NOX2-derived superoxide. *Free Radical Biology and Medicine, 106*, 196-207.

Bardenbacher, M., Ruder, B., Britzen-Laurent, N., et al. (2019). Permeability analyses and three dimensional imaging of interferon gamma-induced barrier disintegration in intestinal organoids. *Stem Cell Research, 35*, 101383.

Batada, A., & Jacobson, M. F. (2016). Prevalence of artificial food colors in grocery store products marketed to children. *Clinical pediatrics, 55*(12), 1113-1119.

Baumgart, D. C., & Sandborn, W. J. (2012). Crohn's disease. *The Lancet, 380*(9853), 1590-1605.

Bawazir, A. (2016). Effects of food colour allura red (No. 129) on some neurotransmitter, antioxidant functions and bioelement contents of kidney and brain tissues in male albino rats. *Life Science Journal, 13*(12).

Bell, C. C. (2013). A comparison of daily consumption of artificial dye-containing foods by american children and adults.

Bellono, N. W., Bayrer, J. R., Leitch, D. B., et al. (2017). Enterochromaffin cells are gut chemosensors that couple to sensory neural pathways. *Cell, 170*(1), 185-198. e116.

Benchimol, E. I., Bernstein, C. N., Bitton, A., et al. (2017). Trends in epidemiology of pediatric inflammatory bowel disease in Canada: distributed network analysis of multiple population-based provincial health administrative databases. *The American journal of gastroenterology, 112*(7), 1120.

Benchimol, E. I., Fortinsky, K. J., Gozdyra, P., et al. (2011). Epidemiology of pediatric inflammatory bowel disease: a systematic review of international trends. *Inflammatory bowel diseases, 17*(1), 423-439.

Benchimol, E. I., Mack, D. R., Guttmann, A., et al. (2015). Inflammatory bowel disease in immigrants to Canada and their children: a population-based cohort study. *Official journal of the American College of Gastroenterology| ACG, 110*(4), 553-563.

Bernstein, C. N., & Forbes, J. D. (2017). Gut microbiome in inflammatory bowel disease and other chronic immune-mediated inflammatory diseases. *Inflammatory intestinal diseases, 2*(2), 116-123.

Bernstein, C. N., Wajda, A., Svenson, L. W., et al. (2006). The epidemiology of inflammatory bowel disease in Canada: a population-based study. *Official journal of the American College of Gastroenterology| ACG, 101*(7), 1559-1568.

Berry, D., Schwab, C., Milinovich, G., et al. (2012). Phylotype-level 16S rRNA analysis reveals new bacterial indicators of health state in acute murine colitis. *The ISME journal, 6*(11), 2091-2106.

Bertaccini, G. (1960). Tissue 5-hydroxytryptamine and urinary 5-hydroxyindoleacetic acid after partial or total removal of the gastro-intestinal tract in the rat. *The Journal of physiology, 153*(2), 239.

Bertrand, P. (2004). Real-time detection of serotonin release from enterochromaffin cells of the guinea-pig ileum. *Neurogastroenterology & Motility, 16*(5), 511-514.

Bertrand, R., Senadheera, S., Markus, I., et al. (2011). A Western diet increases serotonin availability in rat small intestine. *Endocrinology, 152*(1), 36-47.

Birkett, D. (1994). Pharmacokinetics made easy 9: Non-linear pharmacokinetics. *Australian Prescriber, 17*(2).

Bischoff, S. C., Mailer, R., Pabst, O., et al. (2009). Role of serotonin in intestinal inflammation: knockout of serotonin reuptake transporter exacerbates 2, 4, 6-trinitrobenzene sulfonic acid colitis in mice. *American Journal of Physiology-Gastrointestinal and Liver Physiology, 296*(3), G685-G695.

Blair, S. A., Kane, S. V., Clayburgh, D. R., et al. (2006). Epithelial myosin light chain kinase expression and activity are upregulated in inflammatory bowel disease. *Laboratory investigation, 86*(2), 191-201.

Blaser, H., Dostert, C., Mak, T. W., et al. (2016). TNF and ROS crosstalk in inflammation. *Trends in cell biology, 26*(4), 249-261.

Bogunovic, M., Davé, S. H., Tilstra, J. S., et al. (2007). Enteroendocrine cells express functional Toll-like receptors. *American Journal of Physiology-Gastrointestinal and Liver Physiology, 292*(6), G1770-G1783.

Boneh, R. S., Van Limbergen, J., Wine, E., et al. (2021). Dietary therapies induce rapid response and remission in pediatric patients with active Crohn's disease. *Clinical Gastroenterology and Hepatology, 19*(4), 752-759.

Borthakur, A., Bhattacharyya, S., Dudeja, P. K., et al. (2007). Carrageenan induces interleukin-8 production through distinct Bcl10 pathway in normal human colonic epithelial cells. *American Journal of Physiology-Gastrointestinal and Liver Physiology, 292*(3), G829-G838.

Braegger, C. P., Nicholls, S., Murch, S., et al. (1992). Tumour necrosis factor alpha in stool as a marker of intestinal inflammation. *The Lancet, 339*(8785), 89-91.

Brown, M. A., & De Vito, S. C. (1993). Predicting azo dye toxicity. *Critical reviews in environmental science and technology, 23*(3), 249-324.

Bülbring, E., Crema, A., & Saxby, O. (1958). A method for recording peristalsis in isolated intestine. *British Journal of Pharmacology and Chemotherapy, 13*(4), 440.

Burger-van Paassen, N., Vincent, A., Puiman, P. J., et al. (2009). The regulation of intestinal mucin MUC2 expression by short-chain fatty acids: implications for epithelial protection. *Biochemical Journal, 420*(2), 211-219.

Cadwell, K., Liu, J. Y., Brown, S. L., et al. (2008). A key role for autophagy and the autophagy gene Atg16l1 in mouse and human intestinal Paneth cells. *Nature, 456*(7219), 259-263.

Callahan, B. J., McMurdie, P. J., Rosen, M. J., et al. (2016). DADA2: High-resolution sample inference from Illumina amplicon data. *Nature methods, 13*(7), 581-583.

Camoglio, L., Te Velde, A. A., Tigges, A. J., et al. (1998). Altered expression of interferon-γ and interleukin-4 in inflammatory bowel disease. *Inflammatory bowel diseases, 4*(4), 285-290.

Cao, Y.-N., Feng, L.-J., Liu, Y.-Y., et al. (2018). Effect of Lactobacillus rhamnosus GG supernatant on serotonin transporter expression in rats with post-infectious irritable bowel syndrome. *World Journal of Gastroenterology, 24*(3), 338.

Capella, C., Heitz, P. U., Höfler, H., et al. (1995). Revised classification of neuroendocrine tumours of the lung, pancreas and gut. *Virchows Archiv, 425*(6), 547-560.

Carroll, M. W., Kuenzig, M. E., Mack, D. R., et al. (2019). The impact of inflammatory bowel disease in Canada 2018: children and adolescents with IBD. *Journal of the Canadian Association of Gastroenterology, 2*(Supplement_1), S49-S67.

Caruso, R., Mathes, T., Martens, E., et al. (2019). A specific gene-microbe interaction drives the development of Crohn's disease–like colitis in mice. *Science Immunology, 4*(34), eaaw4341.

Cerf-Bensussan, N., & Gaboriau-Routhiau, V. (2010). The immune system and the gut microbiota: friends or foes? *Nature Reviews Immunology, 10*(10), 735-744.

Chapman, M., Grahn, M., Boyle, M., et al. (1994). Butyrate oxidation is impaired in the colonic mucosa of sufferers of quiescent ulcerative colitis. *Gut, 35*(1), 73-76.

Chassaing, B., Koren, O., Goodrich, J. K., et al. (2015). Dietary emulsifiers impact the mouse gut microbiota promoting colitis and metabolic syndrome. *Nature, 519*(7541), 92-96.

Chassaing, B., Van de Wiele, T., De Bodt, J., et al. (2017). Dietary emulsifiers directly alter human microbiota composition and gene expression ex vivo potentiating intestinal inflammation. *Gut, 66*(8), 1414-1427.

Chelakkot, C., Choi, Y., Kim, D.-K., et al. (2018). Akkermansia muciniphila-derived extracellular vesicles influence gut permeability through the regulation of tight junctions. *Experimental & molecular medicine, 50*(2), e450-e450.

Chen, C., Brown, D. R., Xie, Y., et al. (2003). Catecholamines modulate Escherichia coli O157: H7 adherence to murine cecal mucosa. *Shock, 20*(2), 183-188.

Chen, G., Ran, X., Li, B., et al. (2018). Sodium butyrate inhibits inflammation and maintains epithelium barrier integrity in a TNBS-induced inflammatory bowel disease mice model. *EBioMedicine, 30*, 317-325.

Chen, J.-X., Pan, H., Rothman, T. P., et al. (1998). Guinea pig 5-HT transporter: cloning, expression, distribution, and function in intestinal sensory reception. *American Journal of Physiology-Gastrointestinal and Liver Physiology, 275*(3), G433-G448.

Chen, L., He, Z., Reis, B. S., et al. (2022). IFN-γ+ cytotoxic CD4+ T lymphocytes are involved in the pathogenesis of colitis induced by IL-23 and the food colorant Red 40. *Cellular & Molecular Immunology*, 1-14.

Chen, Y., Leon-Ponte, M., Pingle, S., et al. (2015). T lymphocytes possess the machinery for 5-HT synthesis, storage, degradation and release. *Acta Physiologica, 213*(4), 860-867.

Chen, Z., Luo, J., Li, J., et al. (2021). Interleukin-33 promotes serotonin release from enterochromaffin cells for intestinal homeostasis. *Immunity, 54*(1), 151-163. e156.

Christ, A., Lauterbach, M., & Latz, E. (2019). Western diet and the immune system: an inflammatory connection. *Immunity, 51*(5), 794-811.

Chudzik, A., Orzyłowska, A., Rola, R., et al. (2021). Probiotics, prebiotics and postbiotics on mitigation of depression symptoms: modulation of the brain–gut–microbiome axis. *Biomolecules, 11*(7), 1000.

Ciorba, M. A. (2013). Indoleamine 2, 3 dioxygenase (IDO) in intestinal disease. *Current opinion in gastroenterology, 29*(2), 146.

Claus, S. P., Guillou, H., & Ellero-Simatos, S. (2016). The gut microbiota: a major player in the toxicity of environmental pollutants? *Npj biofilms and microbiomes, 2*(1), 1-11.

Clayburgh, D. R., Barrett, T. A., Tang, Y., et al. (2005). Epithelial myosin light chain kinase–dependent barrier dysfunction mediates T cell activation–induced diarrhea in vivo. *The Journal of clinical investigation, 115*(10), 2702-2715.

Colabroy, K. L., & Begley, T. P. (2005). Tryptophan catabolism: identification and characterization of a new degradative pathway. *Journal of bacteriology, 187*(22), 7866-7869.

Committee, C. C. I. (1968). Guidelines for good manufacturing practice: use of certified FD&C colors in food. *Food Technol, 22*(8), 14-17.

Cooper, H. S., Murthy, S., Shah, R., et al. (1993). Clinicopathologic study of dextran sulfate sodium experimental murine colitis. *Laboratory investigation; a journal of technical methods and pathology, 69*(2), 238-249.

Coward, S., Clement, F., Benchimol, E. I., et al. (2019). Past and future burden of inflammatory bowel diseases based on modeling of population-based data. *Gastroenterology, 156*(5), 1345-1353. e1344.

Cristina, M., Lehy, T., Zeitoun, P., et al. (1978). Fine structural classification and comparative distribution of endocrine cells in normal human large intestine. *Gastroenterology, 75*(1), 20-28.

Crowley, S. M., Han, X., Allaire, J. M., et al. (2020). Intestinal restriction of Salmonella Typhimurium requires caspase-1 and caspase-11 epithelial intrinsic inflammasomes. *PLoS pathogens, 16*(4), e1008498.

Cua, D. J., Sherlock, J., Chen, Y., et al. (2003). Interleukin-23 rather than interleukin-12 is the critical cytokine for autoimmune inflammation of the brain. *Nature, 421*(6924), 744-748.

Cui, G., Fan, Q., Li, Z., et al. (2021). Evaluation of anti-TNF therapeutic response in patients with inflammatory bowel disease: Current and novel biomarkers. *EBioMedicine, 66*, 103329.

Cunningham, K. E., & Turner, J. R. (2012). Myosin light chain kinase: pulling the strings of epithelial tight junction function. *Annals of the New York academy of sciences, 1258*(1), 34-42.

Dassopoulos, T., Nguyen, G. C., Talor, M. V., et al. (2010). NOD2 mutations and anti-Saccharomyces cerevisiae antibodies are risk factors for Crohn's disease in African Americans. *The American journal of gastroenterology, 105*(2), 378.

De Preter, V., Arijs, I., Windey, K., et al. (2012). Impaired butyrate oxidation in ulcerative colitis is due to decreased butyrate uptake and a defect in the oxidation pathway. *Inflammatory bowel diseases, 18*(6), 1127-1136.

De Souza, H. S., & Fiocchi, C. (2016). Immunopathogenesis of IBD: current state of the art. *Nature reviews Gastroenterology & hepatology, 13*(1), 13-27.

DeForge, L. E., Fantone, J. C., Kenney, J. S., et al. (1992). Oxygen radical scavengers selectively inhibit interleukin 8 production in human whole blood. *The Journal of clinical investigation, 90*(5), 2123-2129.

Devkota, S., Wang, Y., Musch, M. W., et al. (2012). Dietary-fat-induced taurocholic acid promotes pathobiont expansion and colitis in Il10−/− mice. *Nature, 487*(7405), 104-108.

Dodd, D., Spitzer, M. H., Van Treuren, W., et al. (2017). A gut bacterial pathway metabolizes aromatic amino acids into nine circulating metabolites. *Nature, 551*(7682), 648-652.

Dotan, I., Allez, M., Nakazawa, A., et al. (2007). Intestinal epithelial cells from inflammatory bowel disease patients preferentially stimulate CD4+ T cells to proliferate and secrete interferon-γ. *American Journal of Physiology-Gastrointestinal and Liver Physiology, 292*(6), G1630-G1640.

Dougherty, D. M., Marsh-Richard, D. M., Mathias, C. W., et al. (2008). Comparison of 50-and 100-g L-tryptophan depletion and loading formulations for altering 5-HT synthesis: pharmacokinetics, side effects, and mood states. *Psychopharmacology, 198*(3), 431-445.

Duerr, R. H., Taylor, K. D., Brant, S. R., et al. (2006). A genome-wide association study identifies IL23R as an inflammatory bowel disease gene. *science, 314*(5804), 1461-1463.

Duricova, D., Burisch, J., Jess, T., et al. (2014). Age-related differences in presentation and course of inflammatory bowel disease: an update on the population-based literature. *Journal of Crohn's and Colitis, 8*(11), 1351-1361.

Edsinger, E., & Dölen, G. (2018). A conserved role for serotonergic neurotransmission in mediating social behavior in octopus. *Current Biology, 28*(19), 3136-3142. e3134.

El-Merahbi, R., Löffler, M., Mayer, A., et al. (2015). The roles of peripheral serotonin in metabolic homeostasis. *FEBS letters, 589*(15), 1728-1734.

Engevik, M. A., Luk, B., Chang-Graham, A. L., et al. (2019). Bifidobacterium dentium fortifies the intestinal mucus layer via autophagy and calcium signaling pathways. *MBio, 10*(3), e01087-01019.

Erspamer, V. (1948). Active substances in the posterior salivary glands of octopoda. *Acta Pharmac Toxicol., 4*, 213-247.

Erspamer, V., & Ghiretti, F. (1951). The action of enteramine on the heart of molluscs. *The Journal of physiology, 115*(4), 470.

Erspamer, V., & Vialli, M. (1937). Ricerche sul secreto delle cellule enterocromaffini. *Boll d Soc Med-chir Pavia, 51*, 357-363.

Esmaili, A., Nazir, S. F., Borthakur, A., et al. (2009). Enteropathogenic Escherichia coli infection inhibits intestinal serotonin transporter function and expression. *Gastroenterology, 137*(6), 2074-2083.

Everard, A., Belzer, C., Geurts, L., et al. (2013). Cross-talk between Akkermansia muciniphila and intestinal epithelium controls diet-induced obesity. *Proceedings of the national academy of sciences, 110*(22), 9066-9071.

Fachi, J. L., de Souza Felipe, J., Pral, L. P., et al. (2019). Butyrate protects mice from Clostridium difficile-induced colitis through an HIF-1-dependent mechanism. *Cell reports, 27*(3), 750-761. e757.

Fallico, B., Chiappara, E., Arena, E., et al. (2011). Assessment of the exposure to Allura Red colour from the consumption of red juice-based and red soft drinks in Italy. *Food Additives & Contaminants: Part A, 28*(11), 1501-1515.

Feng, J., Cerniglia, C. E., & Chen, H. (2012). Toxicological significance of azo dye metabolism by human intestinal microbiota. *Frontiers in bioscience (Elite edition), 4*, 568.

Ferrier, L., Mazelin, L., Cenac, N., et al. (2003). Stress-induced disruption of colonic epithelial barrier: role of interferon-γ and myosin light chain kinase in mice. *Gastroenterology, 125*(3), 795-804.

FINOCCHIARO, L. M., ARZT, E. S., FERNÁNDEZ-CASTELO, S., et al. (1988). Serotonin and melatonin synthesis in peripheral blood mononuclear cells: stimulation by interferon-7 as part of an immunomodulatory pathway. *Journal of interferon research, 8*(6), 705-716.

Fish, S., Proujansky, R., & Reenstra, W. (1999). Synergistic effects of interferon γ and tumour necrosis factor α on T84 cell function. *Gut, 45*(2), 191-198.

Foley, K. F., Pantano, C., Ciolino, A., et al. (2007). IFN-γ and TNF-α decrease serotonin transporter function and expression in Caco2 cells. *American Journal of Physiology-Gastrointestinal and Liver Physiology, 292*(3), G779-G784.

Freestone, P. (2013). Communication between bacteria and their hosts. *Scientifica, 2013*.

Fung, T. C., Vuong, H. E., Luna, C. D., et al. (2019). Intestinal serotonin and fluoxetine exposure modulate bacterial colonization in the gut. *Nature microbiology, 4*(12), 2064-2073.

Furman, D., Campisi, J., Verdin, E., et al. (2019). Chronic inflammation in the etiology of disease across the life span. *Nature medicine, 25*(12), 1822-1832.

Furness, J. B., Rivera, L. R., Cho, H.-J., et al. (2013). The gut as a sensory organ. *Nature reviews Gastroenterology & hepatology, 10*(12), 729-740.

Furusawa, Y., Obata, Y., Fukuda, S., et al. (2013). Commensal microbe-derived butyrate induces the differentiation of colonic regulatory T cells. *Nature, 504*(7480), 446-450.

Gao, J., Xu, K., Liu, H., et al. (2018). Impact of the gut microbiota on intestinal immunity mediated by tryptophan metabolism. *Frontiers in cellular and infection microbiology*, 13.

Gershon, M. D. (2013). 5-Hydroxytryptamine (serotonin) in the gastrointestinal tract. *Current opinion in endocrinology, diabetes, and obesity, 20*(1), 14.

Gershon, M. D., & Ross, L. L. (1962). Studies on the relationship of 5-hydroxytryptamine and the enterochromaffin cell to anaphylactic shock in mice. *The Journal of experimental medicine, 115*(2), 367-382.

Ghia, J. E., Li, N., Wang, H., et al. (2009). Serotonin has a key role in pathogenesis of experimental colitis. *Gastroenterology, 137*(5), 1649-1660.

Gibson, P. R. (2004). Increased gut permeability in Crohn's disease: is TNF the link? *Gut, 53*(12), 1724-1725.

Grondin, J. A., Kwon, Y. H., Far, P. M., et al. (2020). Mucins in intestinal mucosal defense and inflammation: learning from clinical and experimental studies. *Frontiers in immunology*, 2054.

Gunawardene, A. R., Corfe, B. M., & Staton, C. A. (2011). Classification and functions of enteroendocrine cells of the lower gastrointestinal tract. *International journal of experimental pathology, 92*(4), 219-231.

Günther, C., Neumann, H., Neurath, M. F., et al. (2013). Apoptosis, necrosis and necroptosis: cell death regulation in the intestinal epithelium. *Gut, 62*(7), 1062-1071.

Hamer, H. M., Jonkers, D., Venema, K., et al. (2008). The role of butyrate on colonic function. *Alimentary pharmacology & therapeutics, 27*(2), 104-119.

Hampe, J., Franke, A., Rosenstiel, P., et al. (2007). A genome-wide association scan of nonsynonymous SNPs identifies a susceptibility variant for Crohn disease in ATG16L1. *Nature genetics, 39*(2), 207-211.

Hannon, J., & Hoyer, D. (2008). Molecular biology of 5-HT receptors. *Behavioural brain research, 195*(1), 198-213.

Haq, S., Wang, H., Grondin, J., et al. (2021). Disruption of autophagy by increased 5-HT alters gut microbiota and enhances susceptibility to experimental colitis and Crohn's disease. *Science advances, 7*(45), eabi6442.

Harig, J. M., Soergel, K. H., Komorowski, R. A., et al. (1989). Treatment of diversion colitis with short-chain-fatty acid irrigation. *New England Journal of Medicine, 320*(1), 23-28.

Haub, S., Ritze, Y., Bergheim, I., et al. (2010). Enhancement of intestinal inflammation in mice lacking interleukin 10 by deletion of the serotonin reuptake transporter. *Neurogastroenterology & Motility, 22*(7), 826-e229.

He, Z., Chen, L., Catalan-Dibene, J., et al. (2021). Food colorants metabolized by commensal bacteria promote colitis in mice with dysregulated expression of interleukin-23. *Cell Metabolism, 33*(7), 1358-1371. e1355.

Heredia, D. J., Dickson, E. J., Bayguinov, P. O., et al. (2009). Localized release of serotonin (5-hydroxytryptamine) by a fecal pellet regulates migrating motor complexes in murine colon. *Gastroenterology, 136*(4), 1328-1338.

Ho, S.-M., Lewis, J. D., Mayer, E. A., et al. (2019). Challenges in IBD research: environmental triggers. *Inflammatory bowel diseases, 25*(Supplement_2), S13-S23.

Holland, N., Dong, J., Garnett, E., et al. (2008). Reduced intracellular T-helper 1 interferon-gamma in blood of newly diagnosed children with Crohn's disease and age-related changes in Th1/Th2 cytokine profiles. *Pediatric research, 63*(3), 257-262.

Hommes, D. W., & van Deventer, S. J. (2004). Endoscopy in inflammatory bowel diseases. *Gastroenterology, 126*(6), 1561-1573.

Hooper, L. V., & Macpherson, A. J. (2010). Immune adaptations that maintain homeostasis with the intestinal microbiota. *Nature Reviews Immunology, 10*(3), 159-169.

Hoyer, D., Clarke, D. E., Fozard, J. R., et al. (1994). International Union of Pharmacology classification of receptors for 5-hydroxytryptamine (Serotonin). *Pharmacological reviews, 46*(2), 157-203.

Hubbard, T. D., Murray, I. A., & Perdew, G. H. (2015). Indole and tryptophan metabolism: endogenous and dietary routes to Ah receptor activation. *Drug Metabolism and Disposition, 43*(10), 1522-1535.

Hugot, J.-P., Chamaillard, M., Zouali, H., et al. (2001). Association of NOD2 leucine-rich repeat variants with susceptibility to Crohn's disease. *Nature, 411*(6837), 599-603.

Inoue, N., Tamura, K., Kinouchi, Y., et al. (2002). Lack of common NOD2 variants in Japanese patients with Crohn's disease. *Gastroenterology, 123*(1), 86-91.

Irvine, E. J., & Marshall, J. K. (2000). Increased intestinal permeability precedes the onset of Crohn's disease in a subject with familial risk. *Gastroenterology, 119*(6), 1740-1744.

Ito, R., Shin-Ya, M., Kishida, T., et al. (2006). Interferon-gamma is causatively involved in experimental inflammatory bowel disease in mice. *Clinical & Experimental Immunology, 146*(2), 330-338.

Ivusic Polic, I. (2018). *Evaluation of the impact of azo dyes on the metabolism of stabilized fecal communities and in vitro cell culture.* University of Guelph.

Jairath, V., & Feagan, B. G. (2020). Global burden of inflammatory bowel disease. *The Lancet Gastroenterology & Hepatology, 5*(1), 2-3.

Johansson, M. E. (2014). Mucus layers in inflammatory bowel disease. *Inflammatory bowel diseases, 20*(11), 2124-2131.

Johansson, M. E., Phillipson, M., Petersson, J., et al. (2008). The inner of the two Muc2 mucin-dependent mucus layers in colon is devoid of bacteria. *Proceedings of the national academy of sciences, 105*(39), 15064-15069.

Johnson, G. E., Quick, E. L., Parry, E. M., et al. (2010). Metabolic influences for mutation induction curves after exposure to Sudan-1 and para red. *Mutagenesis, 25*(4), 327-333.

Johnson, P. L., Molosh, A., Fitz, S. D., et al. (2015). Pharmacological depletion of serotonin in the basolateral amygdala complex reduces anxiety and disrupts fear conditioning. *Pharmacology Biochemistry and Behavior, 138*, 174-179.

Jones-Hall, Y. L., Kozik, A., & Nakatsu, C. (2015). Ablation of tumor necrosis factor is associated with decreased inflammation and alterations of the microbiota in a mouse model of inflammatory bowel disease. *PLoS One, 10*(3), e0119441.

Jørandli, J. W., Thorsvik, S., Skovdahl, H. K., et al. (2020). The serotonin reuptake transporter is reduced in the epithelium of active Crohn's disease and ulcerative colitis. *American Journal of Physiology-Gastrointestinal and Liver Physiology, 319*(6), G761-G768.

Jostins, L., Ripke, S., Weersma, R. K., et al. (2012). Host–microbe interactions have shaped the genetic architecture of inflammatory bowel disease. *Nature, 491*(7422), 119-124.

Kamada, N., Chen, G. Y., Inohara, N., et al. (2013). Control of pathogens and pathobionts by the gut microbiota. *Nature immunology, 14*(7), 685-690.

Kang, C.-s., Ban, M., Choi, E.-J., et al. (2013). Extracellular vesicles derived from gut microbiota, especially Akkermansia muciniphila, protect the progression of dextran sulfate sodium-induced colitis. *PLoS One, 8*(10), e76520.

Kaplan, G. G., Bernstein, C. N., Coward, S., et al. (2019). The impact of inflammatory bowel disease in Canada 2018: epidemiology. *Journal of the Canadian Association of Gastroenterology, 2*(Supplement_1), S6-S16.

Kaplan, G. G., & Ng, S. C. (2017). Understanding and preventing the global increase of inflammatory bowel disease. *Gastroenterology, 152*(2), 313-321. e312.

Kaplan, G. G., & Windsor, J. W. (2021). The four epidemiological stages in the global evolution of inflammatory bowel disease. *Nature reviews Gastroenterology & hepatology, 18*(1), 56-66.

Kelly, C. J., Zheng, L., Campbell, E. L., et al. (2015). Crosstalk between microbiota-derived short-chain fatty acids and intestinal epithelial HIF augments tissue barrier function. *Cell host & microbe, 17*(5), 662-671.

Kendig, D. M., & Grider, J. R. (2015). Serotonin and colonic motility. *Neurogastroenterology & Motility, 27*(7), 899-905.

Khan, W. I., Motomura, Y., Wang, H., et al. (2006). Critical role of MCP-1 in the pathogenesis of experimental colitis in the context of immune and enterochromaffin cells. *American Journal of Physiology-Gastrointestinal and Liver Physiology, 291*(5), G803-G811.

Khayyat, L. I., Essawy, A. E., Sorour, J. M., et al. (2018). Sunset Yellow and Allura Red modulate Bcl2 and COX2 expression levels and confer oxidative stress-mediated renal and hepatic toxicity in male rats. *PeerJ, 6*, e5689.

Khor, B., Gardet, A., & Xavier, R. J. (2011). Genetics and pathogenesis of inflammatory bowel disease. *Nature, 474*(7351), 307-317.

Kidd, M., Gustafsson, B. I., Drozdov, I., et al. (2009). IL1β-and LPS-induced serotonin secretion is increased in EC cells derived from Crohn's disease. *Neurogastroenterology & Motility, 21*(4), 439-450.

Kiesler, P., Fuss, I. J., & Strober, W. (2015). Experimental models of inflammatory bowel diseases. *Cellular and molecular gastroenterology and hepatology, 1*(2), 154-170.

Kim, J. J., Bridle, B. W., Ghia, J.-E., et al. (2013). Targeted inhibition of serotonin type 7 (5-HT7) receptor function modulates immune responses and reduces the severity of intestinal inflammation. *The Journal of Immunology, 190*(9), 4795-4804.

Kim, J. J., Shajib, M. S., Manocha, M. M., et al. (2012). Investigating intestinal inflammation in DSS-induced model of IBD. *JoVE (Journal of Visualized Experiments)*(60), e3678.

Kim, J. J., Wang, H., Terc, J. D., et al. (2015). Blocking peripheral serotonin synthesis by telotristat etiprate (LX1032/LX1606) reduces severity of both chemical-and infection-induced intestinal inflammation. *American Journal of Physiology-Gastrointestinal and Liver Physiology, 309*(6), G455-G465.

Kim, M., Cooke, H. J., Javed, N. H., et al. (2001). D-glucose releases 5-hydroxytryptamine from human BON cells as a model of enterochromaffin cells. *Gastroenterology, 121*(6), 1400-1406.

Kiser, D., SteemerS, B., Branchi, I., et al. (2012). The reciprocal interaction between serotonin and social behaviour. *Neuroscience & Biobehavioral Reviews, 36*(2), 786-798.

Knecht, L. D., O'Connor, G., Mittal, R., et al. (2016). Serotonin activates bacterial quorum sensing and enhances the virulence of Pseudomonas aeruginosa in the host. *EBioMedicine, 9*, 161-169.

Kobayashi, K. S., Chamaillard, M., Ogura, Y., et al. (2005). Nod2-dependent regulation of innate and adaptive immunity in the intestinal tract. *science, 307*(5710), 731-734.

Koppel, N., Maini Rekdal, V., & Balskus, E. P. (2017). Chemical transformation of xenobiotics by the human gut microbiota. *science, 356*(6344), eaag2770.

Korzenik, J. R., & Podolsky, D. K. (2006). Evolving knowledge and therapy of inflammatory bowel disease. *Nature reviews Drug discovery, 5*(3), 197-209.

Krieglstein, C. F., Cerwinka, W. H., Sprague, A. G., et al. (2002). Collagen-binding integrin α 1 β 1 regulates intestinal inflammation in experimental colitis. *The Journal of clinical investigation, 110*(12), 1773-1782.

Kumar, A., Russell, R. M., Pifer, R., et al. (2020). The serotonin neurotransmitter modulates virulence of enteric pathogens. *Cell host & microbe, 28*(1), 41-53. e48.

Kumar, M., Sarma, D. K., Shubham, S., et al. (2020). Environmental endocrine-disrupting chemical exposure: role in non-communicable diseases. *Frontiers in public health*, 549.

Kushnir-Sukhov, N. M., Brown, J. M., Wu, Y., et al. (2007). Human mast cells are capable of serotonin synthesis and release. *Journal of Allergy and Clinical Immunology, 119*(2), 498-499.

Kwon, Y. H., Wang, H., Denou, E., et al. (2019). Modulation of gut microbiota composition by serotonin signaling influences intestinal immune response and susceptibility to colitis. *Cellular and molecular gastroenterology and hepatology, 7*(4), 709-728.

Lamas, B., Richard, M. L., Leducq, V., et al. (2016). CARD9 impacts colitis by altering gut microbiota metabolism of tryptophan into aryl hydrocarbon receptor ligands. *Nature medicine, 22*(6), 598-605.

Latorre, E., Layunta, E., Grasa, L., et al. (2016). Intestinal serotonin transporter inhibition by toll-like receptor 2 activation. A feedback modulation. *PLoS One, 11*(12), e0169303.

Laudisi, F., Di Fusco, D., Dinallo, V., et al. (2019). The food additive maltodextrin promotes endoplasmic reticulum stress–driven mucus depletion and exacerbates intestinal inflammation. *Cellular and molecular gastroenterology and hepatology, 7*(2), 457-473.

Layunta, E., Buey, B., Mesonero, J. E., et al. (2021). Crosstalk Between Intestinal Serotonergic System and Pattern Recognition Receptors on the Microbiota–Gut–Brain Axis. *Frontiers in endocrinology*, 1379.

Lee, Y. K., Turner, H., Maynard, C. L., et al. (2009). Late developmental plasticity in the T helper 17 lineage. *Immunity, 30*(1), 92-107.

Lent, C. M. (1985). Serotonergic modulation of the feeding behavior of the medicinal leech. *Brain research bulletin, 14*(6), 643-655.

Leo, L., Loong, C., Ho, X. L., et al. (2018). Occurrence of azo food dyes and their effects on cellular inflammatory responses. *Nutrition, 46*, 36-40.

León-Ponte, M., Ahern, G. P., & O'Connell, P. J. (2007). Serotonin provides an accessory signal to enhance T-cell activation by signaling through the 5-HT7 receptor. *Blood, 109*(8), 3139-3146.

Leong, R., Armuzzi, A., Ahmad, T., et al. (2003). NOD2/CARD15 gene polymorphisms and Crohn's disease in the Chinese population. *Alimentary pharmacology & therapeutics, 17*(12), 1465-1470.

Leppkes, M., Roulis, M., Neurath, M. F., et al. (2014). Pleiotropic functions of TNF-α in the regulation of the intestinal epithelial response to inflammation. *International immunology, 26*(9), 509-515.

Levine, A., Wine, E., Assa, A., et al. (2019). Crohn's disease exclusion diet plus partial enteral nutrition induces sustained remission in a randomized controlled trial. *Gastroenterology, 157*(2), 440-450. e448.

Lewis, J. D., Chen, E. Z., Baldassano, R. N., et al. (2015). Inflammation, antibiotics, and diet as environmental stressors of the gut microbiome in pediatric Crohn's disease. *Cell host & microbe, 18*(4), 489-500.

Li, N., Ghia, J.-E., Wang, H., et al. (2011). Serotonin activates dendritic cell function in the context of gut inflammation. *The American journal of pathology, 178*(2), 662-671.

Linan-Rico, A., Ochoa-Cortes, F., Beyder, A., et al. (2016). Mechanosensory signaling in enterochromaffin cells and 5-HT release: potential implications for gut inflammation. *Frontiers in neuroscience, 10*, 564.

Liu, J. Z., Van Sommeren, S., Huang, H., et al. (2015). Association analyses identify 38 susceptibility loci for inflammatory bowel disease and highlight shared genetic risk across populations. *Nature genetics, 47*(9), 979-986.

Loy, A., Pfann, C., Steinberger, M., et al. (2017). Lifestyle and horizontal gene transfer-mediated evolution of Mucispirillum schaedleri, a core member of the murine gut microbiota. *Msystems, 2*(1), e00171-00116.

Lund, M. L., Egerod, K. L., Engelstoft, M. S., et al. (2018). Enterochromaffin 5-HT cells–A major target for GLP-1 and gut microbial metabolites. *Molecular metabolism, 11*, 70-83.

Lupp, C., Robertson, M. L., Wickham, M. E., et al. (2007). Host-mediated inflammation disrupts the intestinal microbiota and promotes the overgrowth of Enterobacteriaceae. *Cell host & microbe, 2*(2), 119-129.

Luqman, A., Nega, M., Nguyen, M.-T., et al. (2018). SadA-expressing staphylococci in the human gut show increased cell adherence and internalization. *Cell reports, 22*(2), 535-545.

MacEachern, S. J., Keenan, C. M., Papakonstantinou, E., et al. (2018). Alterations in melatonin and 5-HT signalling in the colonic mucosa of mice with dextran-sodium sulfate-induced colitis. *British journal of pharmacology, 175*(9), 1535-1547.

Machiels, K., Joossens, M., Sabino, J., et al. (2014). A decrease of the butyrate-producing species Roseburia hominis and Faecalibacterium prausnitzii defines dysbiosis in patients with ulcerative colitis. *Gut, 63*(8), 1275-1283.

Madara, J. L., & Stafford, J. (1989). Interferon-gamma directly affects barrier function of cultured intestinal epithelial monolayers. *The Journal of clinical investigation, 83*(2), 724-727.

Mandić, A. D., Woting, A., Jaenicke, T., et al. (2019). Clostridium ramosum regulates enterochromaffin cell development and serotonin release. *Scientific reports, 9*(1), 1-15.

Manichanh, C., Rigottier-Gois, L., Bonnaud, E., et al. (2006). Reduced diversity of faecal microbiota in Crohn's disease revealed by a metagenomic approach. *Gut, 55*(2), 205-211.

Manzella, C. R., Jayawardena, D., Pagani, W., et al. (2020). Serum serotonin differentiates between disease activity states in Crohn's patients. *Inflammatory bowel diseases, 26*(10), 1607-1618.

Margolis, K. G., Stevanovic, K., Li, Z., et al. (2014). Pharmacological reduction of mucosal but not neuronal serotonin opposes inflammation in mouse intestine. *Gut, 63*(6), 928-937.

Martin, M. (2011). Cutadapt removes adapter sequences from high-throughput sequencing reads. *EMBnet. journal, 17*(1), 10-12.

Martinez-Medina, M., Denizot, J., Dreux, N., et al. (2014). Western diet induces dysbiosis with increased E coli in CEABAC10 mice, alters host barrier function favouring AIEC colonisation. *Gut, 63*(1), 116-124.

Mawe, G. M., & Hoffman, J. M. (2013). Serotonin signalling in the gut—functions, dysfunctions and therapeutic targets. *Nature reviews Gastroenterology & hepatology, 10*(8), 473-486.

McCann, D., Barrett, A., Cooper, A., et al. (2007). Food additives and hyperactive behaviour in 3-year-old and 8/9-year-old children in the community: a randomised, double-blinded, placebo-controlled trial. *The Lancet, 370*(9598), 1560-1567.

McMurdie, P. J., & Holmes, S. (2013). phyloseq: an R package for reproducible interactive analysis and graphics of microbiome census data. *PLoS One, 8*(4), e61217.

Mercado, C. P., & Kilic, F. (2010). Molecular mechanisms of SERT in platelets: regulation of plasma serotonin levels. *Molecular interventions, 10*(4), 231.

Mescher, M., & Haarmann-Stemmann, T. (2018). Modulation of CYP1A1 metabolism: From adverse health effects to chemoprevention and therapeutic options. *Pharmacology & Therapeutics, 187*, 71-87.

Mitsuyama, K., Toyonaga, A., Sasaki, E., et al. (1994). IL-8 as an important chemoattractant for neutrophils in ulcerative colitis and Crohn's disease. *Clinical & Experimental Immunology, 96*(3), 432-436.

Modasia, A., Parker, A., Jones, E., et al. (2020). Regulation of enteroendocrine cell networks by the major human gut symbiont Bacteroides thetaiotaomicron. *Frontiers in Microbiology*, 2800.

Morgan, M. E., Zheng, B., Koelink, P. J., et al. (2013). New perspective on dextran sodium sulfate colitis: antigen-specific T cell development during intestinal inflammation. *PLoS One, 8*(7), e69936.

Morgan, M. J., & Liu, Z.-g. (2011). Crosstalk of reactive oxygen species and NF-κB signaling. *Cell research, 21*(1), 103-115.

Moriez, R., Salvador-Cartier, C., Theodorou, V., et al. (2005). Myosin light chain kinase is involved in lipopolysaccharide-induced disruption of colonic epithelial barrier and bacterial translocation in rats. *The American journal of pathology, 167*(4), 1071-1079.

Mössner, R., & Lesch, K.-P. (1998). Role of serotonin in the immune system and in neuroimmune interactions. *Brain, behavior, and immunity, 12*(4), 249-271.

Moubarac, J.-C., Batal, M., Louzada, M., et al. (2017). Consumption of ultra-processed foods predicts diet quality in Canada. *Appetite, 108*, 512-520.

Murphy, C. A., Langrish, C. L., Chen, Y., et al. (2003). Divergent pro-and antiinflammatory roles for IL-23 and IL-12 in joint autoimmune inflammation. *The Journal of experimental medicine, 198*(12), 1951-1957.

Nagalingam, N. A., & Lynch, S. V. (2012). Role of the microbiota in inflammatory bowel diseases. *Inflammatory bowel diseases, 18*(5), 968-984.

Naimi, S., Viennois, E., Gewirtz, A. T., et al. (2021). Direct impact of commonly used dietary emulsifiers on human gut microbiota. *Microbiome, 9*(1), 1-19.

Nakamura, T. (2019). Recent progress in organoid culture to model intestinal epithelial barrier functions. *International immunology, 31*(1), 13-21.

Narula, N., Wong, E. C., Dehghan, M., et al. (2021). Association of ultra-processed food intake with risk of inflammatory bowel disease: prospective cohort study. *bmj, 374*.

Nava, P., Koch, S., Laukoetter, M. G., et al. (2010). Interferon-γ regulates intestinal epithelial homeostasis through converging β-catenin signaling pathways. *Immunity, 32*(3), 392-402.

Neurath, M., Weigmann, B., Finotto, S., et al. (2002). The transcription factor T-bet regulates mucosal T cell activation in experimental colitis and Crohn's disease. *The Journal of experimental medicine, 195*(9), 1129-1143.

Neurath, M. F. (2014). Cytokines in inflammatory bowel disease. *Nature Reviews Immunology, 14*(5), 329-342.

Ng, S. C., Shi, H. Y., Hamidi, N., et al. (2017). Worldwide incidence and prevalence of inflammatory bowel disease in the 21st century: a systematic review of population-based studies. *The Lancet, 390*(10114), 2769-2778.

Nikolaus, S., Schulte, B., Al-Massad, N., et al. (2017). Increased tryptophan metabolism is associated with activity of inflammatory bowel diseases. *Gastroenterology, 153*(6), 1504-1516. e1502.

Niu, H., Li, R., Liang, Q., et al. (2019). Metabolic engineering for improving L-tryptophan production in Escherichia coli. *Journal of Industrial Microbiology and Biotechnology, 46*(1), 55-65.

Nozawa, K., Kawabata-Shoda, E., Doihara, H., et al. (2009). TRPA1 regulates gastrointestinal motility through serotonin release from enterochromaffin cells. *Proceedings of the national academy of sciences, 106*(9), 3408-3413.

O'Connell, P. J., Wang, X., Leon-Ponte, M., et al. (2006). A novel form of immune signaling revealed by transmission of the inflammatory mediator serotonin between dendritic cells and T cells. *Blood, 107*(3), 1010-1017.

Okayasu, I., Hatakeyama, S., Yamada, M., et al. (1990). A novel method in the induction of reliable experimental acute and chronic ulcerative colitis in mice. *Gastroenterology, 98*(3), 694-702.

Ostanin, D. V., Pavlick, K. P., Bharwani, S., et al. (2006). T cell-induced inflammation of the small and large intestine in immunodeficient mice. *American Journal of Physiology-Gastrointestinal and Liver Physiology, 290*(1), G109-G119.

Otte, J. M., Werner, I., Brand, S., et al. (2008). Human beta defensin 2 promotes intestinal wound healing in vitro. *Journal of cellular biochemistry, 104*(6), 2286-2297.

Page, I. H. (1968). Serotonin. Chicago. *Year Book Medical Publishers, Inc*, 44.

Paone, P., & Cani, P. D. (2020). Mucus barrier, mucins and gut microbiota: the expected slimy partners? *Gut, 69*(12), 2232-2243.

Peery, A. F., Crockett, S. D., Barritt, A. S., et al. (2015). Burden of gastrointestinal, liver, and pancreatic diseases in the United States. *Gastroenterology, 149*(7), 1731-1741. e1733.

Pena, R. T., Blasco, L., Ambroa, A., et al. (2019). Relationship between quorum sensing and secretion systems. *Frontiers in Microbiology, 10*, 1100.

Peng, L., Li, Z.-R., Green, R. S., et al. (2009). Butyrate enhances the intestinal barrier by facilitating tight junction assembly via activation of AMP-activated protein kinase in Caco-2 cell monolayers. *The Journal of nutrition, 139*(9), 1619-1625.

Peter, G., & Van Groeningen, C. (1991). Clinical relevance of biochemical modulation of 5-fluorouracil. *Annals of Oncology, 2*(7), 469-480.

Peyrin-Biroulet, L., Beisner, J., Wang, G., et al. (2010). Peroxisome proliferator-activated receptor gamma activation is required for maintenance of innate antimicrobial immunity in the colon. *Proceedings of the national academy of sciences, 107*(19), 8772-8777.

Piovani, D., Danese, S., Peyrin-Biroulet, L., et al. (2020). Systematic review with meta-analysis: biologics and risk of infection or cancer in elderly patients with inflammatory bowel disease. *Alimentary pharmacology & therapeutics, 51*(9), 820-830.

Platzek, T., Lang, C., Grohmann, G., et al. (1999). Formation of a carcinogenic aromatic amine from an azo dye by human skin bacteria in vitro. *Human & experimental toxicology, 18*(9), 552-559.

Plöger, S., Stumpff, F., Penner, G. B., et al. (2012). Microbial butyrate and its role for barrier function in the gastrointestinal tract. *Annals of the New York academy of sciences, 1258*(1), 52-59.

Powrie, F. (1995). T cells in inflammatory bowel disease: protective and pathogenic roles. *Immunity, 3*(2), 171-174.

Powrie, F., Leach, M. W., Mauze, S., et al. (1993). Phenotypically distinct subsets of CD4+ T cells induce or protect from chronic intestinal inflammation in C. B-17 scid mice. *International immunology, 5*(11), 1461-1471.

Rafa, H., Amri, M., Saoula, H., et al. (2010). Involvement of interferon-γ in bowel disease pathogenesis by nitric oxide pathway: a study in Algerian patients. *Journal of Interferon & Cytokine Research, 30*(9), 691-697.

Rafii, F., Hall, J., & Cerniglia, C. (1997). Mutagenicity of azo dyes used in foods, drugs and cosmetics before and after reduction by Clostridium species from the human intestinal tract. *Food and chemical Toxicology, 35*(9), 897-901.

Rapport, M. M., Green, A. A., & Page, I. H. (1948a). Crystalline serotonin. *science, 108*(2804), 329-330.

Rapport, M. M., Green, A. A., & Page, I. H. (1948b). Partial purification of the vasoconstrictor in beef serum. *Journal of Biological Chemistry, 174*(2), 735-741.

Regmi, S. C., Park, S.-Y., Ku, S. K., et al. (2014). Serotonin regulates innate immune responses of colon epithelial cells through Nox2-derived reactive oxygen species. *Free Radical Biology and Medicine, 69*, 377-389.

Rehfeld, J. (2004). A centenary of gastrointestinal endocrinology. *Hormone and Metabolic Research, 36*(11/12), 735-741.

Reigstad, C. S., Salmonson, C. E., III, J. F. R., et al. (2015). Gut microbes promote colonic serotonin production through an effect of short-chain fatty acids on enterochromaffin cells. *The FASEB Journal, 29*(4), 1395-1403.

Reinisch, W., Hommes, D. W., Van Assche, G., et al. (2006). A dose escalating, placebo controlled, double blind, single dose and multidose, safety and tolerability study of fontolizumab, a humanised anti-interferon γ antibody, in patients with moderate to severe Crohn's disease. *Gut, 55*(8), 1138-1144.

Richard, D. M., Dawes, M. A., Mathias, C. W., et al. (2009). L-tryptophan: basic metabolic functions, behavioral research and therapeutic indications. *International Journal of Tryptophan Research, 2*, IJTR. S2129.

Rigottier-Gois, L. (2013). Dysbiosis in inflammatory bowel diseases: the oxygen hypothesis. *The ISME journal, 7*(7), 1256-1261.

Rizzello, F., Spisni, E., Giovanardi, E., et al. (2019). Implications of the westernized diet in the onset and progression of IBD. *Nutrients, 11*(5), 1033.

Rooks, M. G., Veiga, P., Wardwell-Scott, L. H., et al. (2014). Gut microbiome composition and function in experimental colitis during active disease and treatment-induced remission. *The ISME journal, 8*(7), 1403-1417.

SAMUEL TRAN, V., MARION-AUDIBERT, A. M., Karatekin, E., et al. (2004). Serotonin secretion by human carcinoid BON cells. *Annals of the New York academy of sciences, 1014*(1), 179-188.

Sandborn, W. J., Ghosh, S., Panes, J., et al. (2020). Efficacy of upadacitinib in a randomized trial of patients with active ulcerative colitis. *Gastroenterology, 158*(8), 2139-2149. e2114.

Sandborn, W. J., & Targan, S. R. (2002). Biologic therapy of inflammatory bowel disease. *Gastroenterology, 122*(6), 1592-1608.

Sandler, M., Reveley, M., & Glover, V. (1981). Human platelet monoamine oxidase activity in health and disease: a review. *Journal of Clinical Pathology, 34*(3), 292-302.

Sandyk, R. (1992). L-tryptophan in neuropsychiatry disorders: a review. *International journal of neuroscience, 67*(1-4), 127-144.

Sasaki, T., Hiwatashi, N., Yamazaki, H., et al. (1992). The role of interferony in the pathogenesis of Crohn's disease. *Gastroenterologia Japonica, 27*(1), 29-36.

Sasaki, Y. F., Kawaguchi, S., Kamaya, A., et al. (2002). The comet assay with 8 mouse organs: results with 39 currently used food additives. *Mutation Research/Genetic Toxicology and Environmental Mutagenesis, 519*(1-2), 103-119.

Sato, T., Vries, R. G., Snippert, H. J., et al. (2009). Single Lgr5 stem cells build crypt-villus structures in vitro without a mesenchymal niche. *Nature, 459*(7244), 262-265.

Scheppach, W., Sommer, H., Kirchner, T., et al. (1992). Effect of butyrate enemas on the colonic mucosa in distal ulcerative colitis. *Gastroenterology, 103*(1), 51-56.

Scott, K. G. E., Meddings, J. B., Kirk, D. R., et al. (2002). Intestinal infection with Giardia spp. reduces epithelial barrier function in a myosin light chain kinase–dependent fashion. *Gastroenterology, 123*(4), 1179-1190.

Sekirov, I., Russell, S. L., Antunes, L. C. M., et al. (2010). Gut microbiota in health and disease. *Physiological reviews*.

Sellon, R. K., Tonkonogy, S., Schultz, M., et al. (1998). Resident enteric bacteria are necessary for development of spontaneous colitis and immune system activation in interleukin-10-deficient mice. *Infection and immunity, 66*(11), 5224-5231.

Shajib, M. S., Chauhan, U., Adeeb, S., et al. (2019). Characterization of serotonin signaling components in patients with inflammatory bowel disease. *Journal of the Canadian Association of Gastroenterology, 2*(3), 132-140.

Sharkey, K. A., & Mawe, G. M. (2002). Neuroimmune and epithelial interactions in intestinal inflammation. *Current opinion in pharmacology, 2*(6), 669-677.

Sharma, V., McKone, H. T., & Markow, P. G. (2011). A global perspective on the history, use, and identification of synthetic food dyes. *Journal of Chemical Education, 88*(1), 24-28.

Shoda, R., Uchida, M., & Matsueda, K. (2000). Oral administration of a food coloring agent, tartrazine, enhances the development of hapten-induced colitis and delays its healing in rats. *Gastroenterology, 4*(118), A1370.

Siddique, Z.-L., Drozdov, I., Floch, J., et al. (2009). KRJ-I and BON cell lines: defining an appropriate enterochromaffin cell neuroendocrine tumor model. *Neuroendocrinology, 89*(4), 458-470.

Singh, U. P., Singh, N. P., Murphy, E. A., et al. (2016). Chemokine and cytokine levels in inflammatory bowel disease patients. *Cytokine, 77*, 44-49.

Singhal, M., Turturice, B. A., Manzella, C. R., et al. (2019). Serotonin transporter deficiency is associated with dysbiosis and changes in metabolic function of the mouse intestinal microbiome. *Scientific reports, 9*(1), 1-11.

Sjölund, K., Sanden, G., Håkanson, R., et al. (1983). Endocrine cells in human intestine: an immunocytochemical study. *Gastroenterology, 85*(5), 1120-1130.

Smyth, D., Phan, V., Wang, A., et al. (2011). Interferon-γ-induced increases in intestinal epithelial macromolecular permeability requires the Src kinase Fyn. *Laboratory investigation, 91*(5), 764-777.

Stavely, R., Fraser, S., Sharma, S., et al. (2018). The onset and progression of chronic colitis parallels increased mucosal serotonin release via enterochromaffin cell hyperplasia and downregulation of the serotonin reuptake transporter. *Inflammatory bowel diseases, 24*(5), 1021-1034.

Stearns, J. C., Davidson, C. J., McKeon, S., et al. (2015). Culture and molecular-based profiles show shifts in bacterial communities of the upper respiratory tract that occur with age. *The ISME journal, 9*(5), 1246-1259.

Stevens, L. J., Burgess, J. R., Stochelski, M. A., et al. (2014). Amounts of artificial food colors in commonly consumed beverages and potential behavioral implications for consumption in children. *Clinical pediatrics, 53*(2), 133-140.

Stevens, L. J., Burgess, J. R., Stochelski, M. A., et al. (2015). Amounts of artificial food colors in commonly consumed beverages and potential behavioral implications for consumption in children: revisited. *Clinical pediatrics, 54*(12), 1228-1230.

Suez, J., Korem, T., Zeevi, D., et al. (2014). Artificial sweeteners induce glucose intolerance by altering the gut microbiota. *Nature, 514*(7521), 181-186.

Sun, Y., Qiu, R., Li, X., et al. (2020). Social attraction in Drosophila is regulated by the mushroom body and serotonergic system. *Nature communications, 11*(1), 1-14.

Surette, M. G., Miller, M. B., & Bassler, B. L. (1999). Quorum sensing in Escherichia coli, Salmonella typhimurium, and Vibrio harveyi: a new family of genes responsible for autoinducer production. *Proceedings of the national academy of sciences, 96*(4), 1639-1644.

Szamosi, J. C., Forbes, J. D., Copeland, J. K., et al. (2020). Assessment of inter-laboratory variation in the characterization and analysis of the mucosal microbiota in Crohn's disease and ulcerative colitis. *Frontiers in Microbiology*, 2028.

Tai, E. K., Wong, H. P., Lam, E. K., et al. (2008). Cathelicidin stimulates colonic mucus synthesis by up-regulating MUC1 and MUC2 expression through a mitogen-activated protein kinase pathway. *Journal of cellular biochemistry, 104*(1), 251-258.

Takeuchi, A., Badr, M. E. S. G., Miyauchi, K., et al. (2016). CRTAM determines the CD4+ cytotoxic T lymphocyte lineage. *Journal of Experimental Medicine, 213*(1), 123-138.

Tatsuoka, M., Osaki, Y., Ohsaka, F., et al. (2022). Consumption of indigestible saccharides and administration of Bifidobacterium pseudolongum reduce mucosal serotonin in murine colonic mucosa. *British Journal of Nutrition, 127*(4), 513-525.

Thibault, R., De Coppet, P., Daly, K., et al. (2007). Down-regulation of the monocarboxylate transporter 1 is involved in butyrate deficiency during intestinal inflammation. *Gastroenterology, 133*(6), 1916-1927.

Tian, L.-X., Tang, X., Zhu, J.-Y., et al. (2020). Cytochrome P450 1A1 enhances inflammatory responses and impedes phagocytosis of bacteria in macrophages during sepsis. *Cell Communication and Signaling, 18*(1), 1-16.

Torres, J., Mehandru, S., Colombel, J.-F., et al. (2017). Crohn's disease. *The Lancet, 389*(10080), 1741-1755.

Turlejski, K. (1996). Evolutionary ancient roles of serotonin: long-lasting regulation of activity and development. *Acta neurobiologiae experimentalis, 56*, 619-636.

Turner, J. R. (2009). Intestinal mucosal barrier function in health and disease. *Nature Reviews Immunology, 9*(11), 799-809.

Turpin, W., Lee, S.-H., Garay, J. A. R., et al. (2020). Increased intestinal permeability is associated with later development of Crohn's disease. *Gastroenterology, 159*(6), 2092-2100. e2095.

Turvill, J., Connor, P., & Farthing, M. (2000). The inhibition of cholera toxin-induced 5-HT release by the 5-HT3 receptor antagonist, granisetron, in the rat. *British journal of pharmacology, 130*(5), 1031-1036.

Verma, R., Verma, N., & Paul, J. (2013). Expression of inflammatory genes in the colon of ulcerative colitis patients varies with activity both at the mRNA and protein level. *Eur Cytokine Netw, 24*(3), 130-138.

Vernier–Massouille, G., Balde, M., Salleron, J., et al. (2008). Natural history of pediatric Crohn's disease: a population-based cohort study. *Gastroenterology, 135*(4), 1106-1113.

Villablanca, E. J., Selin, K., & Hedin, C. R. (2022). Mechanisms of mucosal healing: treating inflammatory bowel disease without immunosuppression? *Nature reviews Gastroenterology & hepatology*, 1-15.

Vojdani, A., & Vojdani, C. (2015). Immune reactivity to food coloring. *Altern Ther, 21*, 1-100.

Vujkovic-Cvijin, I., Dunham, R. M., Iwai, S., et al. (2013). Dysbiosis of the gut microbiota is associated with HIV disease progression and tryptophan catabolism. *Science translational medicine, 5*(193), 193ra191-193ra191.

Walther, D. J., Peter, J.-U., Bashammakh, S., et al. (2003). Synthesis of serotonin by a second tryptophan hydroxylase isoform. *science, 299*(5603), 76-76.

Walther, D. J., Peter, J.-U., Winter, S., et al. (2003). Serotonylation of small GTPases is a signal transduction pathway that triggers platelet α-granule release. *Cell, 115*(7), 851-862.

Wang, F., Graham, W. V., Wang, Y., et al. (2005). Interferon-γ and tumor necrosis factor-α synergize to induce intestinal epithelial barrier dysfunction by up-regulating myosin light chain kinase expression. *The American journal of pathology, 166*(2), 409-419.

Wang, H., Kwon, Y. H., Dewan, V., et al. (2019). TLR2 plays a pivotal role in mediating mucosal serotonin production in the gut. *The Journal of Immunology, 202*(10), 3041-3052.

Wang, J., Xu, W., Wang, R., et al. (2021). The outer membrane protein Amuc_1100 of Akkermansia muciniphila promotes intestinal 5-HT biosynthesis and extracellular availability through TLR2 signalling. *Food & Function, 12*(8), 3597-3610.

Wang, L., Steele, E. M., Du, M., et al. (2021). Trends in consumption of ultraprocessed foods among US youths aged 2-19 years, 1999-2018. *JAMA, 326*(6), 519-530.

Wang, W., Chen, L., Zhou, R., et al. (2014). Increased proportions of Bifidobacterium and the Lactobacillus group and loss of butyrate-producing bacteria in inflammatory bowel disease. *Journal of clinical microbiology, 52*(2), 398-406.

Ward, J. B., Mroz, M. S., & Keely, S. J. (2013). The bile acid receptor, TGR 5, regulates basal and cholinergic-induced secretory responses in rat colon. *Neurogastroenterology & Motility, 25*(8), 708-711.

Watts, S. W., Morrison, S. F., Davis, R. P., et al. (2012). Serotonin and blood pressure regulation. *Pharmacological reviews, 64*(2), 359-388.

Watts, S. W., Priestley, J. R., & Thompson, J. M. (2009). Serotonylation of vascular proteins important to contraction. *PLoS One, 4*(5), e5682.

Wehkamp, J., Salzman, N. H., Porter, E., et al. (2005). Reduced Paneth cell α-defensins in ileal Crohn's disease. *Proceedings of the national academy of sciences, 102*(50), 18129-18134.

Whitaker-Azmitia, P. M. (1999). The discovery of serotonin and its role in neuroscience. *Neuropsychopharmacology, 21*(1), 2-8.

Whitaker-Azmitia, P. M. (2001). Serotonin and brain development: role in human developmental diseases. *Brain research bulletin, 56*(5), 479-485.

Wikoff, W. R., Anfora, A. T., Liu, J., et al. (2009). Metabolomics analysis reveals large effects of gut microflora on mammalian blood metabolites. *Proceedings of the national academy of sciences, 106*(10), 3698-3703.

Wilks, S. (1859). Morbid appearances in the intestine of Miss Bankes. *Med Times Gazette, 2*(2), 264-265.

Wirtz, S., Neufert, C., Weigmann, B., et al. (2007). Chemically induced mouse models of intestinal inflammation. *Nature protocols, 2*(3), 541-546.

Worthington, J. J., Reimann, F., & Gribble, F. (2018). Enteroendocrine cells-sensory sentinels of the intestinal environment and orchestrators of mucosal immunity. *Mucosal immunology, 11*(1), 3-20.

Xu, P., Becker, H., Elizalde, M., et al. (2018). Intestinal organoid culture model is a valuable system to study epithelial barrier function in IBD. *Gut, 67*(10), 1905-1906.

Xu, P., Becker, H., Elizalde, M., et al. (2021). Interleukin-28A induces epithelial barrier dysfunction in CD patient-derived intestinal organoids. *American Journal of Physiology-Gastrointestinal and Liver Physiology, 320*(5), G689-G699.

Xu, P., Elizalde, M., Masclee, A., et al. (2021). Corticosteroid enhances epithelial barrier function in intestinal organoids derived from patients with Crohn's disease. *Journal of Molecular Medicine, 99*(6), 805-815.

Yamazaki, K., Umeno, J., Takahashi, A., et al. (2013). A genome-wide association study identifies 2 susceptibility loci for Crohn's disease in a Japanese population. *Gastroenterology, 144*(4), 781-788.

Yano, J. M., Yu, K., Donaldson, G. P., et al. (2015). Indigenous bacteria from the gut microbiota regulate host serotonin biosynthesis. *Cell, 161*(2), 264-276.

Yao, Y., Feng, Q., & Shen, J. (2020). Myosin light chain kinase regulates intestinal permeability of mucosal homeostasis in Crohn's disease. *Expert Review of Clinical Immunology, 16*(12), 1127-1141.

Yen, D., Cheung, J., Scheerens, H., et al. (2006). IL-23 is essential for T cell–mediated colitis and promotes inflammation via IL-17 and IL-6. *The Journal of clinical investigation, 116*(5), 1310-1316.

Yoo, J. H., Holubar, S., & Rieder, F. (2020). Fibrostenotic strictures in Crohn's disease. *Intestinal research, 18*(4), 379.

Youakim, A., & Ahdieh, M. (1999). Interferon-γ decreases barrier function in T84 cells by reducing ZO-1 levels and disrupting apical actin. *American Journal of Physiology-Gastrointestinal and Liver Physiology, 276*(5), G1279-G1288.

Zahran, S. A., Ali-Tammam, M., Hashem, A. M., et al. (2019). Azoreductase activity of dye-decolorizing bacteria isolated from the human gut microbiota. *Scientific reports, 9*(1), 1-14.

Zelkas, L., Raghupathi, R., Lumsden, A. L., et al. (2015). Serotonin-secreting enteroendocrine cells respond via diverse mechanisms to acute and chronic changes in glucose availability. *Nutrition & metabolism, 12*(1), 1-9.

Zenewicz, L. A., Antov, A., & Flavell, R. A. (2009). CD4 T-cell differentiation and inflammatory bowel disease. *Trends in molecular medicine, 15*(5), 199-207.

Zeng, R., Bscheider, M., Lahl, K., et al. (2016). Generation and transcriptional programming of intestinal dendritic cells: essential role of retinoic acid. *Mucosal immunology, 9*(1), 183-193.

Zeve, D., Stas, E., de Sousa Casal, J., et al. (2022). Robust differentiation of human enteroendocrine cells from intestinal stem cells. *Nature communications, 13*(1), 1-20.

Zolotarevsky, Y., Hecht, G., Koutsouris, A., et al. (2002). A membrane-permeant peptide that inhibits MLC kinase restores barrier function in in vitro models of intestinal disease. *Gastroenterology, 123*(1), 163-172.

Zou, L., Spanogiannopoulos, P., Pieper, L. M., et al. (2020). Bacterial metabolism rescues the inhibition of intestinal drug absorption by food and drug additives. *Proceedings of the national academy of sciences, 117*(27), 16009-16018.